Author response to referee's comments for acp-2018-159: Production of particulate brown carbon during atmospheric aging of wood-burning emissions by Kumar et al.

Dear editor,

We thank both reviewers for their constructive comments, which significantly enhanced the quality of our manuscript. Below, we provide a point-by-point response (regular typeset) to the comments (blue font) of both reviewers. The modifications made to the manuscript are in grey font, indented and *italicized*. Please note that all references to line numbers are to the submitted manuscript (the ACPD file) and not the revised manuscript.

Anonymous referee 1.

GENERAL COMMENT

The paper presents an analysis of black carbon (BC) and organic aerosol absorption properties upon aging. The experiments were done in a laboratory using a smog chamber where aerosols were exposed to OH radical and UV radiation. Several optical and chemical properties were measured online and filter samples were collected to be analyzed later offline by a multiple wavelength absorbance measurement technique and an EC/OC analyzer. Methanol and water filter extracts were also analyzed and absorbance was measured. The data is very valuable and the paper is well written and presented. I would recommend its publication after addressing the comments I present below.

My main concerns are related to the following aspects:

- The offline techniques used in this study suffer of different artifacts and they are not sufficiently discussed in the manuscript.

We had carefully considered such artifacts, but could have made more reference to them in the manuscript. We consider the reviewer to be referring to unquantifiable uncertainties. Based on both reviewers' comments, we have added a section discussing quantifiable and unquantifiable uncertainties in the method section. This section reads as follows:

> ***Uncertainty analysis.*** *It is important to draw a clear distinction between uncertainties related to measurement precision and accuracy and those related with experimental variability. In this section we discuss the quantifiable and unquantifiable uncertainties related with the different measurements. In the result section, we will present our confidence levels on the average parameters determined based on the experimental variability, which we judge to be the main source of variance in the data.*

➔ ***Quantifiable uncertainties:***

The estimated uncertainty in the AMS-derived OA mass concentrations is ~25%, which includes both potential biases and precision. This estimate is based on the variation in the AMS calibration factors and estimated uncertainties in the SMPS used for the AMS calibration (Bruns et al., 2015, 2016). Uncertainties related to particle transmission efficiency in the AMS are considered negligible for the particles sampled here (Liu et al., 2007), whose volume size distribution falls within the range transmitted efficiently by the AMS aerodynamic lens (see Fig. S4). The bounce-related collection efficiency (CE) of the AMS was concluded to be unity for wood-burning OA in the literature reviewed by Corbin et al. (2015b; in their Section S1.2). For the present data, the comparison between the SMPS mass (predicted from fitted volume distributions using a density of 1.5 g cm^{-3}*) and the total PM predicted as AMS-OA+eBC, suggest a CE value between 0.7 and 1.0 (19% relative uncertainty), consistent with average literature values and the uncertainties estimates. The uncertainty in EC mass concentration, estimated from measurement repeats based on the EUSAAR2 protocol only, is within 7% in our case. The precision uncertainty in the aethalometer attenuation measurements was estimated as 15* Mm^{-1} *based on the standard deviation of its signals prior to aerosol being injected into the smog chamber. The MWAA data have an estimated noise level and precision of 12 /Mm and 10% respectively, and these uncertainties have been added in quadrature to provide the overall uncertainties shown, for example, as error bars in Fig. 1 below. To compare the MWAA and aethalometer measurements, we determined* $b_{abs,MWAA,880nm}$ *by extrapolating the absorption coefficients measured at 850 nm to 880 nm using an α-value determined from the ratio between the absorption coefficients at 850 nm and 635nm. The uncertainty associated with this extrapolation is considered negligible relative to the overall MWAA uncertainty.*

➔ ***Possible unquantified uncertainties:***

There are significant uncertainties in the measurement of aerosol absorption using filter-based techniques (e.g., Collaud Coen et al., 2010). Here, we have used MWAA measurements as a reference to scale the aethalometer data, using a single C value. The correction factor C, which accounts for scattering effects within the filter matrix (Drinovec et al., 2015), may depend on the aerosol sample (Collaud Coen et al., 2010). In this study, we evaluated the variability in this factor for our primary and aged samples, by directly comparing the aethalometer to MWAA measurements, as discussed below. The MWAA has been previously validated against a polar nephelometer and a MAAP (Massabo et al., 2013), which, in turn, has been validated against numerous in situ methods (e.g., Slowik et al., 2007). The excellent correlation between MWAA and EC in our study (discussed below) supports the high confidence in the MWAA filter based absorption measurements conducted here. Another significant source of uncertainty in filter-based absorption measurements is the

possible sorption (or evaporation) of volatile organics on (or from) the filter material. This may lead to an overestimation (or underestimation) of OA absorption. However, we have minimized sorption artefacts by utilizing a charcoal denuder. We have obtained an excellent correlation between OA absorption measurements derived from the MWAA-calibrated aethalometer and from quartz filter samples (see discussion below, Fig. 6 in the main text and S13 in the supplementary information). Although both of these techniques involved filter sampling, their sampling timescale is an order of magnitude different, and a difference is therefore expected if sorption (or evaporation) caused a substantial bias in our results. We therefore conclude that it is unlikely that artifacts associated with filter sampling have biased the absorption measurements. Finally, uncertainties related to pyrolysis during thermo-optical analysis may bias EC measurements. Such uncertainties arise from unstable organic compounds, and can be significant for biomass-burning samples, leading to biases on the order of 20% for EC (e.g. Schauer et al., 2003; Yang and Yu., 2007). To minimize these biases we applied the EUSAAR2 protocol. The optical properties of such organics are generally different from BC; therefore, the excellent correlation between MWAA and EC data in Fig. 1A suggest that pyrolysis effects were not a major source of uncertainty in our data set.

We have added the following abbreviation to the corrected text:

L146. *multi-angle absorption photometer (MAAP, Petzold and Schönlinner, 2004).*

We have also expanded the text in some places to reflect the considerations presented above, as shown in the response to the next comment.

New references added:

Schauer, J. J., Mader, B. T., Deminter, J. T., Heidemann, G., Bae, M. S., Seinfeld, J. H., Flagan, R. C., Cary, R. A., Smith, D., Huebert, B. J., Bertram, T., Howell, S., Kline, J. T., Quinn, P., Bates, T., Turpin, B., Lim, H. J., Yu, J. Z., Yang, H., and Keywood, M. D.: ACE-Asia intercomparison of a thermaloptical method for the determination of particle-phase organic and elemental carbon, Environ. Sci. Technol., 37, 993–1001, https://doi.org/10.1021/es020622f, 2003.

Slowik, J. G., E. S. Cross, J.-H. Han, P. Davidovits, T. B. Onasch, J. T. Jayne, L. R. Williams, M. R. Canagaratna, D. R. Worsnop, R. K. Chakrabarty, H. Moosmüller, W. P. Arnott, J. P. Schwarz, R. S. Gao, D. W. Fahey, G. L. Kok and A. Petzold, An inter-comparison of instruments measuring black carbon content of soot particles, Aerosol Sci. Technol. 41, 3, 295-314, 2007.

Collaud Coen, M., Weingartner, E., Apituley, A., Ceburnis, D., Fierz-Schmidhauser, R., Flentje, H., Henzing, J. S., Jennings, S. G., Moerman, M., Petzold, A., Schmid, O., and Baltensperger, U.: Minimizing light absorption measurement artifacts of the Aethalometer: evaluation of five correction algorithms, Atmos. Meas. Tech., 3, 457-474, https://doi.org/10.5194/amt-3-457-2010, 2010.

Yang, H. and Yu, J. Z.: Uncertainties in charring correction in the analysis of elemental and organic carbon in atmospheric particles by thermal/optical methods, Environ. Sci. Technol., 36 (23), 5199–5204, 2002.

- In this study the BC particles were not observed to be coated with other kind of particles (i.e., no internal mixing but external mixing was observed). However, ambient studies have shown that BC particles in the atmosphere are usually coated and this coating causes an enhancement of BC absorption. Given that, how representative is this study of "atmospheric aging"? Were the experiments not long enough to "age" the BC particles?

The reviewer raised two points, to which we reply separately.

The reviewer questions how representative our study was of atmospheric aging. The emissions studied here are representative of flaming wood in stoves typically used in Western Europe, while aging is equivalent to ~2 days of OH-driven photochemistry, under atmospheric winter day time conditions in the mid-latitude.

The reviewer questions the reasons for the lack of lensing with aging, when such effect had been observed in the field. We have clarified our language here. Our aim has been to assert that our measurements are poorly represented by a pure core-shell conceptual model of internal mixing. This assertion is based on our measured absorption coefficients, and we have modified the text to explain this in more detail as quoted immediately below.

The AMS measurements showed that the amount of OA generated during aging was substantial. Likewise, the SMPS showed a considerable growth of the primary particles with aging. If BC and OA are naively treated as core-shell mixtures, an absorption enhancement of ~1.8 would have been predicted, with an average increase in the coating mass by a factor of 3 (see Bond et al., 2006). However, our absorption-coefficient measurements in Fig. 1a showed that we did not observe any absorption enhancement. Therefore, we do not conclude that "BC particles were not coated" but rather than "the particles studied could not be represented by a core–shell description of coatings that envelop the central BC core". The particles may be internally mixed, but of a morphology more complex than core-shell – e.g. off-centered coatings with complexities due to the aggregated morphology of BC, see e.g. the microscopy images of biomass-burning particles by China et al. 2013. Modelling or even accurately describing such morphologies is well beyond the scope of our experimental study. Current literature reports for the lensing effect are conflicting, showing that absorption enhancements upon significant BC coating can be less than 5% (Cappa et al., 2012) or as large as 150% (Liu et al., 2015). Recent experimental work suggests that such discrepancies are related to the complex black carbon morphology and a core–shell description does not adequately capture mixed-BC optical properties and may considerably overestimate the observed absorption values (Liu et al., 2017). As lensing effect was negligible in our case, we have assumed that the aerosol optically behaves as an external mixture between BC and BrC. We note that while this assumption is important for estimating the BC absorption, the BrC absorption is not very

sensitive to the assumed morphology. Based on both reviewers comments and to avoid confusion we have modified the Results section 4.1 as follows:

Section 4.1.

We have independently determined the MAC_{BC}(880nm) and the aethalometer C values under our conditions, as follows. We determined MAC_{BC}(880nm) from the regression between the absorption coefficients at 880 nm obtained from the MWAA and the EC mass measured by the Sunset analyzer (Fig. 1A). The slope of this regression may be used to estimate the MAC_{BC}(880nm), which we retrieved as 4.7 ± 0.3 $m^2 g^{-1}$ by an uncertainty-weighted linear least-squares fit . The corresponding intercept was not significantly different from zero (-3 ± 3 /Mm). Our MAC_{BC}(880nm) is not statistically significantly different from the value recommended by Bond et al., (2006) for externally-mixed BC (extrapolating their MAC_{BC}(550nm) to 880 nm by assuming α=1 provides MAC_{BC}*(880nm)= 4.7 ± 0.7 $m^2 g^{-1}$). The strong correlation between* $b_{abs,MWAA,880nm}$ *and EC in Fig. 1A shows that MAC_{BC}(880nm) did not vary with aging during our study (see also Fig. S2-a). It also indicates that measurement artefacts for both instruments were negligible, as the fundamental differences between the two techniques mean that any artefacts are unlikely to be similar between them (charring for EC vs. adsorption artefacts for MWAA). Our absorption coefficient measurements also provide insights into particle mixing state in this study. Since a single MAC adequately described our samples at all levels of aging (Fig. 1A and Fig. S2-a), in spite of a factor of 3.3 average increase in the aerosol mass, our samples cannot be adequately described by a core-shell Mie model. Such a core-shell model would predict an absorption enhancement by a factor of ~1.8 (Bond et al., 2006) for the observed OA mass increase with aging, which was not observed in our case. This observation is also supported by the time resolved attenuation measurements at 880 nm using the aethalometer (Fig. S3), suggesting that little (<10%) to no increase in the attenuation coefficients upon SOA formation. We emphasize that this conclusion does not indicate that no internal mixing occurred, but rather that the simplified concept of negligible mixing better describes our data than the equally simplified concept of a core-shell description of coatings that completely envelop the central BC core. This may be due to the complex morphology of internally-mixed BC, which has been previously observed for wood burning particles (e.g., China et al., 2013; Liu et al., 2015; Liu et al., 2017). It may also be related to the fact that OA and BC are emitted during separate phases of combustion. OA rich particles are emitted during the pre-flaming pyrolysis stage of combustion, whereas most BC is emitted during flaming combustion (Corbin et al., 2015a, 2015b; Haslett et al., 2018; Heringa et al., 2011). These two stages of combustion may coexist in different regions of the stove, particularly during simulated real-world usage. As lensing effect was negligible in our case, we have assumed that the aerosol optically behaves as an external mix*

between BC and BrC during Mie calculation (see section 3.4). We note that while this assumption is important for estimating the BC absorption, the conclusion drawn about the BrC absorption are not very sensitive to the assumed morphology.

We determined time-resolved wavelength-dependent absorption coefficients as follows. We used the aethalometer to obtain filter attenuation coefficients with high time resolution, which were then calibrated to obtain absorption coefficients by deriving the factor C (Equation 1) using the MWAA measurements of filter samples. C was obtained from an uncertainty-weighted linear least-squares fit as 3.0 ± 0.2 (Fig. 1B); the intercept of the fit was not significantly different from zero, within two standard deviations (-17 ± 14). A very strong correlation could be observed between MWAA and aethalometer (Fig. 1B), implying that C is independent of the type of the aerosol sampled (see also Fig. S2-B). Therefore, we used a single C value to obtain time-resolved wavelength-dependent absorption coefficients from the aethalometer attenuation measurements at the different wavelengths for primary and aged aerosols.

Note that the manufacturer's default values, which were not applied in our case, are 1.57 for C (using TFE-coated glass fiber filters) and 12.2 m^2 g^{-1} for σ_{ATN} at 880 nm (Gundel et al., 1984 , Drinovec et al., 2015). The C value determined here is larger than the manufacturer-default value for the AE33, resulting in smaller absorption coefficients. However, the calculated σATN at 880 nm (13.8 m^2 g^{-1}), which can be retrieved as the product of the C value and MAC_{BC}(880nm) (Eq. (3)), is similar to the factory-default σATN. Therefore, our calibrated M_{eBC} concentrations, calculated from the attenuation coefficients using σATN (Eq. (2)), are similar to the factory-default M_{eBC}. We note that M_{eBC} has not been used for MAC_{OA} calculations, and is only used for the calculation of the mass fractions of BC and OA for display purposes (Fig. 2, 3, 7 and 8).

References:

China, S., Mazzoleni, C., Gorkowski, K., Aiken, A. C., and Dubey, M. K.: Morphology and mixing state of individual freshly emitted wildfire carbonaceous particles, Nat. Commun., 4, 1–7, doi:10.1038/ncomms-3122-2013, 2013.

Liu, S., Aiken, A. C., Gorkowski, K., Dubey, M. K., Cappa, C. D., Williams, L. R., Herndon, S. C., Massoli, P., Fortner, E. C., Chhabra, P. S., Brooks, W. A., Onasch, T. B., Jayne, J. T., Worsnop, D. R., China, S., Sharma, N., Mazzoleni, C., Xu, L., Ng, N. L., Liu, D., Allan, J. D., Lee, J. D., Fleming, Z. L., Mohr, C., Zotter, P., Szidat, S. and Prévôt, A. S. H.: Enhanced light absorption by mixed source black and brown carbon particles in UK winter, Nat. Commun., 8435, doi:10.1038/ncomms9435, 2015b.

Liu, D. T., Whitehead, J., Alfarra, M. R., Reyes-Villegas, E., Spracklen, D. V., Reddington, C. L., Kong, S. F., Williams, P. I., Ting, Y. C., Haslett, S., Taylor, J. W., Flynn, M. J., Morgan, W. T., McFiggans, G., Coe, H., and Allan, J. D.: Black-carbon

absorption enhancement in the atmosphere determined by particle mixing state, Nat. Geosci., 10, 184–188, doi:10.1038/ngeo2901, 2017.

Haslett, S. L.; Thomas, J. C.; Morgan, W. T.; Hadden, R.; Liu, D.; Allan, J. D.; Williams, P. I.; Keita, S.; Liousse, C. and Coe, H. Highly controlled, reproducible measurements of aerosol emissions from combustion of a common African biofuel source, Atmos. Chem. Phys, 385-403, doi:10.5194/acp-18-385-2018 , 2018.

We slightly modified Fig. 1A to reflect these changes. We included error bars in Fig. 1 which had been missing previously.

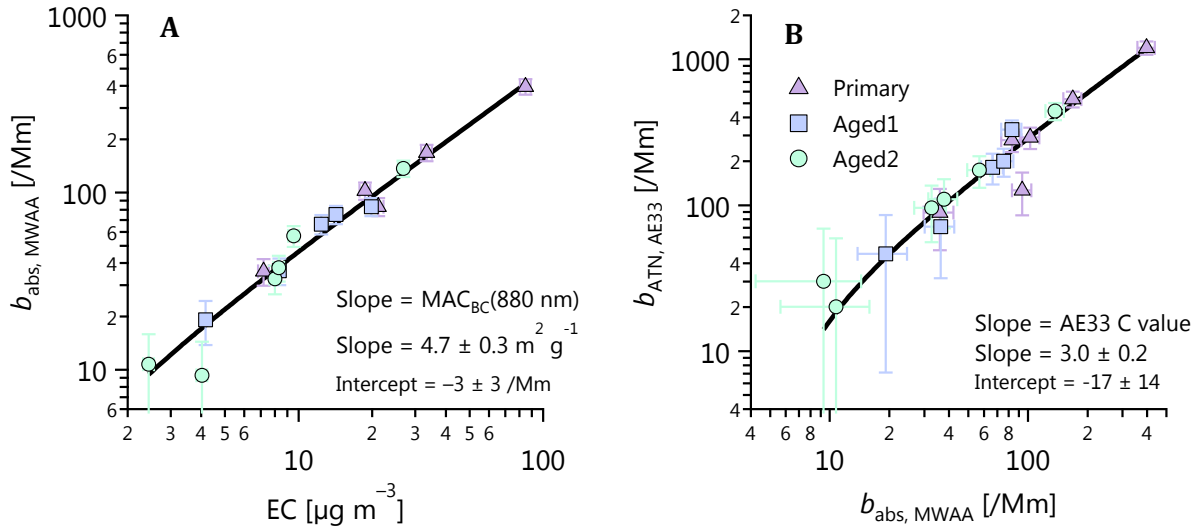

We also included error bars in Fig. 7:

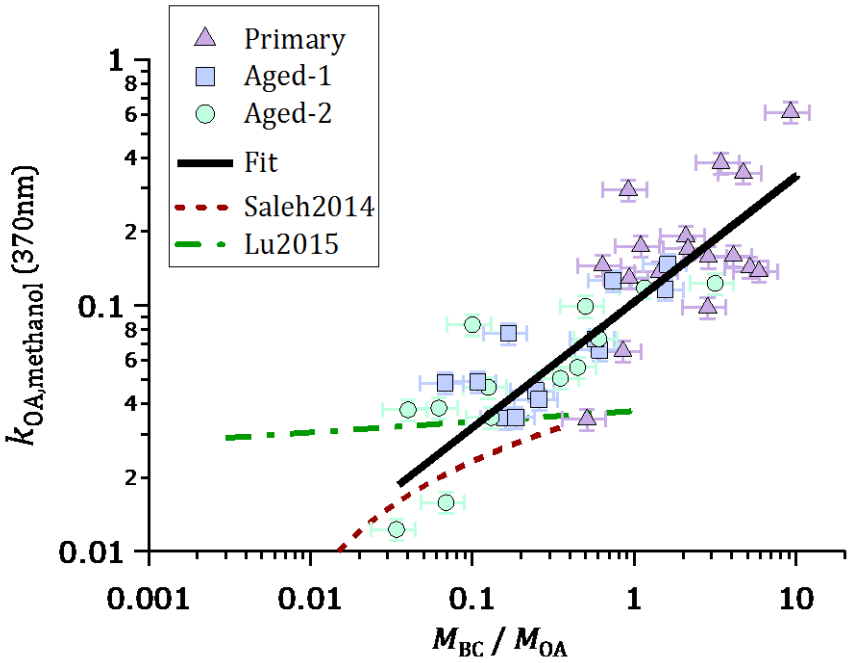

SPECIFIC COMMENTS

1. Lines 107-108: How can you guarantee the correction factor C is wavelength independent?

This is a good question which has often been neglected in the literature. Recently, Corbin et al. (2018), in their Section S3.2, presented a very detailed discussion and reanalysis of the wavelength dependence of the C-value.

In that publication, the authors described the wavelength dependence of the C-value as separated into a filter dependence and a scattering cross-sensitivity measurement, and presented four different arguments for its wavelength dependence being negligible:

1. They compared their wavelength-dependent absorption coefficient measurements with MWAA measurements (which do not rely on a C-value-like correction) and found good agreement between the two techniques. We have also verified our AE33 data with MWAA data in the present study.
2. They pointed out that the measured AAE would be biased by a wavelength-dependent C value, so that their measurements of an AAE of 1.0 for samples dominated by BC (in agreement with extensive literature) indicates a negligible wavelength dependence of C.
3. They combined measurements of aerosol SSA (ranging from 0.5 to 0.9) with size-dependent scattering cross-sensitivity measurements to quantitatively estimate the influence of scattering cross-sensitivity as negligible. SSA measurements were not available in our study, but our measured size distributions indicate that our particles were generally small enough that their conclusions can be extrapolated to our samples.
4. They described previous work where different filter materials were compared, with no significant effect on the wavelength dependence of the C value (Drinovec et al., 2015).

In conclusion, the C value is known to depend on the filter material but its wavelength dependence has been shown to be negligible for samples such as those studied in the manuscript presently under review.

We have updated the manuscript as follow:

> L111. *As discussed in detail by Corbin et al. (2018), the wavelength-dependence of C can be expected to be negligible*

References:

Corbin, J. C.; Pieber, S. M.; Czech, H.; Zanatta, M.; Jakobi, G.; Massabò, D.; Orasche, J.; El Haddad, I.; Mensah, A. A.; Stengel, B.; Drinovec, L.; Mocnik, G.; Zimmermann, R.; Prévôt, A. S. H. and Gysel, M. Brown and black carbon emitted by a marine engine operated on heavy fuel oil and distillate fuels: optical properties, size distributions and emission factors, J. Geophys. Res. Atmos., 123, 6175-6195, doi:10.1029/2017JD027818, 2018.

Drinovec, L., Močnik, G., Zotter, P., Prévôt, A. S. H., Ruckstuhl, C., Coz, E., Rupakheti, M., Sciare, J., Müller, T., Wiedensohler, A. and Hansen, A. D. A.: The"dual-spot" aethalometer: an improved measurement of aerosol black carbon with real-time loading compensation, Atmos. Meas. Tech., 8(5), 1965–1979, doi:10.5194/amt-8-1965-2015, 2015.

2. Line 122: "1.57 for C". Does this mean your Aethalometer was using TFE-coated glass fiber filters? Please mention the filter material.

Our Aethalometer was using TFE-coated glass fiber filters. We have added some clarifications in the text as follows:

*The manufacturer default values are 1.57 for C (**TFE-coated glass fiber filters**) and 12.2 $m^2 g^{-1}$ for σ_{ATN} at 880 nm, which corresponds to a MAC_{BC}(880 nm) of 7.77 $m^2 g^{-1}$ (Gundel et al., 1984 , Drinovec et al., 2015).*

3. Line 128: It should be necessary to add some more discussion about possible artifacts that affect both techniques (MWAA and Sunset analyser).

We have added text, cited and quoted in the preceding responses, to better explain how the MWAA functions and has been validated. We have also added a discussion of artifacts affecting the Sunset analyzer in the new subsubsection quoted above. The relevant text (Section 4.1, as cited at L128) has been updated following this comment and was quoted in our response to this reviewer's overall comments. For clarity, we will not quote the text again here.

References:

Cavalli, F., Viana, M., Yttri, K. E., Genberg, J. and Putaud, J.-P.: Toward a standardised thermal-optical protocol for measuring atmospheric organic and elemental carbon: the EUSAAR protocol, Atmos. Meas. Tech., 3(1), 79–89, doi:doi:10.5194/amt-3-79-2010, 2010.

Massabò, D., Bernardoni, V., Bove, M. C., Brunengo, A., Cuccia, E., Piazzalunga, A., Prati, P., Valli, G. and Vecchi, R.: A multi-wavelength optical set-up for the characterization of carbonaceous particulate matter, J. Aerosol Sci., 60, 34–46, doi:10.1016/j.jaerosci.2013.02.006, 2013.

4. Line 136. MWAA measurements. Which artifacts are to be considered when using this technique in comparison to the Aethalometer? Can you provide more evidence on the comparison of this technique to other absorption measurements like MAAP or PAS?

This good comment has been addressed in our response to this reviewer's first major comment. The MWAA has been validated against the MAAP by Massabo et al. (2013).

5. Line 171: What do you mean with the online kOA? How was this measured?

We apologize for this confusion; we have not measured the k_{OA} online. We corrected this error and rephrased the sentence for clarity:

If the OA extraction efficiency was less than unity, then the absorption (or MAC) predicted from our solvent-extraction measurements would be less than that measured (or calculated) using our real-time measurements (MWAA-calibrated aethalometer).

6. Lines 403-411: How does this result compares to other studies? Ambient measurements have shown quick oxidation of brown carbon chromophores. Please comment about it.

The results of Forrister et al., 2015 suggest that BrC emitted from wildfires has very poor atmospheric stability with most of the aerosol being lost within a day, either due to chemical loss or evaporation. However, other ambient and chamber studies clearly (Zhong et al., 2014, Lee et al., 2014) imply that the optical properties of BrC are strongly dependent on the complex process of aging. Photo-chemical destruction and formation of chromophores is a topic of current research and may strongly depend on the gas phase composition.

References:

Forrister, H., Liu, J., Scheuer, E., Dibb, J., Ziemba, L., Thornhill, L. K., Anderson, B., Diskin, G., Perring, A. E., Schwarz, J. P., Campuzan-Jost, P., Day, D. A., Palm, B. B., Jimenez, J. L., Nenes, A., Weber, R. J.: Evolution of brown carbon in wildfire plumes, Gephys. Res. Lett.,42, 4623-4630, doi: 10.1002/2015GL063897, 2015.

Zhong, M. and Jang, M.: Dynamic light absorption of biomass-burning organic carbon photochemically aged under natural sunlight, Atmos. Chem. Phys., 14, 1517-1525, doi:10.5194/acp-14-1517-2014, 2014.

Lee, H. J., Aiona, P. K., Laskin, A., Laskin, J. and Nizkorodov, S. A.: Effects of solar radiation on the optical properties and molecular composition of laboratory proxies of atmospheric brown carbon, Environ. Sci. Technol. Lett., 48(17), 10217-10226, doi:10.1021/es502515r, 2014.

Technical Corrections:

7. Line 101: It would be convenient to add numbers to these headlines across the manuscript for the sake of readability (e.g., "2.2.1 Aethalometer").

We agree, however, as our manuscript still needs to be converted from Word to LaTeX during typesetting, we will leave this decision to the journal staff.

8. Line 123: at?

The 'at' was removed from the sentence in line 123.

9. Line 141: Which angles?

We modified the text as follows:

> L140. *The first photodiode is placed behind the filter for transmittance measurements (0° relative to the incident light, 1.5 cm from the sample), while the other two photodiodes are positioned at 125º and 165º (11 cm from the sample) to collect the back scattered light.*

10. Lines 294-295: Please rephrase this sentence to improve understanding.

We have rewritten the entire section for improved clarity, as quoted at the beginning of this response.

11. Lines 296-299: It can be found awkward that the two variables needed to calculate MAC are coming from the same measurement technique (Aethalometer). Please try to sustain the reasons why it was done this way.

This was not the case, the two variables for the MAC_{BC} came from the MWAA and EC. The aethalometer provided high time resolution attenuation coefficients which could be calibrated to give absorption coefficients needed for the MAC_{OA} retrieval. eBC was not needed for MAC_{OA} calculations as now clarified in the text, but for display purposes (Fig. 2, 3, 7 and 8). In the revised manuscript we have clarified the text (see new Section 4.1 quoted at the beginning of this response).

12. Line 372: It should be written "Eq. (19)", and "Fig. 4". Please implement this across the manuscript. Check the journal guidelines.

This has been done in the corrected version of the manuscript.

13. Lines 542-543: Please add uncertainty intervals to the reported MAC values.

This has been done in the corrected version of the manuscript:

> *The mean MAC_{SOA}(370nm) was 2.2 $m^2\ g^{-1}$ (one-sigma variability: 1.6 – 3.1 $m^2\ g^{-1}$ according to a **GSD = 1.39**) under our experimental conditions, 2.3 times lower than the mean MAC_{POA}(370nm) but approximately an order of magnitude higher than MAC values estimated for ambient oxygenated aerosols or reported for SOA from biogenic and traditional anthropogenic precursors.*

14. Figures 3A, S6, and S10: The data is presented using discrete colors for each wavelength. Please make the legend discrete too.

We have made this change.

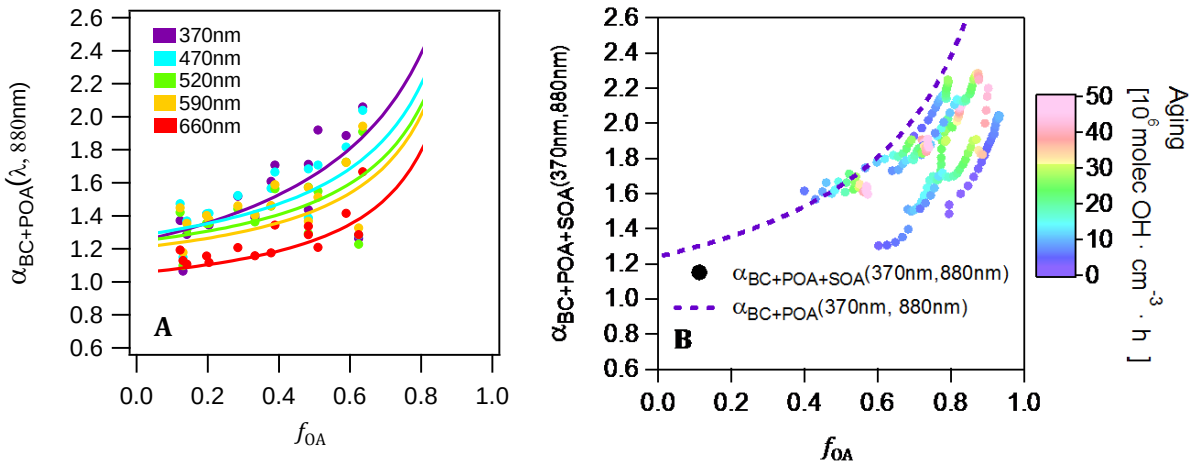

Fig 3A

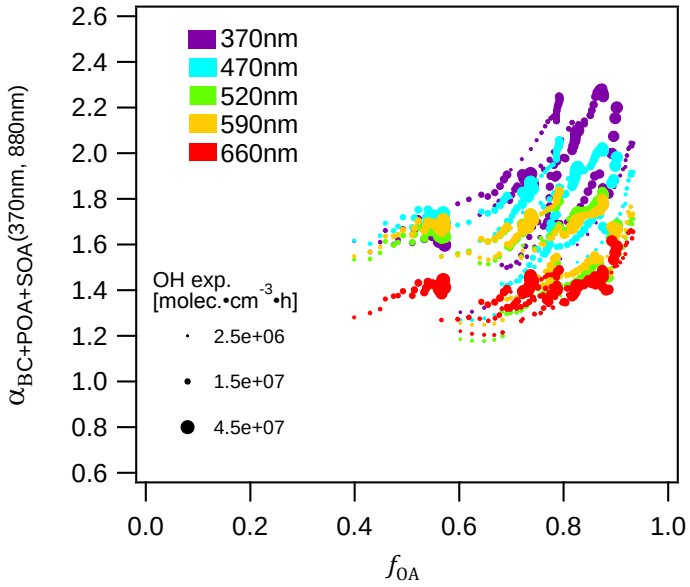

Fig S6

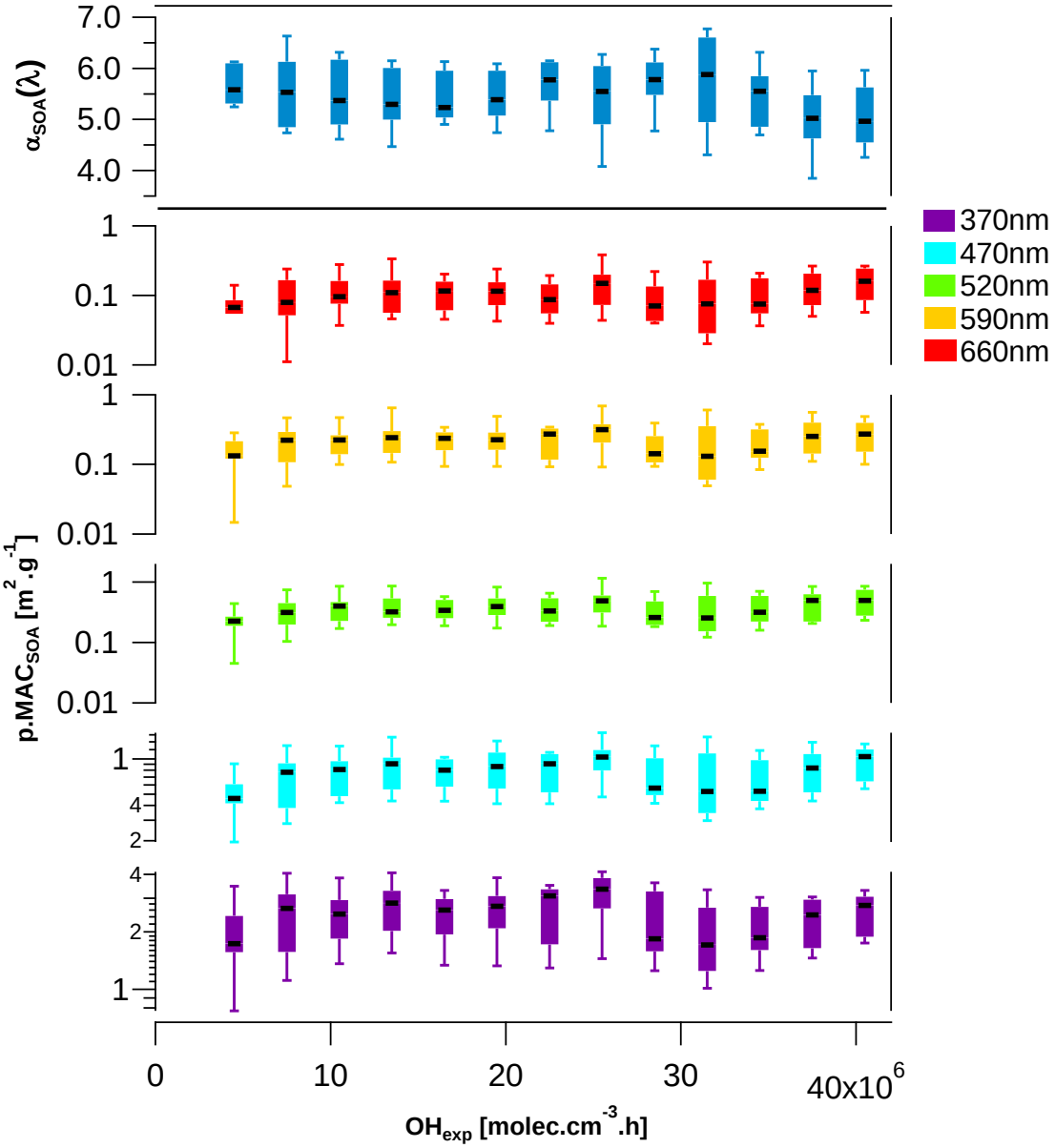

Fig S10

15. Figure 5: What do these boxes and whiskers mean? Please clarify.

We added the following to the caption:

> *The box marks the 25th and 75th percentile, while the whiskers mark the 10th and the 90th percentile.*

16. Figure 6: Could you please add the correlation coefficients to the figure?

We are not sure if the reviewer is referring to a Pearson correlation coefficient *r* or to the coefficient of determination (R^2) of the fit. Although these two quantities are numerically related by a square root function, r is used to describe a data set and R^2 is used to describe a fit. But R^2 is not appropriate to define our fit, as we performed an orthogonal regression. We have reported the standard error of the fit parameters as appropriate diagnostic statistics. We have followed the reviewer's request to include a correlation coefficient in the paper, but, to avoid confusing the reader, we have mentioned the Pearson correlation coefficient in the text but not added it to the figure, as we expect most readers to misinterpret it as reflecting goodness of fit:

> Line 421. *Fig. 6B shows excellent correlation between the MAC_{OA}(370nm) values obtained from the kOA of the solvent-extracted OA with the in-situ method described above. The Pearson correlation coefficient was 0.8, for both solvents.*

17. Figure S6: I guess you meant α as a function of λ or do you mean only the wavelength pair 370-880 nm?

We apologize for the confusion; we modified the figure caption as follows:

> *Figure S6: Relationship of $\alpha_{BC+POA+SOA}(\lambda, \mathbf{880nm})$ to f_{OA} for seven wavelengths, with symbol sizes indicating OH exposure.*

18. Figures S4, S7, and S9: Please stick to journal guidelines and avoid the use of the jet (or rainbow) color map: "For maps and charts, please keep colour blindness in mind and avoid the parallel usage of green and red. For a list of colour scales that are illegible to a significant number of readers, please visit ColorBrewer 2.0".

Based on the referee comment, we have changed the three figures as follows:

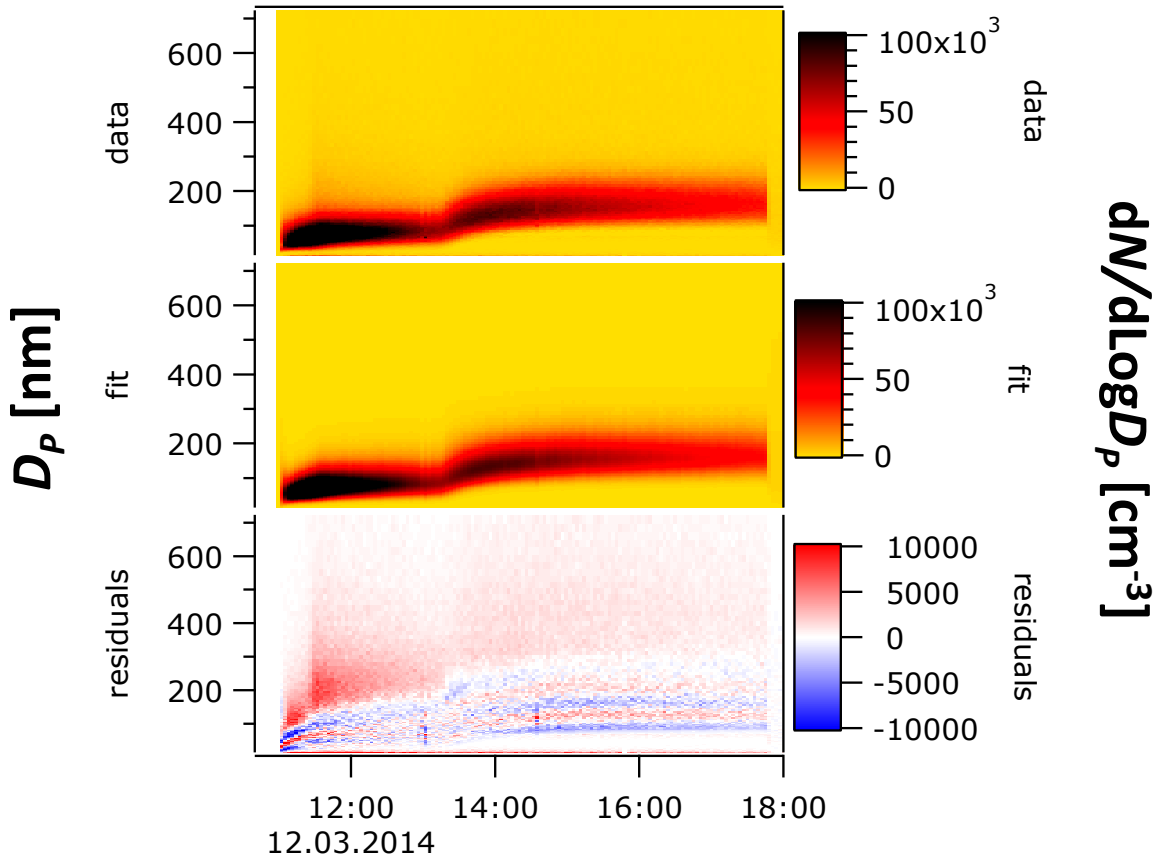

518

519

Fig. S4

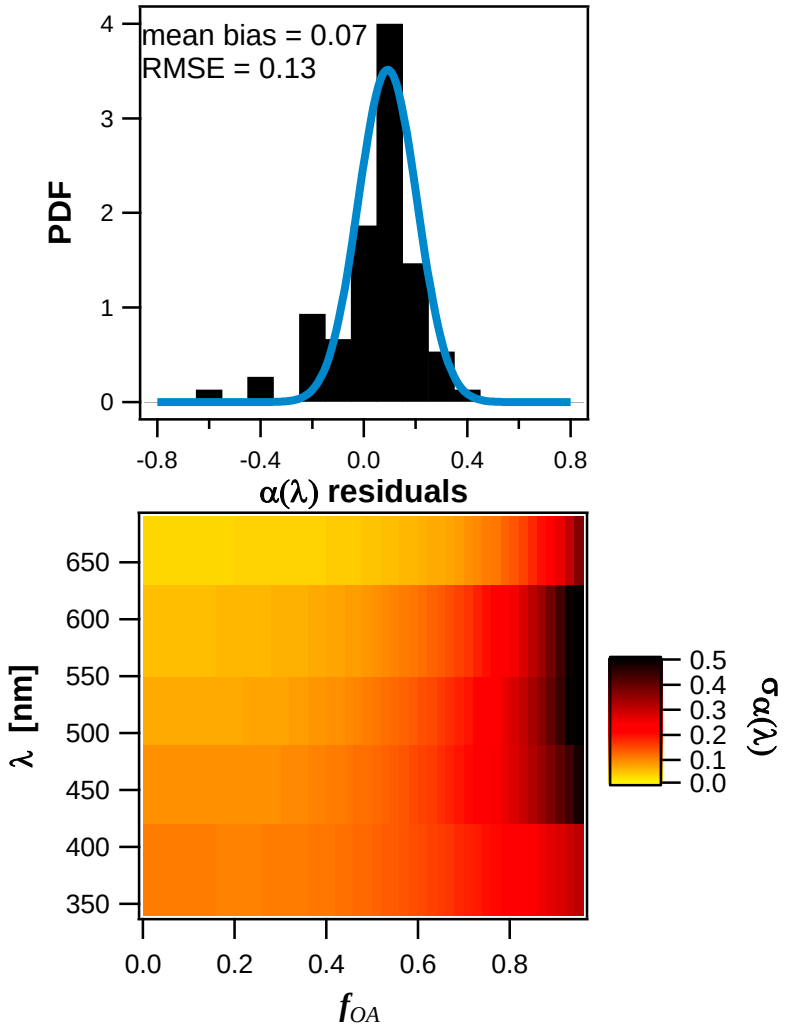

Fig. S7

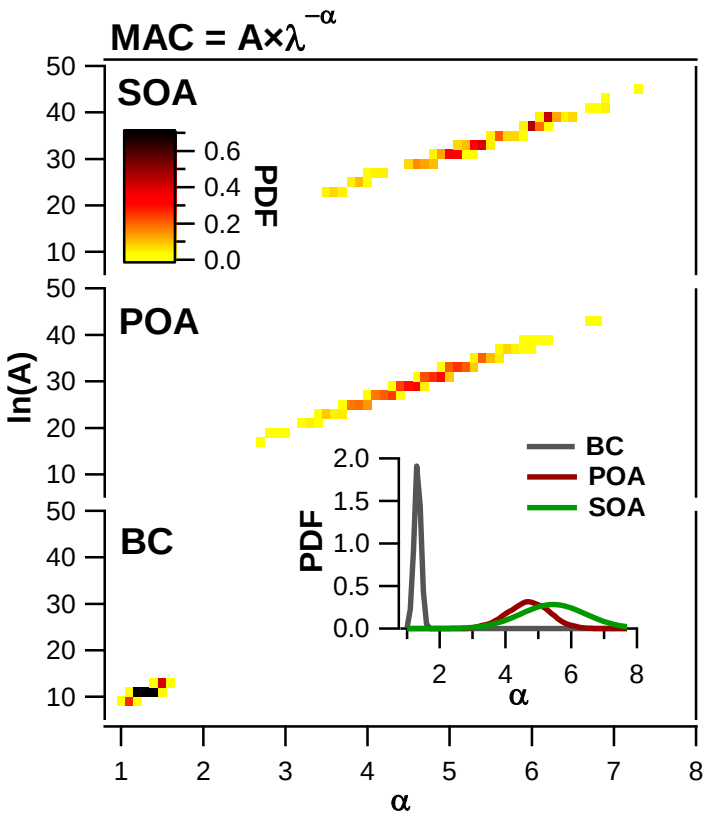

Fig. S9

Anonymous referee 2.

GENERAL COMMENT

Overall, I find that the authors have presented novel and interesting results on the influence of photochemical aging on absorption by residential wood combustion emissions. They have done a better job than I often see in assessing the performance of the aethelometer for their specific situation, but should include additional details regarding measurement uncertainties, and how these measurement uncertainties propogate to their final atmospheric implications. I have numerous comments, mostly just asking for clarification. I believe this paper should be publishable, with revisions.

We thank the referee for her/ his constructive comments, which we address below.

1. Title: It would be good to state "residential wood-burning emissions."

The title has been modified in the corrected version of the manuscript:

> *Production of particulate brown carbon during atmospheric aging of residential wood-burning emissions*

2. L14: It might be good to indicate this was under (likely) high NOx conditions.

The experiments were conducted at estimated NO_x/NMOG ratios of ~ 0.035 – 0.35 ppm ppm C^{-1} (Bruns et al., 2016). These conditions can be considered as high NO_X, where most of the RO_2 radicals react with NO, rather with RO_2/HO_2. This information has been added to the corrected version of the manuscript in section 2.1.

> ***Section 2.1.***
> *Laboratory measurements were conducted in an 8 m^3 Teflon smog chamber (Bruns et al., 2015; Platt et al., 2013) installed within a temperature-controlled housing. Conditions in the chamber were maintained to represent winter time in Europe, i.e. relative humidity ranging between 50 – 90%, at 263 K (Bruns et al., 2015, 2016). Beech wood was combusted in a residential wood stove. Primary emissions were sampled through heated lines at 413 K, diluted by a factor of ~14 using an ejector diluter (DI-1000, Dekati Ltd.), then sampled into the chamber, which provided an additional ten-fold dilution. The overall dilution was a factor of 100 to 200. As we aimed to sample only flaming-phase emissions into the chamber, samples were taken when the modified combustion efficiency (ratio of CO_2 to the sum of CO and CO_2) was > 0.90. Despite maintaining the same combustion conditions, the resulting organic fraction to the total carbonaceous aerosols in the different samples was*

highly variable, indicating that these samples are representative of a mixture of pre-ignition and flaming emissions (with varying contributions of each combustion stage). Finally, the resulting NOx/NMOG ratios, which dramatically influence SOA formation through influencing the fate of peroxy radicals, RO_2, were estimated to be between 0.035 – 0.35 ppm ppm C^{-1} (Bruns et al., 2016). These conditions can be considered as high NO_X representative of urban/sub-urban conditions, where most of the RO_2 radicals react with NO, rather with RO_2/HO_2.

3. L15: It would be good to clarify what wavelength, or if this is integrated in some way.

This has been clarified in the corrected version of the manuscript:

At shorter wavelengths (370 – 470nm), light absorption by brown carbon from primary organic aerosol (POA) and secondary organic aerosol (SOA) formed during aging was around 10 % and 20 %, respectively, of the total aerosol absorption (BrC plus BC).

4. L17: Reporting the GSD is informative, but an actual uncertainty estimate would be better.

Based on this comment and others below, the reviewer is asking for providing uncertainty propagation based on measurement precision and accuracy, instead of a GSD which represents the experimental variability. As we discussed in the reply to the first reviewer, we have added in the corrected version of the manuscript a new section in the Method, discussing quantifiable and unquantifiable uncertainties. However, in the result section we still present the variability in the parameters determined as GSD, as these represent our confidence levels in these average parameters. We believe that such information is relevant if these parameters were to be used for future predictions. We also consider that for most of the parameters experimental variability is much more important than measurement uncertainties and biases.

5. L54: It would be good to also cite the work from the Georgia Tech group (*Forrister et al.*, 2015).

As suggested by the reviewer the work of Forrister et al., 2015 was cited.

Forrister, H., Liu, J., Scheuer, E., Dibb, J., Ziemba, L., Thornhill, L. K., Anderson, B., Diskin, G., Perring, A. E., Schwarz, J. P., Campuzan-Jost, P., Day, D. A., Palm, B. B., Jimenez, J. L., Nenes, A., Weber, R. J.: Evolution of brown carbon in wildfire plumes, Gephys. Res. Lett.,42, 4623-4630, doi: 10.1002/2015GL063897, 2015.

6. L229: It is not clear to me why the MAC for POA would be unaffected. The authors write for Eqn. 13 what amounts to:

$$\alpha(\lambda, 880) = \frac{-1}{\ln\left(\frac{\lambda}{880}\right)} \ln\left(\frac{[EC]MAC_{BC_\lambda}}{[EC]MAC_{BC_{880}}} + \frac{[OA]MAC_{OA_\lambda}}{[EC]MAC_{BC_{880}}}\right)$$

$$= \frac{-1}{\ln\left(\frac{\lambda}{880}\right)} \ln\left(\frac{[EC]MAC_{BC_\lambda}}{[EC]MAC_{BC_{880}}} + \frac{[OA]MAC_{OA_\lambda}}{b_{abs,880}}\right)$$

and where they have only included the second line, not the first. The *b*abs,880 value, while seemingly independent of the EC measurements as the authors have written them, actually do depend on the EC measurements because everything has been referenced to the EC measurement. Perhaps I am simply missing something, but I think that the authors statement must be further justified. Yes, the MAC of OA is fundamentally independent of the MAC of BC. But I am not certain that these are practically separated to the extent indicated by the authors. This is the same challenge that all AAE extrapolation methods face in quantitatively determining OA absorption in the presence of BC. See e.g. the cited Moosmuller paper or (*Lack and Langridge*, 2013). Also, the statement on L231 is self-evident. Of course the AAE at a given wavelength depends on the relative contributions of BC and OA.

The reviewer raises two separate points. The first is whether the $MAC_{OA,\lambda}$ directly depends on the EC mass. The second is whether the BC absorption at a given λ affects the estimation of $MAC_{OA,\lambda}$. Below, we address these points separately.

1. We consider it inaccurate to say that OA MAC has been referenced to EC. This reflects how we have expressed and applied Equation 13. The intermediate steps leading to equation 13 were intentionally omitted, as they tend to mislead the reader. Equation 13 clearly shows that:

- EC mass concentration is not explicitly required.
- A potential bias in $MAC_{BC,880nm}$ due to a bias in EC mass would directly affect the resulting $MAC_{BC,\lambda}$ in a proportional manner, whereas $MAC_{OA,\lambda}$ would remain completely unaffected.
- The resulting $MAC_{OA,\lambda}$ depends on the input parameter M_{OA}, thus being affected by potential AMS calibration bias.
- A potential bias in absorption coefficients measured by the MWAA would propagate to a proportional bias in $MAC_{OA,\lambda}$, as aethalometer measurements of b_{abs} are referenced against the MWAA. Such bias in absorption coefficient would also propagate to a proportional bias in $MAC_{BC,\lambda}$, which would happen through a corresponding bias in $MAC_{BC,880}$
- The resulting $MAC_{OA,\lambda}$ also depends on the input parameter $b_{abs,880nm}$, which is referenced to the MWAA measurement, whereas the EC data are by no means

blended into the b_{abs} data. Such bias in absorption coefficient would also propagate to a proportional bias in $MAC_{BC,\lambda}$, which would happen through a corresponding bias in $MAC_{BC,880nm}$.

2. We acknowledge that the determination of $MAC_{OA,\lambda}$ depends on the estimated absorption of BC at a given λ, which in turn depends on the estimated $MAC_{BC,\lambda}$. This is an issue on any multivariate fitting, where the theoretically independent fitted quantities are not independently determined. We note that such uncertainties are taken into account by the fitting errors presented as GSDs in the manuscript. The $MAC_{BC,\lambda}$ is similar to an extrapolation of the absorption measurements at f_{OA}= 0. We note our experiment covered BC rich particles allowing for an accurate determination of $MAC_{BC,\lambda}$.

Reference:

Saleh, R.; Adams, P. J.; Donahue, N. M. & Robinson, A. L. The interplay between assumed morphology and the direct radiative effect of light-absorbing organic aerosol. Geophys. Res. Lett., 43, 8735-8743, doi:10.1002/2016GL069786, 2016.

We have added the statements below to the manuscript:

> L222. *[…] Equation 10. We have intentionally formulated of Equation 13 as such to highlight that the retrieved* $MAC_{OA}(t,\lambda)$ *depends mainly on the input* M_{OA}. *Correspondingly, the retrieved* $MAC_{OA}(t,\lambda)$ *is mainly sensitive to potential AMS calibration biases.*

7. L264: What about chemically induced changes of POA mass, as opposed to just absorption?

We have mentioned the changes in POA mass and MAC in the sentence before, in L263: "Equation 19 is based on the assumption that POA is "chemically inert", i.e. no chemically induced changes of M_{POA} and MAC_{POA} occur". We have adjusted the text based on the Reviewer's comment to avoid confusion:

> *Such chemically induced changes of absorption coefficient by POA,* ***through a change of*** M_{POA} ***or*** MAC_{POA}***,*** *if they occur, are assigned to the absorption by SOA, thus resulting in a corresponding adjustment of the inferred* MAC_{SOA}.

8. L287: It is unclear what is meant by "a higher than measured lensing effect."

This text has been rewritten following the comments above. The revised text clarifies this meaning and, to avoid confusion, we will simply refer to the revised text in response to Reviewer #1's first comment. The corrected text reads as follows:

Section 4.1.

We have independently determined the MAC_{BC}(880nm) and the aethalometer C values under our conditions, as follows. We determined MAC_{BC}(880nm) from the regression between the absorption coefficients at 880 nm obtained from the MWAA and the EC mass measured by the Sunset analyzer (Figure 1A). The slope of this regression may be used to estimate the MAC_{BC}(880nm), which we retrieved as 4.7 ± 0.3 m^2g^{-1} by an uncertainty-weighted linear least-squares fit . The corresponding intercept was not significantly different from zero (-3 ± 3 /Mm). Our MAC_{BC}(880nm) is not statistically significantly different from the value recommended by Bond et al., (2006) for externally-mixed BC (extrapolating their MAC_{BC}(550nm) to 880 nm by assuming α=1 provides MAC_{BC}*(880nm)= 4.7 ± 0.7 $m^2 g^{-1}$). The strong correlation between* $b_{abs,MWAA,880nm}$ *and EC in Fig. 1A shows that MAC_{BC}(880nm) did not vary with aging during our study (see also Fig. S2-a). It also indicates that measurement artefacts for both instruments were negligible, as the fundamental differences between the two techniques mean that any artefacts are unlikely to be similar between them (charring for EC vs. adsorption artefacts for MWAA). Our absorption coefficient measurements also provide insights into particle mixing state in this study. Since a single MAC adequately described our samples at all levels of aging (Fig. 1A and Fig. S2-a), in spite of a factor of 3.3 average increase in the aerosol mass, our samples cannot be adequately described by a core-shell Mie model. Such a core-shell model would predict an absorption enhancement by a factor of ~1.8 (Bond et al., 2006) for the observed OA mass increase with aging, which was not observed in our case. This observation is also supported by the time resolved attenuation measurements at 880 nm using the aethalometer (Fig. S3), suggesting that little (<10%) to no increase in the attenuation coefficients upon SOA formation. We emphasize that this conclusion does not indicate that no internal mixing occurred, but rather that the simplified concept of negligible mixing better describes our data than the equally simplified concept of a core-shell description of coatings that completely envelop the central BC core. This may be due to the complex morphology of internally-mixed BC, which has been previously observed for wood burning particles (e.g., China et al., 2013; Liu et al., 2015; Liu et al., 2017). It may also be related to the fact that OA and BC are emitted during separate phases of combustion. OA rich particles are emitted during the pre-flaming pyrolysis stage of combustion, whereas most BC is emitted during flaming combustion (Corbin et al., 2015a, 2015b; Haslett et al., 2018; Heringa et al., 2011). These two stages of combustion may coexist in different regions of the stove,*

particularly during simulated real-world usage. As lensing effect was negligible in our case, we have assumed that the aerosol optically behaves as an external mix between BC and BrC during Mie calculation (see section 3.4). We note that while this assumption is important for estimating the BC absorption, the conclusion drawn about the BrC absorption are not very sensitive to the assumed morphology.

We determined time-resolved wavelength-dependent absorption coefficients as follows. We used the aethalometer to obtain filter attenuation coefficients with high time resolution, which were then calibrated to obtain absorption coefficients by deriving the factor C (Equation 1) using the MWAA measurements of filter samples. C was obtained from an uncertainty-weighted linear least-squares fit as 3.0 ± 0.2 (Fig. 1B); the intercept of the fit was not significantly different from zero, within two standard deviations (-17 ± 14). A very strong correlation could be observed between MWAA and aethalometer (Fig. 1B), implying that C is independent of the type of the aerosol sampled (see also Fig. S2-B). Therefore, we used a single C value to obtain time-resolved wavelength-dependent absorption coefficients from the aethalometer attenuation measurements at the different wavelengths for primary and aged aerosols.

Note that the manufacturer's default values, which were not applied in our case, are 1.57 for C (using TFE-coated glass fiber filters) and 12.2 m^2 g^{-1} for σ_{ATN} at 880 nm (Gundel et al., 1984 , Drinovec et al., 2015). The C value determined here is larger than the manufacturer-default value for the AE33, resulting in smaller absorption coefficients. However, the calculated σ_{ATN} at 880 nm (13.8 m^2 g^{-1} see Fig. 1C), which can be retrieved from Fig. 1-C or as the product of the C and MAC_{BC}(880nm) (Equation 3), is almost equal to the factory default σ_{ATN}. Therefore, our M_{eBC}, which can be directly calculated from the attenuation coefficients using σ_{ATN} (Equation 2), would be consistent with factory default M_{eBC}. We note that M_{eBC} has not been used for MAC calculations. However for displaying purposes, we have calculated time resolved M_{eBC} using σ_{ATN} and b_{ATN} to estimate fraction of BC and OA in the aerosol (Fig. 2, 3, 7 and 8).

9. L290: The authors mention uncertainties here for the UV-Vis measurements. But what about for all of the in situ or other measurements? This includes [EC], [OA], absorption. Further discussion of uncertainties is necessary.

We thank the reviewer for emphasizing the importance of uncertainties. In the previous version, uncertainties related with the different measurements were discussed very briefly in sections related with the description of the measurement techniques. As this comment was raised by both reviewers, we have added a new section discussing quantifiable and non-quantifiable uncertainties, which is referenced in the corresponding response and will not be duplicated here for clarity.

10. L305: It is not clear how this uncertainty estimate was arrived at. Also, this differs from the figure. Finally, it is not clear whether this fit has been forced to zero or not.

The reviewer is right, the uncertainty value in the figure and the text are not the same and the correct value is the one indicated in the figure (this has been changed accordingly). The uncertainty is the standard error of the slope of the uncertainty-weighted linear least-squares fit. The fit has not been forced through zero. Rather, we have fit the full linear model and test for the significance of the intercept term. The intercept was at -3 ± 3 m^2/g, not statistically significantly different than 0. This intercept was missing from the submitted manuscript and has now been reported, together with further modifications to the text as quoted in our modified Section 4.1 above.

11. L307: Bond et al. did not "report" a value at 880 nm. They reported at a shorter wavelength. This value is inferred assuming an AAE = 1. It should be noted as such.

The reviewer is right and the text has been modified accordingly, as specified in the quoted response to Reviewer #1's first comment.

12. L308: While the authors obtain a value of the MAC in good agreement with extrapolated values from Bond et al., it is not clear to me how this definitely indicates no lensing effect is present. An uncertainty analysis is necessary. What if, hypothetically, the EC was biased high and the absorption biased low? The obtained MAC might appear in agreement with literature, but only within the bounds of the measurement uncertainty. This statement should be quantified.

The reviewer raises a valid point that unidentified measurement biases in opposing directions may have led to the illusion of agreement between our measured MAC_{BC}(880nm) values and the literature values for bare BC. The major issue here is that of referencing our absorption data and EC measurements to reliable and calibrated technique. Absorption measurements were obtained using MWAA, which has been validated as described in the text, and biases are expected to be within 10%. Measurement biases related to total carbon measurement are negigible (within 5%). The high correlation between absorption and EC measurements also indicates that unquatifiable uncertainties and artefacts (e.g. charring for EC and vapor adsorption artefacts for MWAA) are negligible, as the fundamental differences between the two measurements mean that any artefacts are unlikely to be similar between them. Therefore, measurement biases and unquatifiable artefacts are unlikely to affect the estimated values for MAC_{BC}(880nm) and our conclusions about the lack of lensing. We also note that such conclusions are also supported by independent time resolved attenuation measurements by the aethalometer, suggesting that little (<10%) to no increase in the attenuation coefficients upon SOA formation.

Our analysis has combined multiple analytical techniques and found good agreement between all of them. This good agreement reduces the likelihood that opposing measurement biases led, by chance, to our measurements being in agreement with literature. While it remains

theoretically possible that unknown uncertainties and biases existed in our analysis, it is by Occam's razor more probable that our measurements were in fact accurate and that our cross-validation by employing different techniques was successful.

In the corrected version of the manuscript, we have added a new section discussing the measurement biases estimated for the different measurements. We have additionally discussed potential unquantifiable uncertainties. For clarity, we do not duplicate the mofified text here, but we quote the response to reviewer 1.

13. L315: It is clear that the distribution is reasonably log-normal with a single mode when considered in number space. But what about in surface area or in volume space, which is important for the calculation of the MAC_OA_bulk (Eqn. 20)? Also, to what extent does the volume-weighted distribution exceed the SMPS bounds?

The absolute SMPS volume is not as important for calculating $MAC_{OA,bulk}$ as the reviewer understood. As can be seen from Equation 20, we did not use the SMPS data to calculate total OA volume. We measured total OA mass with an AMS, converted mass into volume using an assumed density (the assumed density has no impact on the results as we use the same density to calculate MAC), and then "distributed" this volume across the size distribution measured by SMPS. That is, the SMPS data provide only a weighting factor for the size dependence of absorption, which means that uncertainties in these data do not have a major effect on our results. We performed the calculations in this way to minimize associated uncertainties, but acknowledge that substantial uncertainties may result. We have estimated that these may be on the order of 20%, based on the magnitude with which particulate absorption varies as a function of size (according to Mie theory).

14. L325 and Fig. S2: I do not understand why in Fig. S2 it says the "reported value" is 2.6 while here 3.0 is given. This should be clarified.

The reported C value is calculated using a σ_{ATN} = 12.2 $m^2 g^{-1}$, as given by the manufacturer, and MAC_{BC}(880nm) = 4.7 $m^2\,g^{-1}$. The C value = 3 is determined from our attenuation and absorption measurements which is used in our calculations. This has been discussed in lines 330-336.

For better clarity, we have now omitted the reported C-value from Fig. S2:

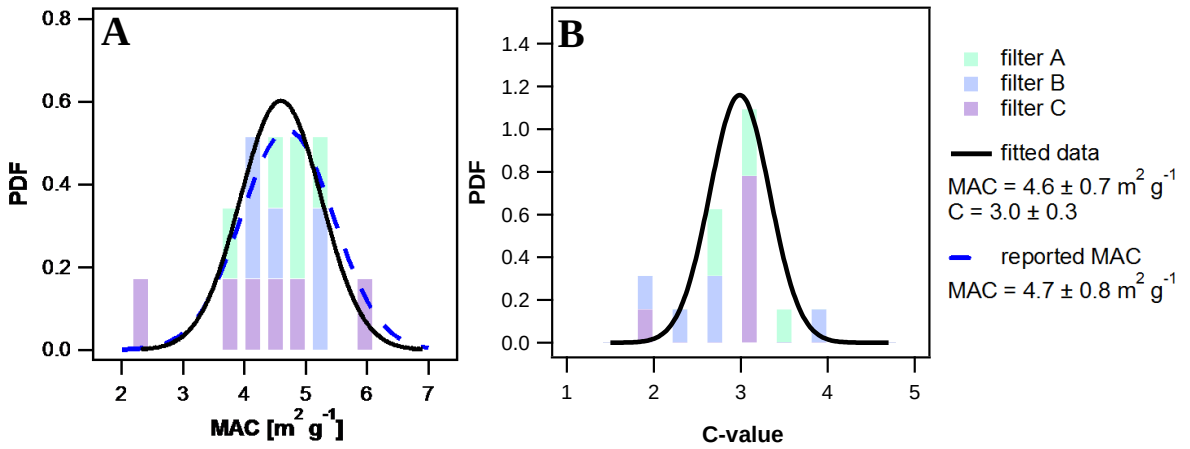

Figure S2: (A) Probability density function (PDF) comparing the MAC values determined by normalizing MWAA absorption measurements of offline primary (filter A), slightly aged (filter B: Aged1) and aged (filter C: Aged2) samples to EC (EUSAAR2) measurements of the same samples (bold line). A literature value for pure BC is also shown (Bond et al., 2006) (dashed blue line). (B) PDF comparing aethalometer attenutation measurements at 880 nm and MWAA absorption measurements at 850 nm to retrieve the aethalometer C value.

15. L332: Not only wood combustion, but really any aerosol if it is assumed that the true MAC for BC at 880 nm is ~4.7 m2/g.

We agree with the reviewer. We specify wood burning because it is the focus of our study. This section has been substantially modified and this sentence was removed.

16. L336: This seems circular to me, if the authors are using C = 3 in coming to this conclusion. This is demanded through the various inequalities.

We do not think that the math here is circular. Below, we present in bullet points the approach followed:

- $\sigma_{ATN} = MAC_{BC} * C$
- The Aethalometer provides b_{ATN}
- We determine a C value of 3 from Equation 1 of the paper:

$$C = b_{ATN,AE33} / b_{abs,MWAA}$$

- We determine a MAC_{BC} of 4.6 $m^2 g^{-1}$ by a fit through $b_{abs,MWAA}$ and EC thermo-optical measurements for primary and aged filter samples.
- We have therefore determined the two variables required to calculate σ_{ATN} and determined it as 13.8 $m^2 g^{-1}$.
- We then compare the σ_{ATN} determined by us to the manufacturer value of 12.2 $m^2 g^{-1}$.
- We then concluded that while the factory default $b_{abs}(\lambda)$ has a substantial bias the eBC mass determined using default σ_{ATN} is consistent with the EC mass. We have rewritten Section 4.1, as quoted at the beginning of this response, to clarify this reasoning.

17. Fig. S5 must indicate which studies are being used to define the literature bounds, and also note that this is not the entire range of reported values over the many papers on this topic. This is a subset of values. Consider e.g. (*Lewis et al.*, 2008) or (*Liu et al.*, 2013). The authors have selected a very narrow subset of literature results to present here, and to reference in the text.

While we agree with the reviewer here, one reason that we have not cited e.g. Lewis et al (2008) is that those authors did not experiment on log-wood burning in a modern stove but rather simulated wildfires. Considering the very low emphasis placed on Fig. S5 in our manuscript, and the importance of avoiding confusion between log-wood burning and wildfire burns, we have simply removed the α ranges in Fig. S5 is only for primary biomass burning emissions. We have also modified the legend to show the two wavelengths of α.

18. Fig. 3: It is not clear why the data in Fig. A do not overlap with the data in Fig. B. Presumably the data in figure B evolved from the data in Fig. A. Also, in Fig. A it is not clear if each point is for one experiment or whether the variability in f_OA is due to variability within an experiment.

Fig. 3A refers to primary emissions and Fig. 3B refers to secondary emissions (as indicated in the caption), so yes, the presumption here was correct, but only partially. More data are included in Fig. 3A because not all burn experiments were aged. This information has been added to the figure caption. In Fig. 3A each point represents an experiment; therefore the variability in f_{OA} is due to the variability in emission composition between experiments. Meanwhile, in Fig. 3B the variability in f_{OA} is due to SOA formation with aging; data from several experiments are shown which explains the wide range of f_{OA} at low OH exposures. Based on the reviewer comment, we have added the following clarifications to the Fig. 3 caption:

> *Figure 3: (A) Relationship of α_{BC+POA} (λ, 880nm) to f_{OA} for seven wavelengths for primary emissions. Data are colored by the wavelength. Curves are fits of Equation 13 to the data. Each point represents the average of one experiment and therefore the variability in f_{OA} is related to the variability in the emission composition between experiments. (B) Relationship of $\alpha_{BC+POA+SOA}$(370nm, 880nm) to f_{OA} for several experiments for aged aerosols. Data are color coded by the OH exposure. The variability in f_{OA} is due to SOA formation with aging; data from several experiments are shown which explains the wide range of f_{OA} at low OH exposures. Note that more data are included in A than B, as primary emissions for some experiments were not aged.*

19. L344: I do not dispute that the AAE values increase with f_OA. However, it is evident that as wavelength decreases the difference from AAE = 0.9-1.1 and the observations increases. This is not clear from the discussion here.

We have stated that the AAE values at low f_{POA} are close to those reported for pure BC. We note that for λ = 660 nm, the AAE value extrapolated at f_{POA} = 0, is equal to 1.04, while for all other wavelengths the value is statistically similar, equal to ~1.2. It can be seen from Fig. 4 that $MAC_{BC}(\lambda)$ profile can be clearly described by a power law, consistent with a constant AAE. To avoid confusion, we have modified the text as follows:

> L344. *The $\alpha(\lambda, 880nm)$ is slightly higher than that of pure BC (~1.2; Bond et al., 2013; Zotter et al., 2017) for small f_{POA}, while increasing f_{POA} corresponded to a distinct increase of $\alpha(\lambda, 880nm)$.*

20. L346: The range reported is inconsistent with what is shown in the graph.

The range presented before denoted the P10 and P90; we apologize that we have forgotten to mention this in the text. Based on the reviewer comment and to avoid confusions we have replaced the [P10-P90] by the total range:

> *The f_{POA} ranges from **0.12 to 0.63**, which is lower than f_{POA} reported for open burning emissions (e.g., f_{POA}~0.75, Ulevicius et al (2016)), because our wood-stove emissions feature a more efficient combustion.*

21. L350: this could be strengthened simply by showing a graph of the observations as a function of wavelength, and showing that a single AAE value does not provide for a good fit.

This is shown in Fig. S5 of the SI. We have added in the corrected version of the manuscript a reference to Fig. S5 and modified the figure caption to highlight the point raised by the reviewer as follows:

> *Figure S5: Absorption coefficients of fresh wood burning emissions measured using an aethalometer normalized to the eBC mass as a function of wavelength. In the legend each color denotes the α_{BC+POA}(370nm,880nm) for an individual experiment. The dashed lines mark the absorption profiles calculated using the literature range of α values obtained for primary biomass burning emissions. The observed absorption spectra have steeper gradients with decreasing wavelength compared to the lines of constant alpha. The systematic decrease in $\alpha(\lambda, 880nm)$ with increasing λ reflects the more-efficient light absorption by BrC at shorter wavelengths (Moosmüller et al., 2011), and shows that the power law wavelength dependence is an inaccurate oversimplification for this mixed aerosol.*

We have added the following in the text in L350:

> *As illustrated in Fig. S5, the observed absorption spectra have steeper gradients with decreasing wavelength compared to the lines of constant alpha. Such systematic increase in $\alpha(\lambda, 880nm)$ with decreasing λ reflects the more-efficient light absorption by BrC at shorter wavelengths (Moosmüller et al., 2011), and shows that the power law wavelength dependence is an inaccurate oversimplification for this mixed aerosol.*

22. Fig. 2: For consistency, it would be helpful if the color scale were labeled as f_OA, similar to Fig. 3 and the text.

This has been modified in the corrected version of the manuscript:

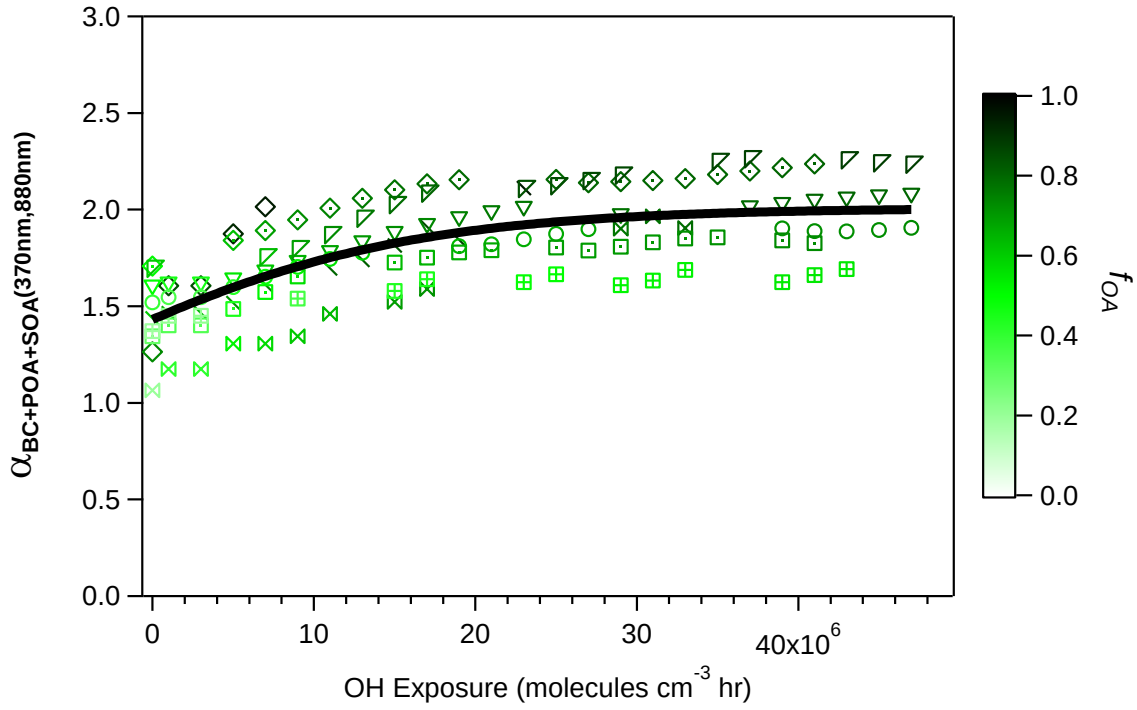

23. L356: Looking at Fig. 3B, it is not clear that this is generally the case. The highest f_OA in Fig. 3B does not have the highest AAE. Perhaps the authors mean this just for the high OH exposures. If so, they might consider plotting AAE vs. f_OA for subsets of data binned according to OH exposure. But, as presented, it is not evident that this is a fully general conclusion.

We do mean at higher OH exposures. This has been added in the corrected version of the manuscript:

> *Also, note in Fig. 2 that at highest OH exposures, the highest $\alpha_{BC+POA+SOA}$(370nm, 880nm) were reached, on average 1.8, during experiments where the fOA was highest.*

24. L362: While I don't necessarily disagree with this point, I will reiterate that the relationship between Fig. 3A and 3B is not clear. The authors give a dashed curve, but it is not clear how, for example, the data in Fig. 3B that start at such low AAE values at high f_OA values come from Fig. 3A. A stronger connection needs to be made to make this clearer

We think that the misunderstanding comes from the fact that we had not adequately highlighted that not all experiments in Fig. A are shown in Fig. B, as for some of the experiments the emissions were not aged. We chose to represent use all the data available in Fig. A to increase our statistics and expand the f_{OA} range. As mentioned above this information has been added and the Figure caption now reads as follows:

> *Figure 3: (A) Relationship of α_{BC+POA} (λ, 880nm) to f_{OA} for seven wavelengths for primary emissions. Data are colored by the wavelength. Curves are fits of Equation 13 to the data. Each point represents the average of one experiment and therefore the variability in f_{OA} is related to the variability in the emission composition between experiments. (B) Relationship of $\alpha_{BC+POA+SOA}$(370nm, 880nm) to f_{OA} for several experiments for aged aerosols. Data are color coded by the OH exposure. The variability in f_{OA} is due to SOA formation with aging; data from several experiments are shown which explains the wide range of f_{OA} at low OH exposures. Note that more data are included in A than B, as primary emissions for some experiments were not aged.*

25. L364: For the data in Fig. 3B, extrapolation to f_OA -> 0 for wavelengths < 600 nm suggests an AAE ~1.2- 1.3, larger than the 0.9-1.1 range the authors have taken for BC. This is consistent with the derived MAC(370) = 13.7 m2/g for BC, given the value at 880 nm. There is, however, a bit of an inconsistency with how the authors compare with Bond. They state that 13.7 is within the 95% confidence interval of the 11.1 m2/g value reported by Bond. But, they have also stated that the AAE = 0.9-1.1. If this is the case, then isn't the range actually narrower? Really, my question here is about the consistency of the statistical interpretation/uncertainty representation.

We thank the reviewer once again for raising opportunities for clarificating the text, where some of the information were missing. The range of $MAC_{BC}(370)$ we calculate is based on an error propagation calculation considering not only the range of AAE reported (0.9-1.1) but also the errors on the absolute $MAC_{BC}(520)$. This has now been clarified in the text:

> *The obtained fit value of $MAC_{BC}(370nm)$ was 13.7 m^2 g^{-1} (GSD 1.1, one-sigma uncertainty 12.4—15.1 m^2/g), higher but not statistically significantly different from the range estimated based on Bond et al. (2013), considering the uncertainties on both the α_{BC} values and the $MAC_{BC}(520nm)$.*

26. Fig. 7: I find the legend to be incomplete in that it leaves the reader thinking that the Lu and Saleh measurements are from methanol extraction, which they are not. Also, for Saleh (2014), the authors do not at all make clear that the Saleh measurements are at 550 nm, not 370. This is not a fair comparison. Neither is which fuel type of Saleh's has been considered. The authors should provide a fuller picture. Also, the Saleh reference is missing from the bibliography.

Thank you for pointing out the missing reference. The Saleh et al. (2014) data in Fig. 7 were extrapolated to 370 nm using the wavelength dependence of k_{OA} i.e. $k_{OA} = k_{OA,550} \times (550 / \lambda)^{w}$, given by those authors. Likewise, the Lu et al., 2015 data have also been determined at 370 nm using the wavelength dependence of k_{OA} provided by the authors ($k_{OA} = 0.017 \times (550 / \lambda)^{1.62}$) and the parameterization of k_{OA} against BC/OA ratio. We have updated the figure legend and caption according to the reviewer comment:

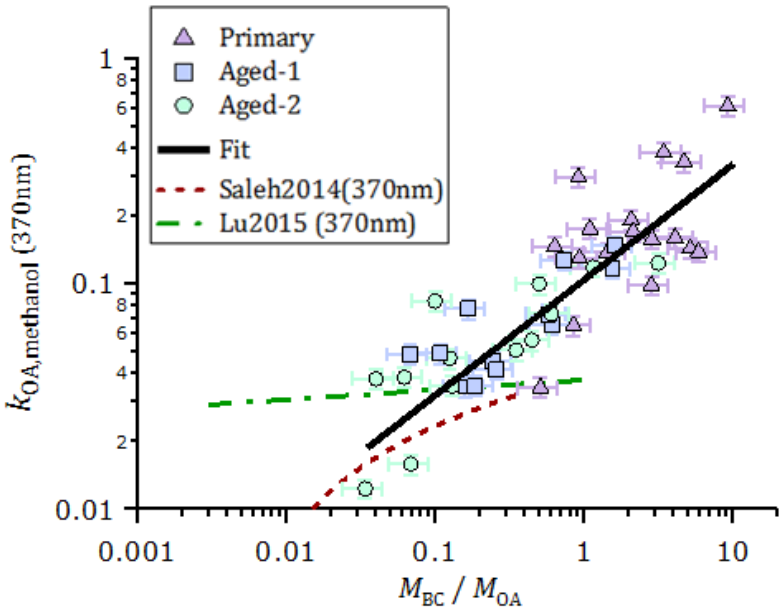

Figure 7: Imaginary part of the OA refractive index at 370 nm, obtained from offline UV/vis spectroscopy of methanol OA extracts, plotted as a function of f_{OA}*. The data could be empirically represented by a linear function in the log-log space, in the measurement range. The ordinary least-squares fit is* $(k_{OA,nm}) = \log(M_{BC}/M_{OA})(0.51\pm0.07) + (-0.98\pm0.05)$*. Also shown are parameterizations of* $k_{OA}(370\text{nm})$ *for open burning against* M_{BC}/M_{OA} *estimated based on the online* $k_{OA}(550\text{nm})$ *measurements in Saleh et al. (2014) and Lu et al. (2015), using the* k_{OA} *wavelength dependence reported by the respective authors.*

Reference added:

Saleh, R., Robinson, E. S., Tkacik, D. S., Ahern, A. T., Liu,S., Aiken, A. C., Sullivan, R. C., Presto, A. A., Dubey, M. K., Yokelson, R. J., Donahue, N. M., and Robinson, A.L.:Brownness of organics in aerosols from biomass burning linked to their black carbon content, Nat. Geosci., 7, 2–5, doi:10.1038/ngeo2220, 2014.

27. Fig. S7: It is not clear why the propagated uncertainty in the AAE increases with wavelength or f_OA. The AAE is a measured quantity that depends only on the measured absorption at two wavelengths. . Why would uncertainty in absorption depend on f_OA? And are the authors saying that the uncertainty in absorption increases with wavelength? Uncertainty in the AAE should directly propagate from Eqn. 10, which is independent of f_OA. Perhaps I am misunderstanding?

We believe that there is a misunderstanding. Fig. S7A is obtained from the error propagation of equation 13 solved for different wavelengths, using the geometric mean and standard deviation of $MAC_{POA}(\lambda)$ and $MAC_{BC}(\lambda)$. The resulting error term represents the variability in/ the confidence level on the $\alpha(t_0, \lambda, 880nm)$ at different wavelengths. Equation 13 is expressed below:

$$\alpha(t_0, \lambda, 880nm) = \alpha_{\mathrm{BC+POA}}(t_0, \lambda, 880nm)$$

$$= \frac{1}{\ln(880\mathrm{nm}/\lambda)} \ln\left(\frac{\mathrm{MAC_{BC}}(t_0,\ \lambda)}{\mathrm{MAC_{BC}}(t_0, 880nm)} + \frac{M_{\mathrm{OA}}(t_0)\mathrm{MAC_{POA}}(t_0, \lambda)}{b_{\mathrm{abs}}(t_0, 880nm)}\right)$$

As $\alpha(t_0, \lambda, 880nm)$ depends on $\mathrm{M_{OA}}/b_{\mathrm{abs}}(t_0, 880nm)$ $\sigma_{\alpha(t_0,\lambda,880nm)}$ also does. We expressed $\mathrm{M_{OA}}/b_{\mathrm{abs}}(880nm)$ as f_{OA}, using σ_{ATN} to estimate EC mass from $b_{\mathrm{ATN}}(880nm)$.
The image plot in panel B shows that at short wavelengths and low fractions of OA, the confidence level on α is within 0.1. However, with increasing f_{OA}, and at longer wavelength the uncertainty in predicting α increases. The idea behind this figure is to provide an error on the predicted α when the $f_{OA}$is extrapolated to values higher than measured here (typical of open burning).

We have updated the figure caption adding the explanations above:

> *Figure S7: Analysis of the fitting errors of $\alpha(\lambda, 880nm)$ of primary emissions as a function of f_{OA}. Panel A shows the α residual as a probability density function. Panel B is an image plot of the $\alpha(\lambda, 880nm)$ error, $\sigma_{\alpha(t_0,\lambda,880nm)}$, as a function of f_{OA} at different wavelengths. $\sigma_{\alpha(t_0,\lambda,880nm)}$ is obtained from the error propagation of Eq. (13) solved for different wavelengths, using the geometric mean and standard deviation of $MAC_{POA}(\lambda)$ and $MAC_{BC}(\lambda)$. This error term represents the variability in or the confidence level on the $\alpha(t_0, \lambda, 880nm)$ at different wavelengths. As $\alpha(t_0, \lambda, 880nm)$ depends on $M_{OA}/b_{abs}(t_0, 880nm)$ in Equation 13, $\sigma_{\alpha(t_0,\lambda,880nm)}$ also does. We expressed $M_{OA}/b_{abs}(t_0, 880nm)$ as f_{OA},, using σ_{ATN} to estimate EC mass from b_{ATN}(880nm). At short wavelengths and low OA fractions, the confidence level on α is within 0.1. However, with increasing f_{OA}, and at longer wavelength the uncertainty in predicting α increases.*

28. L384: A larger GSD does not necessarily mean a larger uncertainty. This could be variability that is independent of uncertainty. I do not regard this as a true assessment of "uncertainty." It is only an assessment of variability. The authors should, however, consider uncertainties explicitly.

The reviewer is correct, the word "variability" rather than "uncertainty" should have been used in this sentence. That is, the GSD values relate to variability in the MAC values that is not explained by the variability in f_{OA}. Overall, our data show that this variability is related to a real change in the chemical nature of the compounds present and their intrinsic absorptivity, as online MAC values correlate well with k_{OA} values independently measured offline after methanol extraction. As mentioned above, we have now added a new section discussing the quantifiable and unquantifiable uncertainties. We have also updated the related to the variability in the determined parameters as follows:

> ***Uncertainties and variability in MAC_{BC}, MAC_{POA} and MAC_{SOA}.*** *Table 1 shows the fitting errors related with $MAC_{BC}(\lambda)$, $MAC_{POA}(\lambda)$ and $MAC_{SOA}(\lambda)$, arising from our measurement precision and experimental variability. These fitting errors are greater than our estimated uncertainties in the absorption coefficients measured by MWAA (10%), and comparable to our estimated uncertainty in OA mass measured by AMS (30%). The residuals in the fitted $MAC_{BC}(\lambda)$ are relatively low (< 10%), increasing with decreasing λ. By contrast, the uncertainties in the fitted $MAC_{POA}(\lambda)$ are much higher (GSD = 1.2–1.5) and increase with increasing λ. The relative residuals between the measured and fitted α(λ,880nm) for primary emissions showed a mean bias and RMSE of 0.07 and 0.13, respectively (Fig. S7), indicating that our fitted MAC results provide a good description of the data set. $MAC_{SOA}(\lambda)$ values determined were highly variable between experiments with a GSD = 1.39 and 2.42 for λ=370 nm and 660 nm, respectively. In Fig. S10, we show the distribution of $MAC_{SOA}(\lambda)$ values as box and whiskers against OH exposure, showing no particular dependence of these values with aging as it will be discussed below. Therefore, we expect the fitting errors in MAC_{SOA} and of MAC_{POA} to be mainly related to true changes in the organic aerosol chemical composition between different burns, since the variability of $MAC_{BC}(\lambda)$ was relatively small. In Section 4.3, we discuss this variability further using the results of an additional and independent analysis.*

29. L386: Given that the authors show distributions and fits for the AAE, it would seem appropriate to also show similar for the MAC_POA and MAC_SOA so that the reviewer can judge. Given the width of the SOA distribution, is a normal fit even appropriate? (Probably not, in a fundamental sense, since MAC values cannot be < 0. But perhaps a normal distribution is appropriate in a practical sense.)

The MACs of primary species (POA and BC) at different wavelengths are obtained through fitting equation 13, which used the AAE as dependent variable. Therefore, we have assessed the model goodness of fit by showing the residuals in the AAE values (Fig. S7). While we cannot show the residuals distributions for MAC_{POA} and MAC_{BC} resulting from the fit, the obtained fitting errors (GSD) can be used to represent these distributions. The normal fit of the AAE residuals in Fig. S7A serves only to illustrate the distribution of fitting errors and is not essential to our analysis. We note that we have never claimed that MAC values to be normally distributed and hence we performed our fits in log-transformed space to constrain the MAC to be greater than zero. MAC_{SOA} is the only unknown parameter in equation 19. Therefore, we have shown the distributions of MAC_{SOA} as a function of wavelength and OH exposure, in Fig. 4 and 5, respectively.

30. L398: The authors should provide the resulting uncertainties, or at least ranges, based on the multivariate analysis, for the AAE values.

The ranges for AAE values have been already provided in Fig. S9 and Table S1, and following the reviewer's comment we have added the following to the main text:

> *"This yielded αBC = 1.2, […], with corresponding uncertainties of approximately 20% (complete details of the uncertainties are provided in Table S1)."*

31. L402: I suggest removing the "this is the first study" statement. Saleh (2014) reported very closely related "w" values, from which AAE values can be calculated, for SOA from biomass burning.

The new sentence reads as follows:

> *The high α values obtained for the organic fractions are consistent with previous measurements for BrC containing POA (e.g. Chakrabarty et al., 2010, 2013).*

32. Fig. S10: I find that the use of the log scale for the y-axis makes it difficult for the reader to see what sort of changes did/did not occur. Variability in the AAE over so many orders of magnitude is not expected, but a factor of 2 would be reasonable. Thus, a linear scale should be used.

In response to the reviewer comment, we have modified the figure to better illustrate the variability in our data.

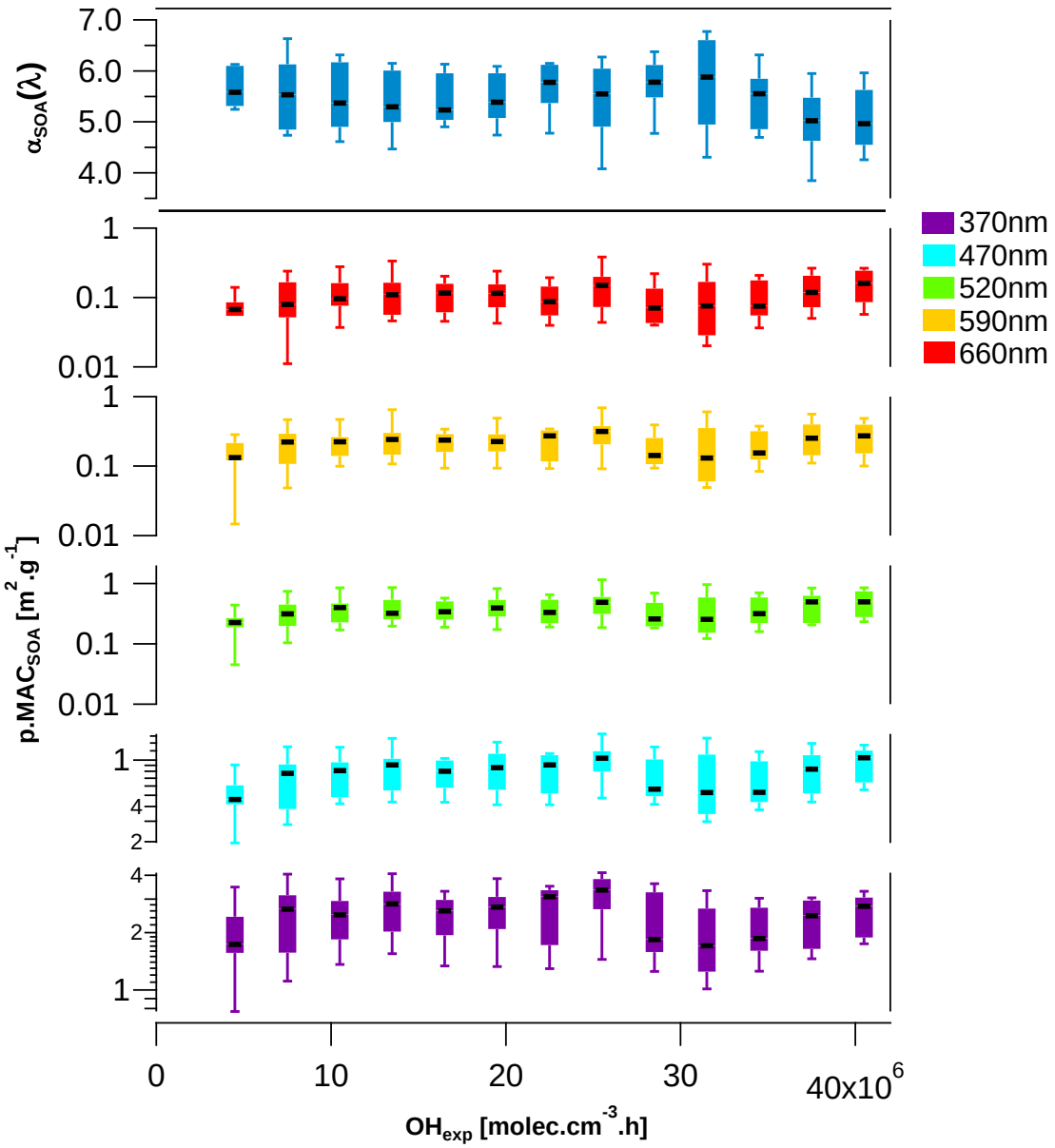

33. L424: In Fig. S13, and Fig. 6, it is unclear why the authors fit only the "aged" data. Why exclude the primary, especially in Fig. S13? Because the relationship is visibly much worse? This goes to the statement about sensitivity to Mie calculations.

We apologize; this information went missing during revisions of an earlier manuscript draft. We excluded the primary because our assumption of particle sphericity inherent in the Mie calculations is generally more likely to be violated for fresh than for aged combustion particles. Similarly, our interpretation of the SMPS-measured mobility diameter as representative of a physical particle diameter is violated in the presence of fractal-like soot particles, which have a shape factor significantly different from unity.

The variability in our primary results is interpreted as illustrating directly the impact of this variability on our analysis. This variability will reflect differences in burn conditions as well as the chaotic impacts of the combustion process (for example, uncontrolled differences between time spent in pre-ignition [where most OA is emitted] versus flaming phases [where most BC is emitted], between the physical distribution of flames during each burn, etc.).

In spite of these simplifications, the fresh data in Fig. 6 generally fall on the best-fit line for the aged data. The fact that they fall on the best-fit line is a direct demonstration of the magnitude of the uncertainties in our retrieved OA MAC.

We have revised the figures and captions for clarity. The revised figures are:

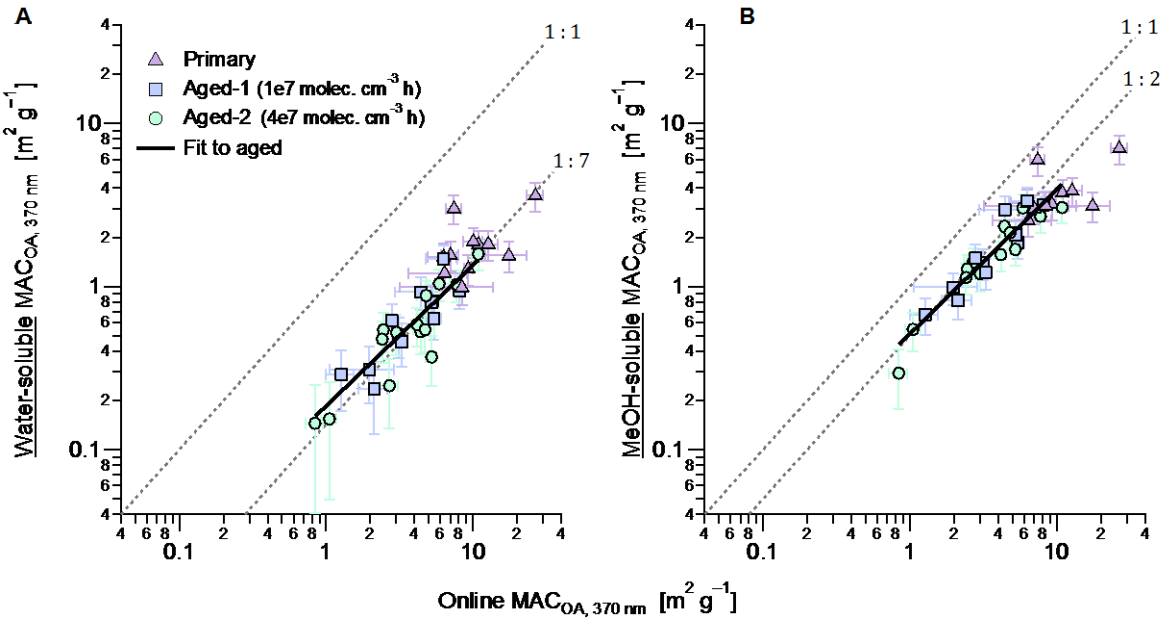

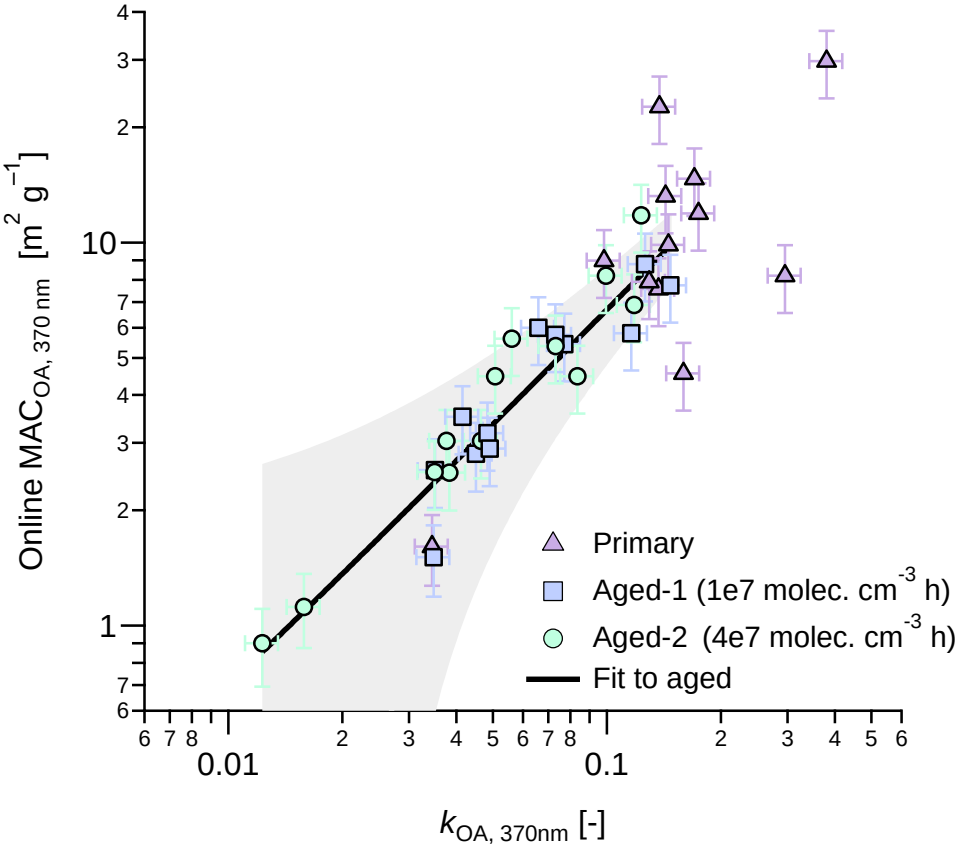

We modified the text:

L431. *The data in Fig. 6B show that the methanol extracts correspond to a MAC about 50% smaller than the online data. The scatter in the data is significantly reduced for the aged data (note that, in this analysis, aged OA refers to the sum of POA and SOA, since the reported values represent all OA after aging). This reduced*

scatter is expected, considering that aging is likely to result in more-spherical particles. We have assumed particle sphericity when interpreting the SMPS data and performing the Mie analysis. While the propagation of quantifiable uncertainties leads to an error estimate of ~25%, considering the simplifiations that were necessary for the Mie analysis, we consider a 50% closure to be an adequate agreement. Despite this, we cannot exclude additional methanol insoluble brown carbon. Conversely, the fit in Figure 6A indicates that the apparent MAC of water-soluble species was a fourth of the respective methanol MAC, according to the slope of only 12 ± 3%. Only the aged data have been fit to illustrate this point. This strong disagreement shows that the BrC in our samples was hardly water soluble, even for the most aged samples. As we expect that the majority of OA in our samples formed by wood pyrolysis (Di Blasi, 2008; Corbin et al., 2015b; Shafizadeh, 1984), we can compare our results directly to those of Chen and Bond (2010), who also found that primary wood-pyrolysis BrC was water insoluble. Moreover, the water-insoluble nature of the light absorbing components of SOA is in line with the results by Bruns et al. (2016) who showed that SOA precursors during these experiments were predominantly aromatic compounds.

We modified the Figure 6 caption:

Figure 6: Comparison of the MAC_{OA}(370nm) of aged aerosols determined from online and offline absorption measurements. The offline filter-extraction method directly quantified properties of total OA (ordinate), while the average of MAC_{SOA} and MAC_{POA} weighted with respective mass concentrations is shown on the abscissa. The panels show offline measurements of (A) water-soluble OA, (B) methanol-soluble OA. Fits are to aged data only due to the significantly smaller scatter of those data, although primary data on average follow similar trends. The fitted slopes and intercepts are, respectively, (A) 0.13 ± 0.02 and 0.05 ± 0.06 m^2g^{-1} and (B) 0.12 ± 0.1 and 0.38 ± 0.03 m^2g^{-1}.

We modified the Figure S13 caption:

Figure S13: MAC_{OA} at λ = 370 nm calculated from aethalometer measurements vs. k_{OA} at λ = 370 nm from the UV/visible measurements of the methanol extracts. The shaded region shows the 90% confidence interval of a weighted orthogonal regression (slope 66 ± 9 m^2g^{-1}, intercept 0.0 ± 0.3 m^2g^{-1}) to illustrate the relatively small range of variability in the data for aged samples.

34. L427: Fig. 6 normalizes out any uncertainty/variability in the measured [OA], because both absorption values are normalized by this. Fig. 4, in contrast, does not. How can the authors rule out the possibility that there is not some variability in the measurement of OA between burns, perhaps dependent on particle shape or variability in bounce in the AMS (which can differ between POA and SOA)?

Fig. 4 actually does normalize the absorption by [OA], so we are not sure which figure the reviewer had in mind. Our goal with Fig. 6 is to relate the offline and online absorption measurements, in such a way that any unknown uncertainties would influence scatter in the plot.

The bounce-related collection efficiency of the AMS was concluded as close to 1.0 for wood-burning OA in the literature reviewed by Corbin et al. (2015b; in their Section S1.2). From recent results from our group using a similar setup, we have measured with an AMS primary organic aerosol rich emissions from smoldering biomass and found the POA collection efficiency to be close to 1.

We reanalyzed our SMPS, AMS, and eBC (MWAA-calibrated AE33) data for the present study by fitting the SMPS mass (predicted with a density of 1.5 g/cm3) against the total PM mass predicted as AMS OA + eBC. The 95% CI of the slope of this fit corresponds to a CE of 0.7-1.0 (relative 19% relative uncertainty), consistent with the literature cited above. Combining this 19% uncertainty (slope uncertainty) with the 30% uncertainty already assigned to the AMS OA (largely reflecting uncertainties in RIE) in quadrature results in a 36% uncertainty in AMS OA, which we have updated in the text.

Shape-related collection efficiency issues in the AMS are unlikely as such issues mainly come into play when transmission through the AMS lens is considered. That is, shape itself is not an issue in the AMS except as it affects aerodynamic diameters (DeCarlo et al., 2014). In our study, particles were large enough that transmission and therefore shape-related issues were minor.

We modified the text:

> L94. *Uncertainties related to particle collection efficiency in the AMS are considered negligible for the relatively-large particles sampled here, which in terms of volume are within the size range transmitted efficiently by the AMS aerodynamic lens (Liu et al., 2007). The collection efficiency of wood-combustion OA is expected to be unity (Corbin et al., 2015b).*

References:

Corbin, J. C., Keller, A., Lohmann, U., Burtscher, H., Sierau, B. and Mensah, A. A.: Organic emissions from a wood stove and a pellet stove before and after simulated atmospheric aging, Aerosol Sci. Technol., 49(11), 1037–1050, doi:10.1080/02786826.2015.1079586, 2015b.

DeCarlo, P. F., Slowik, J. G., Worsnop, D. R., Davidovits, P., and Jimenez, J. L.: Particle morphology and density characterization by combined mobility and aerodynamic diameter measurements. Part 1: Theory, Aerosol Sci. Technol., 38, 1185– 1205, 2004.

Liu, P. S. K., Deng, R., Smith, K. A., Jayne, J. T., Williams, L.R., Canagaratna, M. R., Moore, K., Onasch, T. B., Worsnop, D.R., and Deshler, T.: Transmission efficiency of an aerodynamic focusing lens system: comparison of model calculations and laboratory measurements for the aerodyne aerosol mass spectrometer,Aerosol Sci. Tech., 41, 721–733, 2007.

35. L432: This 46% must state that it is for aged OA only. It remains unclear to me why the primary is excluded.

This statement was removed following comment #33.

36. L440: Is this a fair comparison, given that the authors have focused on the aged OA?

This comment is deprecated following our response to comment #33, but we would also like to point out that we did point out in the text that Chen and Bond studied primary and not aged OA.

37. L431: Are these fits forced through zero?

No fits in this work were forced through zero, but all intercepts were not significantly different from zero. We acknowledge that it is our responsibility to report those intercepts clearly and have updated the text where fits are still reported (the present fits are no longer discussed, see response to comment 33).

38. L441: The authors seem to be implying that SOA formed from oxidation of aromatic precursors is not especially water soluble, or at least less soluble than in methanol. The authors might consider citing e.g. (*Zhang et al.*, 2011), to strengthen this argument.

Thank you, we have added this citation in the corrected version of the manuscript.

Reference:

Zhang, X., Lin, Y. –H., Surratt, J. D., Zotter, P. and Prévôt, A. S. H.: Light-absorbing soluble organic aerosol in Los-Angeles and Atlanta: A contrast in secondary organic aerosol, Geophys. Res. Lett, 38, 2011.

39. Fig. 7: As already noted above, I find the comparison here insufficient. Saleh et al. (2014) and Lu et al. (2015) report values not at 370 nm. This is unclear. Also, the line shown for Lu et al. (2015) appears to be incorrect. See their Fig. 1D. Further, and importantly, the Lu et al. (2015) data are largely, although not entirely, derived from the Saleh measurements. Thus, they are not really an independent assessment.

We have replied to comment #26 about the data in Fig. 7 and we think we have addressed all the points raised by the reviewer in this question. We acknowledge that the Saleh and Lu data sets are not entirely independent, but have treated the corresponding parameterizations as independent for lack of any method to disentangle their interdependence. We expect other studies to cite Saleh and Lu's separately. Note that we have not focused on the more comprehensive Lu data set because the Saleh dataset represents biomass burning specifically, which we have also studied in the present work.

Figure 7: Imaginary part of the OA refractive index at 370 nm, obtained from offline UV/vis spectroscopy of methanol OA extracts, plotted as a function of $\boldsymbol{fOA}$*. The data could be empirically represented by a linear function in the log-log space, in the measurement range. The ordinary least-squares fit is* $(\boldsymbol{k_{OA,nm}}) = \boldsymbol{\log(M_{BC}/M_{OA})(0.51\pm0.07) + (-0.98\pm0.05)}$*. Also shown are parameterizations of* $\boldsymbol{k_{OA}(370}$*nm) for open burning against* M_{BC}/M_{OA} *estimated based on the* $\boldsymbol{k_{OA}(550}$*nm) measurements in Saleh et al. (2014) and Lu et al. (2015), using the* $\boldsymbol{k_{OA}}$ *wavelength dependence reported by the respective authors.*

We have also updated the text at line 460:

The parameterizations reported by these authors are included in Fig. 7, where the wavelength dependence reported by those authors has been used to adjust their parameterizations to 370nm.

40. Fig. 7: The logic of a linear fit to the observations is not clear to me. The authors have argued that the SOA is absorbing, and differently absorbing than the POA. If I use the equation given and extrapolate towards M_BC/M_OA - >0, the k_OA -> 0. If the SOA is absorbing, and if SOA formation drives the decrease in the M_BC/M_OA, then the limiting value of k_OA should be equal to the value for k_SOA. As such, the provided fit does not seem appropriate and requires justification. Some of this may be experiment-to-experiment variability. But the limiting case issue remains.

We do agree with the reviewer that k_{OA} will likely tend towards k_{POA} and k_{SOA} when M_{BC}/M_{OA} is very large and very small, respectively. However, within the range covered, a line is the simplest model which can describe our data adequately and the linear fit used is simply empirical. We do not aim to include a complete physical interpretation in this simple fit With our fit in Fig. 7, we mainly wish to emphasize that k_{OA} can be described as a function of M_{BC}/M_{OA} only. For clarification we have modified the figure caption as follows:

> *Figure 7: Imaginary part of the OA refractive index at 370 nm, obtained from offline UV/vis spectroscopy of methanol OA extracts, plotted as a function of* $\boldsymbol{fOA}$*. The ordinary least-squares fit is* $\boldsymbol{\log(k_{OA,370nm}) = \log(M_{BC}/M_{OA})(0.51\pm0.07) + (-0.98\pm0.05)}$ *and illustrates that the observed* k_{OA} *can be described as a function of* M_{BC}/M_{OA} *with reasonable accuracy, regardless of the degree of aging. Also shown are parameterizations of* $\boldsymbol{k_{OA}(370nm)}$ *for open burning against* M_{BC}/M_{OA} *estimated based on the online* $\boldsymbol{k_{OA}(550nm)}$ *measurements in Saleh et al. (2014) and Lu et al. (2015), using the* $\boldsymbol{k_{OA}}$ *wavelength dependence reported by the respective authors.*

41. Fig. 7: The authors should be able to, from their observations and within their assumptions, calculate M_POA/M_SOA. They might consider plotting k_OA vs. this ratio instead of versus M_BC. These will be related, of course, since the authors assume POA is proportional to BC during aging for a given experiment.

We agree, however, we do not think that this calculation will shed any new insights into our data set. In Fig. 7, we have only chosen to use M_{BC}/M_{OA} as an abscissa because previous studies have used this quantity; our goal in Fig. 7 is a comparison of our results with related literature. We do not find this ratio to be particularly meaningful or interesting physically, but we acknowledge that future studies are likely to measure it as well and so it provides a useful basis for comparison.

42. The origin of these "uncertainties" is unclear. They are explained later for f_OA, but for the MAC values it is not abundantly clear.

We apologize but we do not see which part of the manuscript the reviewer is referring to. We assume that the reviewer is referring to the fitted MAC values, which we have commented on above and adjusted the manuscript to include.

43. L486: This statement regarding mass yields of SOA requires much further detail.

The analysis of SOA gas phase precursors has been thoroughly presented in Bruns et al. (2016) and the discussion about SOA yields is beyond the scope of this study. As this statement is not required for the understanding of the paper we have removed it in the corrected version of the manuscript. The section now reads as follows:

> *The $M_{SOAP,WLC}/M_{POA,WLC}$ was on average equal to 7.8 (GSD = 1.4) and kOH was estimated as 2.7×10^{-11} molecule^{-1} cm^3 (GSD = 1.4), consistent with the SOA precursors chemical nature measured (e.g. PAH and phenol derivatives) by a proton-transfer-reaction mass spectrometer (PTR-MS) (Bruns et al., 2016, 2017). These high rates and enhancement ratios indicate the rapid production of SOA.*

44. L512: A note about terminology. I am not certain that "error analysis" is appropriate here. Variance in the POA fraction is not "error." It is variability. A substantial aspect of this "error analysis" is really just a "sensitivity analysis." I suggest that the authors limit the term "error analysis" to when they are truly considering errors, and use some other term when they are considering variability. This is true here and elsewhere.

We agree with the reviewer and have changed the word "error" to "sensitivity".

We have also made the requested modifications related with the section entitled "***Uncertainties and variability in MAC_{BC}, MAC_{POA} and MAC_{SOA}***".

45. L499: The authors should clarify the origin of the solar irradiance data that they have used.

We have now added the reference on which the solar irradiance data are based:

> *Gueymard, C.; Myers, D.; Emery, K. "Proposed Reference Irradiance Spectra for Solar Energy Systems Testing," Solar Energy, 73, 6, 443–467, 2002.*

Production of particulate brown carbon during atmospheric aging of residential wood-burning emissions

Nivedita K. Kumar[1], Joel C. Corbin[1*], Emily A. Bruns[1], Dario Massabó[2], Jay G. Slowik[1], Luka Drinovec[3,4], Griša Močnik[3,4], Paolo Prati[2], Athanasia Vlachou[1], Urs Baltensperger[1], Martin Gysel[1], Imad El-Haddad[1] and André S. H. Prévôt[1]

[1]Laboratory of Atmospheric Chemistry, Paul Scherrer Institute, 5232 Villigen, Switzerland

[2]Department of Physics & INFN, University of Genoa, via Dodecaneso 33, 16146, Genova, Italy

[3]Aerosol d.o.o, Kamniška 41, 1000 Ljubljana, Slovenia

[4]Condensed Matter Physics, Jožef Stefan Institute, 1000 Ljubljana, Slovenia

*Now at National Research Council Canada, Ottawa, Canada

Correspondence to: I. El-Haddad (imad.el-haddad@psi.ch), A. S. H. Prévôt (andre.prevot@psi.ch)

ABSTRACT

We investigate the optical properties of light-absorbing organic carbon (brown carbon) from domestic wood combustion as a function of simulated atmospheric aging. ~~At shorter wavelengths, light absorption by brown carbon from primary organic aerosol (POA) and secondary organic aerosol (SOA) formed during aging was around 10 % and 20 %, respectively, of the total aerosol absorption (brown carbon plus black carbon)~~. At shorter wavelengths (370 – 470nm), light absorption by brown carbon from primary organic aerosol (POA) and secondary organic aerosol (SOA) formed during aging was around 10 % and 20 %, respectively, of the total aerosol absorption (brown carbon plus black carbon). The mass absorption cross-section (MAC) determined for black carbon (BC, 13.7 $m^2 g^{-1}$ (geometric standard deviation GSD = 1.1) at 370 nm) was consistent with that recommended by Bond et al. (2006). The corresponding MAC of POA (5.5 $m^2 g^{-1}$ (GSD =1.2)) was higher than that of SOA (2.4 $m^2 g^{-1}$ (GSD = 1.3)) at

370 nm. However, SOA presents a substantial mass fraction, with a measured average SOA/POA mass ratio after aging of ~5 and therefore contributes significantly to the overall light absorption, highlighting the importance of wood-combustion SOA as a source of atmospheric brown carbon. The wavelength dependence of POA and SOA light absorption between 370 nm and 660 nm is well described with absorption Ångström exponents of 4.6 and 5.6, respectively. UV-visible absorbance measurements of water and methanol-extracted OA were also performed showing that the majority of the light-absorbing OA is water insoluble even after aging.

1. INTRODUCTION

Atmospheric aerosols contribute to radiative forcing either directly by absorbing and scattering light or indirectly by acting as cloud-condensation and ice nuclei. While black carbon (BC) from combustion processes is the most efficient light-absorbing aerosol component, organic aerosols (OA) may also absorb solar radiation (Alexander et al., 2008; Chen and Bond, 2009; Kirchstetter et al., 2004). This light-absorbing OA, denoted as brown carbon (BrC), absorbs most strongly at shorter UV-visible wavelengths (Andreae and Gelencsér, 2006; Hoffer et al., 2005). Global chemical-transport model estimates indicate that the BrC contribution to the positive radiative forcing of climate by anthropogenic aerosols may not be negligible (Feng et al., 2013; Jo et al., 2016; Lin et al., 2014; Wang et al., 2014).

Unlike BC, whose light absorption properties are relatively constant across sources (Bond et al., 2013), BrC is composed of a wide range of largely unknown compounds, which exhibit highly variable spectral dependence and absorption efficiencies. For example, reported imaginary indices of refraction for different organic species, which describe the absorption of these compounds, span two orders of magnitude (Lu et al., 2015). Because it is impractical to experimentally separate BrC from non-absorbing OA, optical properties are typically determined for the bulk OA of a given source. The large variability of BrC fraction in combustion aerosol may contribute to the wide variation in reported properties of BrC containing OA.

Biomass burning OA, which contributes two-thirds of the global budget of directly-emitted primary OA (POA), is expected to be a considerable source of BrC (Chakrabarty et al., 2010; Hecobian et al., 2010; Lack and Langridge,

2013; Liu et al., 2014). The variability in reported light absorption properties of biomass burning OA with fuel type and burn conditions remains a major obstacle complicating its treatment in climate models (Lu et al., 2015; Saleh et al., 2013). Residential biomass burning is typically characterized by a more efficient combustion, than open burning. Residential wood burning represents a substantial contribution to anthropogenic combustion emissions (Bond et al., 2013), especially in urban atmospheres, and is considered the largest source of OA in Europe during winter (Denier Van Der Gon et al., 2015).

Upon photo-oxidation, biomass-burning emissions produce secondary organic aerosol (SOA) at concentrations similar to or exceeding the primary organic aerosol (POA) (Bertrand et al., 2017; Bruns et al., 2015, 2016; Corbin et al., 2015a; Grieshop et al., 2009). There is a growing body of evidence that light absorption by OA change with OH exposure (aging) owing to the production of secondary BrC or to the transformation of primary BrC (Forrister et al., 2015; Heringa et al., 2011; Lee et al., 2014; Zhao et al., 2015). However, these effects have not yet been systematically investigated and must be quantified to assess the climate effects of primary and aged biomass burning OA.

Here, we show that both POA and SOA from residential biomass burning emissions aged in controlled smog chamber experiments contain BrC. Wavelength dependent, mass-normalized absorption cross-sections (MACs) of POA and SOA are presented from online aerosol measurements as a function of aging for the first time. Complementary measurements of filter-extract absorbance (conducted in different solvents) are used to obtain the imaginary refractive index and to investigate the solubility of BrC in fresh and aged OA. While results presented here are related to flaming residential wood combustion emissions and cannot therefore be generalized, the approach used can be extrapolated for the characterization and quantification of the contribution of BrC in other primary and aged emissions.

2. METHODS

2.1 Smog chamber experiments

~~Laboratory measurements were conducted in an 8 m^3 Teflon smog chamber (Bruns et al., 2015; Platt et al., 2013) installed within a temperature-controlled housing. Conditions in the chamber were maintained to represent winter~~

~~time in Europe, i.e. relative humidity ranging between 50 – 90%, at 263 K (Bruns et al., 2015, 2016). Beech wood was combusted in a residential wood stove. Primary emissions were sampled through heated lines at 413 K, diluted by a factor of ~14 using an ejector diluter (DI-1000, Dekati Ltd.), then sampled into the chamber, which provided an additional ten-fold dilution. The overall dilution was a factor of 100 to 200. As we aimed to sample only flaming-phase emissions into the chamber, samples were taken when the modified combustion efficiency (ratio of CO_2 to the sum of CO and CO_2) was > 0.90. Despite maintaining the same combustion conditions, the resulting organic fraction in the different samples was highly variable, indicating that these samples are representative of a mixture of pre-ignition and flaming emissions (with varying contributions of each combustion stage).~~

Laboratory measurements were conducted in an 8 m^3 Teflon smog chamber (Bruns et al., 2015; Platt et al., 2013) installed within a temperature-controlled housing. Conditions in the chamber were maintained to represent winter time in Europe, i.e. relative humidity ranging between 50 – 90%, at 263 K (Bruns et al., 2015, 2016). Beech wood was combusted in a residential wood stove. Primary emissions were sampled through heated lines at 413 K, diluted by a factor of ~14 using an ejector diluter (DI-1000, Dekati Ltd.), then sampled into the chamber, which provided an additional ten-fold dilution. The overall dilution was a factor of 100 to 200. As we aimed to sample only flaming-phase emissions into the chamber, samples were taken when the modified combustion efficiency (ratio of CO_2 to the sum of CO and CO_2) was > 0.90. Despite maintaining the same combustion conditions, the resulting organic fraction to the total carbonaceous aerosols in the different samples was highly variable, indicating that these samples are representative of a mixture of pre- ignition and flaming emissions (with varying contributions of each combustion stage). Finally, the resulting NOx/NMOG ratios, which dramatically influence SOA formation through influencing the fate of peroxy radicals, RO_2, were estimated to be between 0.035 – 0.35 ppm ppm C^{-1} (Bruns et al., 2016). These conditions can be considered as high NO_X representative of urban/sub-urban conditions, where most of the RO_2 radicals react with NO, rather with RO_2/HO_2.

After injection of the primary emissions and stabilization of the concentrations, nitrous acid (HONO) was continuously added, which dissociates upon irradiation (λ<400 nm) and forms the hydroxyl radical (OH). Then, 9-times deuterated butanol sample (butanol- D9, 98%, Cambridge Isotope Laboratories) was subsequently injected into the chamber. The decay of butanol-D9 was used to infer the time-resolved OH exposure of the sampled aerosol (Barmet et al., 2012). The chamber was exposed to UV lights for ~3.5 hours.

Particles were collected onto filters (47 mm Tissue-quartz, Pall Corporation, 26 L min^{-1} for 30-32 min) for offline optical measurements and the determination of elemental carbon (EC) mass. Three filters were collected during each experiment, namely i) a primary aerosol filter sample ("primary"), ii) a slightly aged aerosol ("Aged1", OH exposure ~ $1x10^7$ molecules cm^{-3} h), collected 30 minutes after the UV lights were switched on, and iii) an aged aerosol ("Aged2", OH exposure ~ $4x10^7$ molecules cm^{-3} h), collected at the end of the experiment (see Fig. S1 for the sampling periods). A charcoal denuder was installed upstream of the filter sampler to remove organic gases. Filters were stored at 253K until analysis.

In addition to the characterization of the particle optical properties detailed in the next section, a set of online and offline techniques were used for the characterization of the gaseous and particulate emissions before and after aging. The non-refractory particle size-segregated chemical composition was measured with a high resolution (HR) time-of-flight aerosol mass spectrometer (AMS) (DeCarlo et al., 2006). Uncertainties related to particle collection efficiency in the AMS are considered negligible for the relatively-large particles sampled here, which in terms of volume are within the size range transmitted efficiently by the AMS aerodynamic lens (Liu et al., 2007). The collection efficiency of wood-combustion OA is expected to be unity (Corbin et al., 2015b). Details related to the AMS data analysis and calibration can be found elsewhere (Bruns et al., 2015, 2016). A scanning mobility particle sizer was used to measure the size distribution of the evolving aerosol. Organic gases were monitored by a proton transfer reaction time-of-flight mass spectrometer (PTR-MS, $[H_3O^+]$ reagent ion, Ionicon Analytik GmbH) (Bruns et al., 2017), following the same procedure as in Klein et al. (2016). Additionally, elemental carbon (EC) mass concentration was measured offline using a sunset thermo-optical analyzer, following the EUSAAR2 protocol (Cavalli et al., 2010).

2.2 Optical measurements

Aethalometer. A dual-spot aethalometer (Magee Scientific aethalometer AE33, Aerosol d.o.o.) was used for real-time aerosol light attenuation measurements at seven wavelengths (λ = 370, 470, 520, 590, 660, 880 and 950 nm) (Drinovec et al., 2015). The instrument measures the attenuation coefficient (b_{ATN}) of a light beam transmitted through a filter tape loaded with aerosol samples. The use of the sampling flow (here, 2 L min^{-1}), integration time for the measurement (here, 1 minute), and automated dual-spot loading compensation to obtain b_{ATN} has been described by Drinovec et al. (2015).

The loading compensated b_{ATN} was used to infer the aerosol absorption coefficient, b_{abs}, using a constant wavelength independent correction factor *C*, which accounts for multiple scattering within the filter matrix (Weingartner et al., 2003):

$$b_{\mathrm{abs}}(\lambda) = b_{\mathrm{ATN}}(\lambda)/C \quad (1)$$

As discussed in detail by Corbin et al. (2018), the wavelength-dependence of C can be expected to be negligible. The loading compensated b_{ATN} at 880 nm from the AE33 is further used to infer the equivalent-BC mass concentration, M_{eBC}:

$$M_{\mathrm{eBC}} = \frac{b_{\mathrm{ATN}}(880\ nm)}{\sigma_{\mathrm{ATN}}(880\ nm)} \quad (2)$$

where σ_{ATN} is the mass attenuation cross-section of BC deposited on the filter of the AE33. M_{eBC} inferred from Eq. (2) only equals the true BC mass concentration, M_{BC}, if the applied σ_{ATN} is identical to the true attenuation cross-section of BC, $\sigma_{\mathrm{ATN,BC}}$, and if light attenuation at 880 nm is exclusively due to BC. $\sigma_{\mathrm{ATN,BC}}(880\,nm)$ can be inferred from the true MAC of BC, $\mathrm{MAC_{BC}}$, and the true *C* value:

$$\sigma_{\mathrm{ATN,BC}}(880\ nm) = \mathrm{MAC_{BC}}(880\ nm) * C \quad (3)$$

with $\mathrm{MAC_{BC}}$ being defined as:

$$\mathrm{MAC_{BC}}(\lambda) = \frac{b_{\mathrm{abs,BC}}(\lambda)}{M_{\mathrm{BC}}} \quad (4)$$

where $b_{abs,BC}$ is the absorption coefficient due to BC.

The manufacturer default values are 1.57 for C (TFE-coated glass fiber filters) and 12.2 $m^2 g^{-1}$ for σ_{ATN} at 880 nm, which corresponds to a MAC_{BC}(880 nm) of 7.77 $m^2 g^{-1}$ ~~at~~ (Gundel et al., 1984 , Drinovec et al., 2015). However, these three parameters depend on aerosol properties. Here, we have determined the C value by applying Eq. (1) to b_{ATN} measured by the aethalometer and the absorption coefficient, $b_{abs_{MWAA}}$, measured by a multi-wavelength absorbance analyser, MWAA (Massabò et al., 2015; Massabò et al., 2013). The MAC_{BC}(880 nm) was determined using Eq. (4) to compare $b_{abs_{MWAA}}$ from the MWAA measurements with EC mass from the Sunset thermo-optical analyzer (see Fig. 1A&B and Section 4.1 for detailed discussion). Following this procedure, the MWAA and Sunset analyser will be defined as reference methods for absorption coefficient and EC mass concentration, respectively. Note that data from these reference methods were only available with low time resolution and for a subset of all samples. Thus, the aethalometer anchored against these reference methods, was used to obtain the wavelength dependent absorption coefficients and the eBC mass concentrations with high time resolution using Eq. (1) and (2), respectively. Processing the loading compensated AE33 attenuation coefficients with C value and MAC_{BC}, determined with independent MWAA and Sunset analyser measurements, ensures that the inferred $b_{abs}(\lambda)$ (Eq. (1)) and M_{eBC} (Eq. (2)) have minimal bias compared to respective true values.

MWAA measurements. The MWAA (Massabò et al., 2015; Massabò et al., 2013) was used as reference method for the aerosol absorption coefficient. It measures the absorption coefficient $b_{abs_{MWAA}}(\lambda)$ of particles deposited on on standard filter samples. It is composed of five laser diodes, with λ = 375, 407, 532, 635 and 850 nm, acting as light sources and placed above the filter, an automated sample-changer, and three low-noise UV-enhanced photodiodes. ~~The first photodiode is placed behind the filter for the analysis of transmittance measurements, while the other two photodiodes are positioned at specific angles between the sources and the loaded filter to perform reflectance measurements~~. The first photodiode is placed behind the filter for transmittance measurements (0° relative to the incident light, 1.5 cm from the sample), while the other two photodiodes are positioned at 125º and 165º (11 cm from the sample) to collect the back scattered light. These transmittance and reflectance measurements are used together with a radiative transfer model (Hänel et al., 1987) , which takes into account multiple scattering within the particle/filter layer, to retrieve both the total optical thickness and the particle-filter-layer single scattering albedo, providing the absorption coefficient $b_{abs_{MWAA}}(\lambda)$ values. These calculations largely follow the approach

implemented in the multi-angle absorption photometer (MAAP, Petzold and Schönlinner, 2004).

UV-visible absorbance measurements of extracted aerosols. Filter samples were extracted for UV-visible absorbance measurements in 10 mL ultrapure water or methanol in an ultrasonic bath for 20 min at 30 °C. Samples were subsequently briefly vortexed (1 min) and filtered with 0.45 µm nylon membrane syringe filters following the procedure described in Daellenbach et al. (2016). Absorption spectra were measured from 280 to 500 nm using a UV-visible spectrophotometer (Ocean Optics) coupled to a 50-cm long-path detection cell (Krapf et al., 2016). Light attenuation by the OA in solution, $ATN_{\text{OA-sol}}$, at a given wavelength was recorded as the logarithm of the ratio of signal intensities of the reference (solvent) (I_0) and the sample (I), both corrected for background signals with the light source off. From $ATN_{\text{OA-sol}}$, the absorption coefficient of OA in solution, $b_{\text{abs,OA-sol}}(\lambda)$, can be quantified as:

$$b_{\text{abs,OA-sol}}(\lambda) = \frac{ATN_{\text{OA-sol}}(\lambda)}{l} \quad (5)$$

where l is the optical path length.

The absorbance measurements are aimed at inferring the imaginary part of the refractive index. For this, $b_{\text{abs,OA-sol}}(\lambda)$ is transformed to the absorption coefficient of the bulk OA in the pure form, $b_{\text{abs,OA-bulk}}$ (Sun et al., 2007):

$$b_{\text{abs,OA-bulk}}(\lambda) = b_{\text{abs,OA-sol}}(\lambda) \Big/ \frac{m_{\text{OA}}}{\rho_{\text{OA}} V_{\text{solvent}}} \quad (6)$$

where ρ_{OA} is the bulk density of OA (assumed to be 1.5 g cm^{-3}, typical of wood-burning OA; (Corbin et al., 2015a; Moosmüller et al., 2009; Sun et al., 2007)), m_{OA} is the extracted OA mass, and V_{solvent} is the solvent volume. The bulk absorption coefficient directly leads to the imaginary part of the OA refractive index, k_{OA}, in pure form (Moosmüller et al., 2009):

$$k_{\text{OA}}(\lambda) = b_{\text{abs,OA-bulk}}(\lambda) \frac{\lambda}{4\pi} \quad (7)$$

Inserting Eq. (6) into Eq. (7) eventually provides (Liu et al., 2015a):

$$k_{\text{OA}}(\lambda) = \frac{\lambda \rho_{\text{OA}} V_{\text{solvent}}}{4\pi m_{\text{OA}}} b_{\text{abs,OA-sol}}(\lambda) \quad (8)$$

The mass of organics dissolved in the solution could not be quantified. Therefore, we use an upper limit value for m_{OA}, approximated as the integral of AMS-measured OA mass concentration times sample flow rate over the filter-sampling period. Accordingly, the resulting k_{OA} values represent lower limits for the true values, as the OA extraction efficiency was not accounted for. ~~Higher k_{OA} values based on online absorption coefficient measurements compared to those calculated based on Equation 8 may be related to low OA extraction efficiency or to non-extractable highly absorbing material and results shall be discussed accordingly.~~ If the OA extraction efficiency was less than unity, then the absorption (or MAC) predicted from our solvent-extraction measurements would be less than that measured (or calculated) using our real-time measurements (MWAA-calibrated aethalometer).

2.3 Uncertainty analysis

It is important to draw a clear distinction between uncertainties related to measurement precision and accuracy and those related with experimental variability. In this section we discuss the quantifiable and unquantifiable uncertainties related with the different measurements. In the result section, we will present our confidence levels on the average parameters determined based on the experimental variability, which we judge to be the main source of variance in the data.

Quantifiable uncertainties. The estimated uncertainty in the AMS-derived OA mass concentrations is ~25%, which includes both potential biases and precision. This estimate is based on the variation in the AMS calibration factors and estimated uncertainties in the SMPS used for the AMS calibration (Bruns et al., 2015, 2016). Uncertainties related to particle transmission efficiency in the AMS are considered negligible for the particles sampled here (Liu et al., 2007), whose volume size distribution falls within the range transmitted efficiently by the AMS aerodynamic lens (see Fig. S4). The bounce-related collection efficiency (CE) of the AMS was concluded to be unity for wood-burning OA in the literature reviewed by Corbin et al. (2015b; in their Section S1.2). For the present data, the comparison between the SMPS mass (predicted from fitted volume distributions using a density of 1.5 g cm^{-3}) and the total PM predicted as AMS-OA+eBC, suggest a CE value between 0.7 and 1.0 (19% relative uncertainty), consistent with average literature values and the uncertainties estimates. The uncertainty in EC mass concentration, estimated from measurement repeats based on the EUSAAR2 protocol only, is within 7% in our case. The precision uncertainty in the aethalometer attenuation measurements was estimated as 15 Mm^{-1} based on the

standard deviation of its signals prior to aerosol being injected into the smog chamber. The MWAA data have an estimated noise level and precision of 12 /Mm and 10% respectively, and these uncertainties have been added in quadrature to provide the overall uncertainties shown, for example, as error bars in Fig. 1 below. To compare the MWAA and aethalometer measurements, we determined $b_{abs,MWAA,880nm}$ by extrapolating the absorption coefficients measured at 850 nm to 880 nm using an α-value determined from the ratio between the absorption coefficients at 850 nm and 635nm. The uncertainty associated with this extrapolation is considered negligible relative to the overall MWAA uncertainty.

Possible unquantified uncertainties. There are significant uncertainties in the measurement of aerosol absorption using filter-based techniques (e.g., Collaud Coen et al., 2010). Here, we have used MWAA measurements as a reference to scale the aethalometer data, using a single C value. The correction factor C, which accounts for scattering effects within the filter matrix (Drinovec et al., 2015), may depend on the aerosol sample (Collaud Coen et al., 2010). In this study, we evaluated the variability in this factor for our primary and aged samples, by directly comparing the aethalometer to MWAA measurements, as discussed below. The MWAA has been previously validated against a polar nephelometer and a MAAP (Massabo et al., 2013), which, in turn, has been validated against numerous in situ methods (e.g., Slowik et al., 2007). The excellent correlation between MWAA and EC in our study (discussed below) supports the high confidence in the MWAA filter based absorption measurements conducted here. Another significant source of uncertainty in filter-based absorption measurements is the possible sorption (or evaporation) of volatile organics on (or from) the filter material. This may lead to an overestimation (or underestimation) of OA absorption. However, we have minimized sorption artefacts by utilizing a charcoal denuder. We have obtained an excellent correlation between OA absorption measurements derived from the MWAA-calibrated aethalometer and from quartz filter samples (see discussion below, Fig. 6 in the main text and S13 in the supplementary information). Although both of these techniques involved filter sampling, their sampling timescale is an order of magnitude different, and a difference is therefore expected if sorption (or evaporation) caused a substantial bias in our results. We therefore conclude that it is unlikely that artifacts associated with filter sampling have biased the absorption measurements. Finally, uncertainties related to pyrolysis during thermo-optical analysis may bias EC measurements. Such uncertainties arise from unstable organic compounds, and can be significant for biomass-burning samples, leading to biases on the order of 20% for EC (e.g. Schauer et al., 2003; Yang and Yu., 2007). To minimize these biases we applied the EUSAAR2 protocol. The optical properties of such organics are

generally different from BC; therefore, the excellent correlation between MWAA and EC data in Fig. 1A suggest that pyrolysis effects were not a major source of uncertainty in our data set.

3. OPTICAL PROPERTIES ANALYSIS

3.1 Determination of absorption Ångström exponents and mass absorption cross-sections

In this section we describe the methodology adapted for the determination of the mass absorption cross-sections (MACs) for the different aerosol material from the Sunset, MWAA and aethalometer measurements. The assumptions and limitations underlying these calculations are clearly stated. We also explain the relationship between the MACs and the wavelength dependence of the overall absorption.

Definition of the absorption Ångström exponent . The wavelength dependence of the overall absorption due to both BC and BrC has often been described assuming a power law:

$$b_{abs}(\lambda) \propto \lambda^{-\alpha} \quad (9)$$

where α is the Ångström absorption exponent, often determined by fitting the absorption coefficient measurements across the entire wavelength range. Eq. (9) is an empirical simplification, which breaks down when different components having different spectral dependence contribute to the absorption, e.g. a mix of BrC and black carbon (e.g., Moosmüller et al., 2011). In practice, different values of α would be obtained for different choices of λ ranges, and therefore we alternatively calculated two-wavelength absorption exponents according to

$$\alpha(\lambda, \lambda_{ref}) = -\frac{\ln\left(\frac{b_{abs}(\lambda)}{b_{abs}(\lambda_{ref})}\right)}{\ln\left(\frac{\lambda}{\lambda_{ref}}\right)} \quad (10)$$

where λ is a wavelength of interest (in nm) and λ_{ref} is the reference wavelength, here 880 nm. This reference wavelength was chosen, because BC is expected to fully dominate light absorption in this range (Laskin et al., 2015).

Black carbon is known to have an α between 0.9 and 1.1 (Bond et al., 2013; Kirchstetter et al., 2004; Liu et al., 2015b), whereas BrC, which preferentially absorbs at shorter wavelength, has a higher α (Laskin et al., 2015; Saleh et al., 2013). Thus, we interpret an increase of $\alpha(\lambda, \lambda_{ref})$ of the total aerosol as due to an increased contribution of BrC to the total absorption. $\alpha(\lambda, \lambda_{ref})$ can potentially change due to other effects such as a wavelength dependent lensing effect on absorption by BC (e.g., Lack and Langridge, 2013) or the restructuring of BC aggregates during aging. The former effect was negligible under our conditions, as elaborated on below. The latter, if it occurs during aging, would be attributed to SOA absorption in our approach. However, this is not an issue if our values are accordingly applied in e.g. model simulations, following the same assumption as in our approach. This means that the potential restructuring effects must implicitly be considered within the MAC(λ) of SOA, while the MAC(λ) of BC must be kept fixed.

3.2 Determination of MAC_{BC} and MAC_{POA} using the absorption Ångström exponent

In a mixture of *n* absorbing species, the total absorption at any wavelength may be written as the sum of the absorbance of each of the species. Accordingly, Eq. (10) can be expressed for a multi-component system

$$\alpha(\lambda, \lambda_{\mathrm{ref}}) = \frac{1}{\ln(\lambda_{ref}/\lambda)} \ln\left(\frac{\sum_{i=1}^{n} b_{\mathrm{abs,i}}(\lambda)}{\sum_{i=1}^{n} b_{\mathrm{abs,i}}(\lambda_{ref})}\right) = \frac{1}{\ln(\lambda_{\mathrm{ref}}/\lambda)} \ln\left(\frac{\sum_{i=1}^{n} M_i MAC_{\mathrm{i}}(\lambda)}{\sum_{i=1}^{n} M_i MAC_{\mathrm{i}}(\lambda_{ref})}\right) \quad (11)$$

where the right hand side follows the general definition of MAC along the lines of Eq. (4). M_{i} and MAC_i are the mass concentration and MAC, respectively, of the i^{th} species, with *n* absorbing species in total. By considering that the light absorption at λ_{ref} = 880 nm is exclusively due to BC, and by defining BC to be the n^{th} species, Eq. (11) can be written as

$$\alpha(\lambda, 880nm) = \frac{1}{ln(880nm/\lambda)} ln\left(\frac{\mathrm{MAC_{BC}}(\lambda)}{\mathrm{MAC_{BC}}(880nm)} + \sum_{i=1}^{n-1} \frac{M_i \mathrm{MAC}_i(\lambda)}{b_{\mathrm{abs}}(880nm)}\right) \quad (12)$$

In Eq. (12), the summation now only goes over the n-1 organic species, which contribute to light absorption.

The fresh combustion aerosol exclusively contains BC and POA as absorbing species. For the data at time t_0 before the start of photo-oxidative aging, Eq. (12) simplifies to:

$$\alpha(t_0, \lambda, 880nm) = \alpha_{\mathrm{BC+POA}}(t_0, \lambda, 880nm)$$

$$= \frac{1}{\ln(880\text{nm}/\lambda)} \ln\left(\frac{\text{MAC}_{\text{BC}}(t_0,\lambda)}{\text{MAC}_{\text{BC}}(t_0,880nm)} + \frac{M_{\text{OA}}(t_0)\text{MAC}_{\text{POA}}(t_0,\lambda)}{b_{\text{abs}}(t_0,880nm)}\right) \quad (13)$$

In Eq. (13), $M_{\text{OA}}(t_0)$ is the mass concentration of primary organic aerosol measured by the AMS at t_0. $\text{MAC}_{\text{BC}}(t_0,880\text{nm})$ was inferred from the MWAA and Sunset thermo-optical analysis and shown to be independent of the experimental conditions (Section 4.1; Fig. 1A). Absorption coefficients $b_{\text{abs}}(t_0,\lambda)$ are obtained from the high time resolution attenuation measurements by the aethalometer referenced to the MWAA absorption measurements as described above. $\alpha(t_0,\lambda,880\text{ nm})$ is derived from $b_{\text{abs}}(t_0,\lambda)$ and $b_{\text{abs}}(t_0,880\text{ nm})$ using Eq. (10). We have intentionally formulated of Eq. (13) as such to highlight that the retrieved $\text{MAC}_{\text{OA}}(t,\lambda)$ depends mainly on the input M_{OA}. Correspondingly, the retrieved $\text{MAC}_{\text{OA}}(t,\lambda)$ is mainly sensitive to potential AMS calibration biases. This leaves only 2 free parameters in Eq. (13), $\text{MAC}_{\text{BC}}(t_0,\lambda)$ and $\text{MAC}_{\text{POA}}(t_0,\lambda)$. These were determined by fitting Eq. (13) to $\alpha(t_0,\lambda,880\text{ nm})$, $M_{\text{OA}}(t_0)$, $\text{MAC}_{\text{BC}}(t_0,880\text{nm})$ and $b_{\text{abs}}(t_0,880nm)$ data measured in all experiments for fresh emissions at t_0. This approach contains the implicit assumption that the two MAC values are also independent of experimental conditions, and therefore these MACs should be considered as average values. The accuracy of these MAC values obviously depends on the accuracy of the absorption and mass measurements. First, a systematic bias in the *C* value potentially caused by a systematic bias in the MWAA measurements propagates to an identical bias in both $\text{MAC}_{\text{BC}}(t_0,\lambda)$ and $\text{MAC}_{\text{POA}}(t_0,\lambda)$. Second, a systematic bias in the Sunset EC mass measurements yields a corresponding inverse bias in $\text{MAC}_{\text{BC}}(t_0,\lambda)$, while $\text{MAC}_{\text{POA}}(t_0,\lambda)$ remains unaffected. Third, a systematic bias in the AMS POA mass yields a corresponding inverse bias in $\text{MAC}_{\text{POA}}(t_0,\lambda)$, while $\text{MAC}_{\text{BC}}(t_0,\lambda)$ remains unaffected. Eq. (13) shows that α of the primary aerosol at a certain wavelength is largely driven by $\text{MAC}_{\text{POA}}(t_0,\lambda)$, i.e. the optical properties of POA, and by the ratio $\frac{M_{\text{OA}}(t_0)}{b_{\text{abs}}(t_0,880nm)}$, which reflects the relative contributions of POA and BC to total primary aerosol mass.

3.3 Determination of MAC_{SOA}

The MAC of SOA, MAC_{SOA}, can be generally defined as:

$$\text{MAC}_{\text{SOA}} = \frac{b_{\text{abs,SOA}}}{M_{\text{SOA}}} \quad (14)$$

where $b_{\text{abs,SOA}}$ and M_{SOA} are the absorption coefficient and mass concentration of SOA, respectively. In the aged aerosol, which contains the absorbing species BC, POA and SOA, $b_{\text{abs,SOA}}$ is the difference of the total absorption minus the absorption by POA and BC:

$$b_{\mathrm{abs,SOA}}(t,\lambda) = b_{\mathrm{abs}}(t,\lambda) - b_{\mathrm{abs,POA+BC}}(t,\lambda) \quad (15)$$

The absorption by POA and BC in the aged aerosol is a priori unknown, but can be calculated under certain assumptions. The first assumption is that SOA does not contribute to absorption at 880 nm: $b_{\mathrm{abs,POA+BC}}(t, 880\ nm) \equiv b_{\mathrm{abs}}(t, 880\ nm)$. The second assumption is that the two-λ α values of primary emissions do not change during aging $\alpha_{\mathrm{POA+BC}}(t,\lambda,880\ nm) \equiv \alpha_{\mathrm{POA+BC}}(t_0,\lambda,880\ nm)$. The latter approximation is based on the underlying assumptions that the MAC of POA is not altered by aging and that the proportions of POA and BC mass lost to the wall are identical. Under these assumptions $b_{\mathrm{abs,POA+BC}}$ becomes:

$$b_{\mathrm{abs,POA+BC}}(t,\lambda) = b_{\mathrm{abs}}(t, 880\ nm)\left(\frac{880\ nm}{\lambda}\right)^{\alpha_{\mathrm{POA+BC}}(t_0,\lambda,880\ nm)} \quad (16)$$

Note that inferring $b_{\mathrm{abs,POA+BC}}(t,\lambda)$ from $b_{\mathrm{abs}}(t, 880\ nm)$ implicitly accounts for the decrease in the BC and POA absorption due to wall losses.

M_{SOA} was obtained as total organic minus POA mass concentration:

$$M_{\mathrm{SOA}}(t) = M_{\mathrm{OA}}(t) - M_{\mathrm{POA}}(t) \quad (17)$$

The POA mass concentration in the aged aerosol can be inferred from the initial OA mass concentration in the fresh emissions by accounting for the wall losses using Eq. (S1) and the wall loss time constant τ (see Section Wall loss corrections in the SI):

$$M_{\mathrm{POA}}(t) = M_{\mathrm{OA}}(t_0)\exp(\tau^{-1}t) \quad (18)$$

Inserting Eq. (15) - (18) into Eq. (14) provides the final equation for inferring $\mathrm{MAC_{SOA}}$.

$$\mathrm{MAC_{SOA}}(t,\lambda) = \frac{b_{\mathrm{abs}}(t,\lambda) - b_{\mathrm{abs}}(t,880\ nm)\left(\frac{880\ nm}{\lambda}\right)^{\alpha_{\mathrm{POA+BC}}(t_0,\lambda,880\ nm)}}{M_{\mathrm{OA}}(t) - M_{\mathrm{OA}}(t_0)\exp(\tau^{-1}t)} \quad (19)$$

$\mathrm{MAC_{SOA}}$ can be calculated for every data point in time and for all aethalometer wavelengths from 370 to 660 nm ($\mathrm{MAC_{SOA}}$ defined to be zero at $\lambda \geq 880$ nm), as all quantities on the right hand side of Eq. (19) are available from either the aethalometer or AMS measurements or are otherwise known. It can be seen from Eq. (19) that the mass concentrations used to calculate $\mathrm{MAC_{SOA}}$ solely originate from AMS data, thus being consistent with the calculation of $\mathrm{MAC_{POA}}$ (see above). Eq. (19) is based on the assumption that POA is "chemically inert", i.e. no chemically

induced changes of M_{POA} and MAC_{POA} occur. ~~Such chemically induced changes of absorption by POA, if they occur, are assigned to the absorption by SOA, thus resulting in a corresponding adjustment of the inferred MAC_{SOA}~~ Such chemically induced changes of absorption coefficient by POA, through a change of M_{POA} or MAC_{POA}, if they occur, are assigned to the absorption by SOA, thus resulting in a corresponding adjustment of the inferred MAC_{SOA}.

3.4 Mie calculation to relate k_{OA} with MAC_{OA}

The imaginary part of the refractive index of an aerosol component is an intensive material property. However, the MAC of such an aerosol component additionally depends on the size and morphology of the aerosol (except for the Rayleigh regime). The online aerosol absorption measurements provide estimates for MAC values, while the UV-visible absorbance measurements of filter extracts provide the imaginary part of the refractive index. We used Mie calculations in order to compare the two quantities. The $k_{OA}(\lambda)$obtained from the filter extracts is converted to a $MAC_{OA,bulk}$ by assuming that all OA is present in homogeneous spherical particles with a diameter distribution identical to the mobility diameter distribution measured by the SMPS. In this manner, $MAC_{OA,bulk}$ becomes equal to the mass-weighted average (=volume-weighted average) of the diameter dependent MAC:

$$MAC_{OA,bulk}(\lambda, n_{OA}, k_{OA}, \rho_{OA}) = \frac{\sum_i N_i d_i^3 MAC_i^{Mie}(\lambda, n_{OA}, k_{OA}, \rho_{OA})}{\sum_i N_i d_i^3} \quad (20)$$

Here, N_i and d_i are the number of particles and particle diameter, respectively, in the i^{th} size bin, and n_{OA} is the real part of the refractive index of the OA (which is assumed to be n_{OA} = 1.5 typical for organic material; Lu et al., 2015). The MAC of particles with diameter d_i, MAC_i^{Mie}, was calculated using the Mie Code by Peña and Pal (2009) (incorporated into Igor Pro 6.3, WaveMetrics, OR, USA by Taylor et al., 2015). MAC_i^{Mie} also depends on the density of OA, for which we assume a value of ρ_{OA}= 1.5 g cm^{-3} (see Section 2.2), as the volume specific absorption cross-section obtained from Mie theory needs to be converted to a mass specific absorption cross-section. We note that as we have used the same value of ρ_{OA} in the calculation of both MAC_i^{Mie} and $k_{OA}(\lambda)$, $MAC_{OA,bulk}$ becomes independent of the assumed ρ_{OA} value.

Assuming spherical particles and neglecting the presence of BC in these particles may seem inappropriate. However, calculations considering BC and assuming core-shell morphology revealed (1) limited sensitivity of the resulting MAC_{OA} to this assumption and (2) a higher than measured lensing effect. Therefore, a substantial fraction of the OA seems to be externally mixed and to dominate the measured size distribution (see also Section 4.1). ~~The uncertainty~~

in the MAC_{OA} inferred from k_{OA} of the UV visible absorbance measurements was estimated by combining an estimated 20 % precision with a detection limit of 0.3 $m^2 g^{-1}$ in quadrature.

4. RESULTS AND DISCUSSION

4.1 Verification of MAC_{BC} and *C* value

As mentioned above, the determination of MAC_{BC}(880nm) requires the determination of the absorption coefficients at λ and the BC mass. We used the aethalometer to obtain the absorption coefficients with high time resolution, while absolute values were scaled to match MWAA data, which we defined as our reference method. The aethalometer was also used to obtain eBC mass concentrations with high time resolution, while absolute values were scaled to match EC mass measured by the Sunset thermo optical measurement using the EUSAAR 2 protocol, which we defined as our reference method. Here we start by proving the concept of our scaling approaches and provide average values for MAC_{BC}(880nm) and aethalometer-*C* which are required subsequently.

Figure 1A shows the correlation between the MWAA measured absorption coefficient at 880 nm and the Sunset thermo optical EC mass measurements. MWAA absorption measurements at 880 nm is determined by extrapolating the absorption coefficients at 850 nm using an α determined from the ratio between the absorption coefficients at 850 nm and 635nm. The corresponding MAC_{BC}(880nm), determined as the slope of the linear fit through all data, is 4.6 ± 0.7 $m^2 g^{-1}$. This value matches the data at all three levels of aging, i.e. for the primary, Aged1 and Aged2 filter samples, within experimental uncertainty (see Figure S2 in the Supplement for more information). This average MAC_{BC}(880nm) is also very similar to values reported for "pure" BC (4.7 ± 0.7 $m^2 g^{-1}$ at 880 nm) (Bond et al., 2006), indicating no significant lensing effect on absorption by BC from primary or secondary OA. This can also be observed from the time resolved attenuation measurements by the aethalometer at 880 nm (Figure S3), suggesting that little (<10%) to no increase in the attenuation coefficients upon SOA formation. If the OA and the BC were internally mixed, the observed variability in the mass fraction of OA (f_{OA}) from 0.1 to 0.9 for the fresh and aged samples would result in a high variability in the MAC_{BC}(880nm), with values higher than those reported in the literature, according to Mie calculations assuming core-shell internal mixtures. However, this is not the case. Based on this observation, we conclude that the particles studied are likely not core-shell internal

~~mixtures, although we have measured a mono-modal aerosol population growing during SOA production (Figure S4). An explanation for the occurrence of an external mixture could be that the primary OA and BC particles may have been externally mixed after these species were emitted separately during combustion, preferentially during the pre-ignition and flaming phases, respectively (Corbin et al., 2015a, 2015b; Heringa et al., 2011). These phases may occur consecutively during a burn or simultaneously in different parts of the stove. MAC_{BC}(880nm) found to be constant supports our approach described in Section 2.2 using scaled aethalometer data for BC mass and treating MAC_{BC} at all other wavelengths as a constant across all experiments during the data retrieval process described in Section 3.1.~~

~~Figure 1B shows the correlation between $b_{ATN,AE33}$ and $b_{abs,MWAA}$ measured by the aethalometer and MWAA, respectively. The two variables correlated very well, indicating a constant aethalometer C value, which is the ratio between $b_{ATN,AE33}$ and $b_{abs,MWAA}$ (Equation 1), of 3.0±0.3, independent of the type of the aerosol sampled. This is also reflected in the probability density function of individual C values shown in Figure S2 where the standard deviation is found to be as small as σ_C~ ± 10% . Such constant ratio justifies our approach of applying this single C value for all conditions in order to scale the time resolved attenuation measurements by the aethalometer to the MWAA reference method.~~

~~Note, the manufacturer's default values, which were not applied in our case, are 1.57 for C and 12.2 $m^2 g^{-1}$ for σ_{ATN} at 880 nm, which implies an underlying MAC_{BC}(880 nm) of 7.77 $m^2 g^{-1}$ (Gundel et al., 1984 , Drinovec et al., 2015). Therefore, factory default $b_{abs}(\lambda)$ would have a substantial systematic high bias for the wood combustion aerosols of this study. Meanwhile, the σ_{ATN} calculated at 880 nm, which is the product of the C value and MAC_{BC} (Equation 3), is consistent with the manufacturer value of σ_{ATN} (σ_{ATN} values determined here are 15% higher, 13.8 $m^2 g^{-1}$ in this study compared to the value of 12.2 $m^2 g^{-1}$ provided by the manufacturer), and the factory default M_{eBC} would agree well with the true M_{BC}, determined here.~~

We have independently determined the MAC_{BC}(880nm) and the aethalometer C values under our conditions, as follows. We determined MAC_{BC}(880nm) from the regression between the absorption coefficients at 880 nm obtained from the MWAA and the EC mass measured by the Sunset analyzer (Fig. 1A). The slope of this regression may be used to estimate the MAC_{BC}(880nm), which we retrieved as 4.7 ± 0.3 $m^2 g^{-1}$ by an uncertainty-weighted linear least-squares fit . The corresponding intercept was not significantly different from zero (-3 ± 3 /Mm). Our MAC_{BC}(880nm) is not statistically significantly different from the value recommended by Bond et al., (2006) for

externally-mixed BC (extrapolating their MAC_{BC}(550nm) to 880 nm by assuming α=1 provides MAC_{BC}(880nm)= 4.7 ± 0.7 $m^2 g^{-1}$). The strong correlation between $b_{abs,MWAA,880nm}$ and EC in Fig. 1A shows that MAC_{BC}(880nm) did not vary with aging during our study (see also Fig. S2-a). It also indicates that measurement artefacts for both instruments were negligible, as the fundamental differences between the two techniques mean that any artefacts are unlikely to be similar between them (charring for EC vs. adsorption artefacts for MWAA). Our absorption coefficient measurements also provide insights into particle mixing state in this study. Since a single MAC adequately described our samples at all levels of aging (Fig. 1A and Fig. S2-a), in spite of a factor of 3.3 average increase in the aerosol mass, our samples cannot be adequately described by a core-shell Mie model. Such a core-shell model would predict an absorption enhancement by a factor of ~1.8 (Bond et al., 2006) for the observed OA mass increase with aging, which was not observed in our case. This observation is also supported by the time resolved attenuation measurements at 880 nm using the aethalometer (Fig. S3), suggesting that little (<10%) to no increase in the attenuation coefficients upon SOA formation. We emphasize that this conclusion does not indicate that no internal mixing occurred, but rather that the simplified concept of negligible mixing better describes our data than the equally simplified concept of a core-shell description of coatings that completely envelop the central BC core. This may be due to the complex morphology of internally-mixed BC, which has been previously observed for wood burning particles (e.g., China et al., 2013; Liu et al., 2015; Liu et al., 2017). It may also be related to the fact that OA and BC are emitted during separate phases of combustion. OA rich particles are emitted during the pre-flaming pyrolysis stage of combustion, whereas most BC is emitted during flaming combustion (Corbin et al., 2015a, 2015b; Haslett et al., 2018; Heringa et al., 2011). These two stages of combustion may coexist in different regions of the stove, particularly during simulated real-world usage. As lensing effect was negligible in our case, we have assumed that the aerosol optically behaves as an external mix between BC and BrC during Mie calculation (see section 3.4). We note that while this assumption is important for estimating the BC absorption, the conclusion drawn about the BrC absorption are not very sensitive to the assumed morphology.

We determined time-resolved wavelength-dependent absorption coefficients as follows. We used the aethalometer to obtain filter attenuation coefficients with high time resolution, which were then calibrated to obtain absorption coefficients by deriving the factor C (Eq. (1)) using the MWAA measurements of filter samples. C was obtained from an uncertainty-weighted linear least-squares fit as 3.0 ± 0.2 (Fig. 1B); the intercept of the fit was not significantly different from zero, within two standard deviations (-17 ± 14). A very strong correlation could be observed between MWAA and aethalometer (Fig. 1B), implying that C is independent of the type of the aerosol

sampled (see also Fig. S2-B). Therefore, we used a single C value to obtain time-resolved wavelength-dependent absorption coefficients from the aethalometer attenuation measurements at the different wavelengths for primary and aged aerosols.

Note that the manufacturer's default values, which were not applied in our case, are 1.57 for C (using TFE-coated glass fiber filters) and 12.2 m^2 g^{-1} for σ_{ATN} at 880 nm (Gundel et al., 1984 , Drinovec et al., 2015). The C value determined here is larger than the manufacturer-default value for the AE33, resulting in smaller absorption coefficients. However, the calculated σ_{ATN} at 880 nm (13.8 m^2 g^{-1}), which can be retrieved as the product of the C value and MAC_{BC}(880nm) (Eq. (3)), is similar to the factory-default σ_{ATN}. Therefore, our calibrated M_{eBC}, calculated from the attenuation coefficients using σ_{ATN} (Eq. (2)), are similar to the factory-default M_{eBC}. We note that M_{eBC} has not been used for MAC_{OA} calculations, and is only used for the calculation of the mass fractions of BC and OA for display purposes (Fig. 2, 3, 7 and 8).

4.2 Optical properties of BC, POA, and SOA

In this section we derive the wavelength dependent mass absorption cross-sections for BC, POA and SOA. In Fig. 2, we display the evolution of $\alpha(370nm, 880nm)$ as a function of OH exposure. Fig. 3 shows the relationship between $\alpha(\lambda, 880nm)$ and f_{OA} for primary and aged aerosols.

α of primary emissions. The $\alpha(370nm, 880nm)$ values computed for the primary aerosol (OH exposure = 0 molecules cm^{-3} h) ranged between 1.3 and 1.7 (Fig. S5), which is within the range reported previously for biomass-burning emissions (Kirchstetter et al., 2004; Lewis et al., 2008; Zotter et al., 2016). The $\alpha(\lambda, 880nm)$ is slightly higher than that of pure BC (~1.2; Bond et al., 2013; Zotter et al., 2017) for small f_{POA}, while increasing f_{POA} corresponded to a distinct increase of $\alpha(\lambda, 880nm)$. ~~The $\alpha(\lambda, 880nm)$ is close to that of pure BC (~ 0.9-1.1; Bond et al., 2013; Zotter et al., 2017) for small f_{POA}, while increasing f_{POA} corresponded to a distinct increase of $\alpha(\lambda, 880nm)$~~. This increase provides clear evidence for the contribution of primary BrC to the absorption at lower wavelengths (shown explicitly in Eq. (13)). ~~The f_{POA} ranges from 0.23 to 0.59, which is lower than f_{POA} reported for open burning emissions (e.g., f_{POA}~0.75, Ulevicius et al (2016)), because our wood-stove emissions feature a more efficient combustion~~ The f_{POA} ranges from 0.12 to 0.63, which is lower than f_{POA} reported for open burning emissions (e.g., f_{POA}~0.75, Ulevicius et al (2016)), because our wood-stove emissions feature a more efficient combustion. ~~The systematic decrease in $\alpha(\lambda, 880nm)$ with increasing λ reflects the more efficient light absorption by BrC at shorter wavelengths (Moosmüller et al., 2011), and shows that the power law wavelength dependence is an inaccurate~~

~~oversimplification for this mixed aerosol~~ As illustrated in Fig. S5, the observed absorption spectra have steeper gradients with decreasing wavelength compared to the lines of constant α. Such systematic increase in $\alpha(\lambda, 880nm)$ with decreasing λ reflects the more-efficient light absorption by BrC at shorter wavelengths (Moosmüller et al., 2011), and shows that the power law wavelength dependence is an inaccurate oversimplification for this mixed aerosol.

Evolution of α with aging. Fig. 3B shows that upon aging, the OA fraction rapidly increased (a typical time series of raw data is shown in Fig. S1), reaching an average value of 0.81 (full range for aged OA: 0.74 < f_{OA} < 0.89) at high OH exposures (> 2×10^7 molecules cm^{-3} h), and resulting in a corresponding increase of $\alpha_{\mathrm{BC+POA+SOA}}(370\mathrm{nm}, 880\mathrm{nm})$. The increase of $\alpha_{\mathrm{BC+POA+SOA}}(370\mathrm{nm}, 880\mathrm{nm})$ and f_{OA} were always correlated and plateaued at OH exposures beyond ~2×10^7 molecules cm^{-3} h, as seen in Fig 2. ~~Also, note in Fig. 2 that the highest $\alpha_{\mathrm{BC+POA+SOA}}(370\mathrm{nm}, 880\mathrm{nm})$ were reached, on average 1.8, during experiments where the f_{OA} was highest~~ Also, note in Fig. 2 that at highest OH exposures, the highest $\alpha_{\mathrm{BC+POA+SOA}}$(370nm, 880nm) were reached, on average 1.8, during experiments where the f_{OA} was highest. Such strong correlation between SOA formation and $\alpha_{\mathrm{BC+POA+SOA}}(370\mathrm{nm}, 880\mathrm{nm})$ suggests the production of substantial amounts of brown SOA. A similar relationship is observed between $\alpha_{\mathrm{BC+POA+SOA}}(\lambda, 880\mathrm{nm})$ and f_{OA} for higher wavelengths as shown in Fig. S6. Similar to the case of POA, a systematic decrease in $\alpha(\lambda, 880nm)$ with increasing λ is observed, reflecting the preferential absorption of BrC SOA at shorter wavelengths. We note that $\alpha_{\mathrm{BC+POA+SOA}}(370nm, 880nm)$ as a function of f_{OA} for all experiments lies below the overall trend for the primary aerosol (dashed line in Fig. 3B), implying that $\mathrm{MAC_{SOA}}$(370nm) was smaller than $\mathrm{MAC_{POA}}$(370nm).

Determination of $\mathbf{MAC_{BC}}$ and $\mathbf{MAC_{POA}}$. We determined best-fit values for $\mathrm{MAC_{BC}}(\lambda)$ and $\mathrm{MAC_{POA}}(\lambda)$ from the data shown in Fig. 3A. Fig. 3A includes least-squares fits of Eq. (13) to the data, with $\mathrm{MAC_{BC}}(\lambda)$ and $\mathrm{MAC_{POA}}(\lambda)$ as fit parameters. The fit results are shown in Table 1. ~~The obtained fit value of $\mathrm{MAC_{BC}}$(370nm) was 13.7 $m^2\ g^{-1}$ (GSD 1.1), higher but not statistically significantly different from the value suggested by Bond et al. (2013) of 11.1 $m^2\ g^{-1}$ with a 95% confidence interval of 3.5 $m^2\ g^{-1}$, considering α_{BC} =1~~ The obtained fit value of $\mathrm{MAC_{BC}}$(370nm) was 13.7 $m^2\ g^{-1}$ (GSD 1.1, one-sigma uncertainty 12.4—15.1 m^2/g), higher but not statistically significantly different from the range estimated based on Bond et al. (2013), considering the uncertainties on both the α_{BC} values and the $\mathrm{MAC_{BC}}$(520nm). Meanwhile, the mean $\mathrm{MAC_{POA}}$(370nm) value, equal to 5.5 $m^2\ g^{-1}$, obtained under our conditions for domestic wood burning is ~2.4 times higher than that obtained by Saleh et al. (2014) for open biomass burning

primary emissions, suggesting the presence of more-strongly absorbing organic material under our conditions (this comparison is continued in Section 4.3).

Determination of MAC_{SOA}. The $MAC_{SOA}(\lambda)$ values, determined using Eq. (19), are shown in Fig. 4 and Table 1. MAC_{SOA}(370nm) was 2.2 m^2 g^{-1} (GSD 1.39), a factor of 2.5 smaller than MAC_{POA}(370nm), but approximately an order of magnitude higher than values reported for ambient oxygenated aerosols or laboratory SOA from biogenic and traditional anthropogenic precursors such as terpenes and methyl-benzenes (Clarke et al., 2007; Lambe et al., 2013; Liu et al., 2016; Romonosky et al., 2015). The predominant SOA precursors identified in wood smoke comprise (methyl)naphthalene(s) and phenol derivatives from lignin pyrolysis (Bruns et al., 2016; Ciarelli et al., 2016), the oxidation products of which are expected to be highly light absorbing due to the presence of aromatic moieties in the SOA (Bruns et al., 2016; Laskin et al., 2015). In this regard, it is not surprising that the MAC_{SOA}(370nm) values obtained here are similarly high as those obtained from methanol-extracted SOA from guaiacol and naphthalene oxidation (0.5–3.0 m^2 g^{-1}, Romonosky et al., 2015).

Uncertainties and variability in MAC_{BC}, MAC_{POA} and MAC_{SOA}. ~~Table 1 shows that the uncertainties in the fitted $MAC_{BC}(\lambda)$ are relatively low (< 10%), increasing with decreasing λ. By contrast, the uncertainties in the fitted MAC_{POA} are much higher (GSD = 1.2–1.5) and increase with increasing λ. The relative residuals between the measured and fitted $\alpha(\lambda, 880nm)$ for primary emissions showed small biases of only 0.07 (Fig. S7). The corresponding RMSE (root mean square error) was 0.13, showing that the obtained average values may represent the data well. MAC_{SOA} values determined were highly variable between experiments with a GSD = 1.39 and 2.42 for λ=370 nm and 660 nm, respectively. We expect the variabilities in MAC_{SOA} and of MAC_{POA} to be related to changes in the organic aerosol chemical composition between different burns, since the variability of $MAC_{BC}(\lambda)$ was relatively small. In Section 4.3, we discuss this variability further using the results of an additional and independent analysis.~~

Table 1 shows the fitting errors related with $MAC_{BC}(\lambda)$, $MAC_{POA}(\lambda)$ and $MAC_{SOA}(\lambda)$, arising from our measurement precision and experimental variability. These fitting errors are greater than our estimated uncertainties in the absorption coefficients measured by MWAA (10%), and comparable to our estimated uncertainty in OA mass measured by AMS (30%). The residuals in the fitted $MAC_{BC}(\lambda)$ are relatively low (< 10%), increasing with decreasing λ. By contrast, the uncertainties in the fitted $MAC_{POA}(\lambda)$ are much higher (GSD = 1.2–1.5) and increase with increasing λ. The relative residuals between the measured and fitted $\alpha(\lambda,880nm)$ for primary emissions showed

a mean bias and RMSE of 0.07 and 0.13, respectively (Fig. S7), indicating that our fitted MAC results provide a good description of the data set. $MAC_{SOA}(\lambda)$ values determined were highly variable between experiments with a GSD = 1.39 and 2.42 for λ=370 nm and 660 nm, respectively. In Fig. S10, we show the distribution of $MAC_{SOA}(\lambda)$ values as box and whiskers against OH exposure, showing no particular dependence of these values with aging as it will be discussed below. Therefore, we expect the fitting errors in MAC_{SOA} and of MAC_{POA} to be mainly related to true changes in the organic aerosol chemical composition between different burns, since the variability of $MAC_{BC}(\lambda)$ was relatively small. In Section 4.3, we discuss this variability further using the results of an additional and independent analysis.

MAC_{BC}, MAC_{POA} and MAC_{SOA} wavelength dependence. The relationships between the $MAC_{SOA}(\lambda)$, $MAC_{POA}(\lambda)$ and $MAC_{BC}(\lambda)$ and wavelength appear to fall on three unique lines in the range 660 nm to 370 nm when plotted in log-log space, as shown in Fig. 4 (Fig. S8 shows the same data plotted on a linear scale). This indicates that a power-law approximation provides a good description of the behavior of individual components within this wavelength range from 370 nm to 660 nm. Accordingly we fitted the power law coefficients to the data shown in Fig. 4 ($\ln(MAC_i) = \ln(A_i) + \alpha_i \ln(\lambda)$, with i= BC, POA, or SOA) and fitting parameters are shown as multivariate probability density functions in Fig. S9. This yielded $\alpha_{BC} = 1.2$, $\alpha_{POA} = 4.6$, and $\alpha_{SOA} = 5.6$, with corresponding uncertainties of approximately 20% (complete details of the uncertainties are provided in Table S1). Note that α_{BC} in the range 660 nm to 370 nm obtained from this fit is very similar to α_{BC} values that can be inferred by extrapolating the data shown in Fig. 3A to f_{OA}=0. ~~The high α values obtained for the organic fractions are consistent with previous measurements for BrC containing POA (e.g. Chakrabarty et al., 2010, 2013) although, to our knowledge, this is the first study to report α_{SOA} without performing a solvent extraction.~~ The high α values obtained for the organic fractions are consistent with previous measurements for BrC containing POA (e.g. Chakrabarty et al., 2010, 2013).

Evolution of MAC_{OA} with aging. In Fig. 5, we examine whether the absorption profile of SOA evolved with aging. A change in $MAC_{SOA}(370nm)$ or α_{SOA} with increasing OH exposure may indicate either a change in the mass-specific absorption of the condensing SOA species with time, or a change (e.g. "bleaching") in the MAC of pre-existing POA. Fig. 5 indicates that neither of these scenarios was the case. Both $MAC_{SOA}(370nm)$ and α_{SOA} were statistically independent of the OH exposure, for exposures up to 40 molec. OH cm^{-3} h. This signifies that under our conditions and within our measurement uncertainties the optical properties of the additional organic mass formed was constant with aging, under the assumption that the light-absorption properties of POA were negligibly

influenced by aging. Most of the variability in $MAC_{SOA}(\lambda)$ discussed above is therefore related to experiment-to-experiment differences rather than to the extent of OH exposure, as it is also shown below.

4.3 Solubility of BrC in methanol and water

Fig. 6 shows the MAC_{OA}(370nm) determined from the water and methanol extracts against the MAC_{OA}(370nm) determined from the online measurements. The MAC_{OA}(370nm) from online measurements was estimated by subtracting the contribution of BC assuming a constant MAC_{BC}(370nm) = 13.7 $m^2.g^{-1}$ as obtained in this work (Table 1). We performed all the calculations and comparisons at λ = 370 nm, as the signal to noise ratio of the absorption coefficients measured by UV-visible spectroscopy and the contribution of BrC to the total carbonaceous absorption are highest at this wavelength. The MAC of the extracts was computed from the k_{OA} through Mie calculations. Repetition of both water and methanol extracts yielded results that were consistent within 10% (Fig. S11). Average raw absorption spectra are shown in Fig. S12.

~~Fig. 6B shows excellent correlation between the MAC values obtained from the the k_{OA} of the methanol extracted OA with the in-situ method described above~~. Fig. 6B shows excellent correlation between the MAC_{OA}(370nm) values obtained from the kOA of the solvent-extracted OA with the in-situ method described above. The Pearson correlation coefficient was 0.8, for both solvents. This correlation suggests that none of the assumptions employed in either method led to substantial errors in precision, providing direct support for our results. A similar relationship was observed between k_{OA} and the MAC_{OA}(370nm) determined from the online measurements (Fig. S13), showing that this relationship is not sensitive to assumptions underlying the Mie calculations. It further suggests that the wide variability observed in the MAC_{OA} values of different burns, as seen Fig. 6, most likely reflects real variability in the optical properties of POA and SOA rather than random noise or experimental errors in the retrieved quantities. MAC_{OA} retrieved based on the k_{OA} of the water soluble OA show substantially more scatter than observed in Fig. 6B (for both primary and aged data), suggesting a variable extraction efficiency in the case of water, which we also attribute to variability in the OA composition.

~~The orthogonal, uncertainty weighted linear regression in Fig. 6B shows that the methanol extracts explain 46 ± 10% of the online MAC. (Note that, in this analysis, aged OA refers to the sum of POA and SOA for aged samples.) Considering the simplifying assumptions that were necessary for our Mie analysis and those related to online MAC_{OA} calculations, we consider this an adequate agreement. In particular, the assumption of a perfect extraction efficiency of OA in methanol may have been violated (see Section 3.4). Conversely, the fit in Fig. 6A~~

~~indicates that the apparent MAC of water-soluble species was a fourth of the respective methanol MAC, according to the slope of only 12 ± 3%. . This strong disagreement shows that the BrC in our samples was hardly water soluble, even for the most aged samples. As we expect that the majority of OA in our samples formed by wood pyrolysis (Di Blasi, 2008; Corbin et al., 2015b; Shafizadeh, 1984), we can compare our results directly to those of Chen and Bond (2010), who also found that primary wood-pyrolysis BrC was water insoluble. Moreover, the water-insoluble nature of the light-absorbing components of SOA is in line with the results by Bruns et al. (2016) who showed that the precursors of SOA in these experiments were predominantly aromatic compounds.~~

The data in Fig. 6B show that the methanol extracts correspond to a MAC about 50% smaller than the online data. The scatter in the data is significantly reduced for the aged data (note that, in this analysis, aged OA refers to the sum of POA and SOA, since the reported values represent all OA after aging). This reduced scatter is expected, considering that aging is likely to result in more-spherical particles. We have assumed particle sphericity when interpreting the SMPS data and performing the Mie analysis. While the propagation of quantifiable uncertainties leads to an error estimate of ~25%, considering the simplifiations that were necessary for the Mie analysis, we consider a 50% closure to be an adequate agreement. Despite this, we cannot exclude additional methanol insoluble brown carbon. Conversely, the fit in Fig. 6A indicates that the apparent MAC of water-soluble species was a fourth of the respective methanol MAC, according to the slope of only 12 ± 3%. Only the aged data have been fit to illustrate this point. This strong disagreement shows that the BrC in our samples was hardly water soluble, even for the most aged samples. As we expect that the majority of OA in our samples formed by wood pyrolysis (Di Blasi, 2008; Corbin et al., 2015b; Shafizadeh, 1984), we can compare our results directly to those of Chen and Bond (2010), who also found that primary wood-pyrolysis BrC was water insoluble. Moreover, the poor water solubility of the light absorbing components of SOA (Zhang et al., 2011) is in line with the results by Bruns et al. (2016) who showed that SOA precursors during these experiments were predominantly aromatic compounds.

4.4 Comparison of k_{OA} with literature

The results above highlight the variability in the OA absorption properties. In this section, we discuss potential reasons for this variability and compare our results to literature. Fig. 7 shows the imaginary refractive index of methanol-extracted OA at 370 nm, $k_{OA,methanol}$(370nm) (Eq. (8)), as a function of M_{BC}/M_{OA} and aging. The data are plotted against M_{BC}/M_{OA} instead of f_{OA} to allow for a direct comparison with literature (see Fig. S14 for a plot against f_{OA}). An approximately linear trend of $k_{OA,methanol}$(370nm) with M_{BC}/M_{OA} is seen in log space. This aging-

independent relationship may be useful in, for example, atmospheric scenarios where wood-burning OA is a dominant aerosol component but its exact degree of aging is unknown. The decrease of M_{BC}/M_{OA} caused by formation of SOA during aging results in a concurrent decrease of $k_{OA,methanol}$(370nm), implying that $k_{SOA} < k_{POA}$. This result is consistent with the smaller MAC of SOA compared to POA obtained from online measurements (Table 1) and with recent results reported by Sumlin et al. (2017) . We emphasize that the derived quantity here is the imaginary refractive index *k* of the total aged OA, not the SOA.

The increase of $k_{OA,methanol}$(370nm) with increasing M_{BC}/M_{OA} indicates that the OA compounds present at higher M_{BC}/M_{OA} absorbed more efficiently than at low M_{BC}/M_{OA}. If the variability in M_{BC}/M_{OA} was driven partly by OA partitioning, then this implies that lower-volatility compounds were more absorbing than high-volatility compounds, consistent with the results by Saleh et al. (2014) who investigated the relation between OA absorption and volatility using thermodesorber measurements. A correlation between k_{OA} and M_{BC}/M_{OA} has also been reported by Lu et al. (2015). ~~The parameterizations reported by these authors are included in Fig. 7, both showing a smaller trend with M_{BC}/M_{OA} than seen in our data.~~ The parameterizations reported by these authors are included in Fig. 7, where the wavelength dependence reported by those authors has been used to adjust their parameterizations to 370nm. Despite these differences, our results confirm the generality of the correlation proposed by Saleh et al. (2014), but using a method that is independent of potential biases related to internal mixing effects, filter-based absorption measurements or Mie calculations. Indeed, we emphasize that the k_{OA} obtained here is a lower limit: as our approach does not account for the OA extraction efficiency; $k_{OA,methanol}$(370nm) may be underestimated by up to a factor of ~2, based on Fig. 6B.

5. ATMOSPHERIC IMPLICATIONS

In this section, we seek to estimate the relative importance of OA absorption at different wavelengths relative to that of the total carbonaceous aerosol as a function of aging. For these calculations, the MAC(λ) values for the different components and their relative mass abundance are required. We used the power law parameters reported above to generate continuous $MAC_{BC}(\lambda)$, $MAC_{POA}(\lambda)$, and $MAC_{SOA}(\lambda)$ functions together with their associated uncertainties (Fig. 8A), which allow the extrapolation of these parameters in the range [280nm; 880nm].

The contributions of the different components as a function of OH exposure were calculated by assuming that SOA production follows the first order decay of its precursors, i.e., the reaction with OH. Under this assumption, the time-dependent mass concentration of SOA compared to POA can be expressed as

$$M_{\mathrm{SOA,WLC}}(t)/M_{\mathrm{POA,WLC}}(t) = M_{\mathrm{SOAP,WLC}}/M_{\mathrm{POA,WLC}} \times \left(1 - \exp\left(-k_{\mathrm{OH}} OH_{\mathrm{exp}}\right)\right) \quad (21)$$

In this equation, $M_{\mathrm{SOA,WLC}}(t)$, $M_{\mathrm{POA,WLC}}(t)$ and $M_{\mathrm{SOAP,WLC}}$ are the wall loss corrected mass concentrations of SOA, POA and the SOA potential (the maximum SOA formed upon the consumption of all precursors). k_{OH} represents an estimation of reaction rate of SOA precursors towards OH based on SOA production rates. By fitting the observed $M_{\mathrm{SOA,WLC}}(t)/M_{\mathrm{POA,WLC}}(t)$ against the OH exposure, k_{OH} and $M_{\mathrm{SOAP,WLC}}/M_{\mathrm{POA,WLC}}$ can be estimated. For these calculations, we have estimated the wall losses using two approaches as described in the SI.

~~The $M_{\mathrm{SOAP,WLC}}/M_{\mathrm{POA,WLC}}$ was on average equal to 7.8 (GSD = 1.4) and k_{OH} was estimated as 2.7×10^{-11} molecule^{-1} cm^3 (GSD = 1.4), consistent with the chemically speciated data obtained by a proton-transfer-reaction mass spectrometer (PTR-MS) (Bruns et al., 2016, 2017). These high rates and enhancement ratios indicate the rapid production of SOA.~~ The $M_{\mathrm{SOAP,WLC}}/M_{\mathrm{POA,WLC}}$ was on average equal to 7.8 (GSD = 1.4) and kOH was estimated as 2.7×10^{-11} molecule^{-1} cm^3 (GSD = 1.4), consistent with the SOA precursors chemical nature measured (e.g. PAH and phenol derivatives) by a proton-transfer-reaction mass spectrometer (PTR-MS) (Bruns et al., 2016, 2017). These high rates and enhancement ratios indicate the rapid production of SOA.

Based on the bulk gas phase measurements of SOA precursors (Bruns et al., 2016), the obtained enhancements are consistent with high bulk SOA yields of ~50%. These high values are not surprising, considering the nature of these gases (e.g. PAH and phenol derivatives), the low temperatures (263 K), and the relatively high concentrations (Aged OA ~100 μg m^{-3}) at which the experiments have been conducted (Bruns et al. 2016).

Combining these calculated enhancements with the average contributions of POA in primary emissions, the evolution of f_{OA} with aging was determined and is shown in Fig. 8B. The uncertainties in Fig. 8B (dotted lines) represent one standard deviation on f_{OA} obtained by a Monte Carlo propagation of uncertainties due to experiment-to-experiment variability, fitting errors and wall loss correction errors (see SI). While this calculation represents a simplification of the SOA production mechanisms (the dependence of SOA yields on OH exposures/multigeneration chemistry and OA mass concentrations was neglected), it results in residuals much smaller than the experiment-to-experiment variability. We therefore used these calculations to assess the relative contribution of OA to the total

carbonaceous absorption. We show in Fig. 8C that below 400 nm and upon aging, the absorption coefficient of the total organics was at least as high as the one of BC.

Using the MAC values of the different components (in $m^2\ g^{-1}$), their abundance (in $g\ m^{-3}$) and the solar irradiance data (S, in $W\ m^{-2}\ nm^{-1}$) calculated at sea level for a cloudless day, the fractional energy transfer due to the BrC light absorption relative to that due to the total carbonaceous aerosol absorption , $W_{\mathrm{OA}}(OH_{\mathrm{exp}})$, in air masses dominated by residential burning emissions can be determined as

$$W_{\mathrm{OA}}(OH_{\mathrm{exp}}) = RET_{\mathrm{OA}}(OH_{\mathrm{exp}})/RET_{\mathrm{tot}}(OH_{\mathrm{exp}})$$

$$= \frac{\int_{300}^{880}\{M_{\mathrm{POA}}(OH_{\mathrm{exp}})\times MAC_{\mathrm{POA}}(\lambda)+M_{\mathrm{SOA}}(OH_{\mathrm{exp}})\times MAC_{\mathrm{SOA}}(\lambda)\}\times S(\lambda)\times d\lambda}{\int_{300}^{880}\{M_{\mathrm{BC}}(OH_{\mathrm{exp}})\times MAC_{\mathrm{BC}}(\lambda)+M_{\mathrm{POA}}(OH_{\mathrm{exp}})\times MAC_{\mathrm{POA}}(\lambda)+M_{\mathrm{SOA}}(OH_{\mathrm{exp}})\times MAC_{\mathrm{SOA}}(\lambda)\}\times S(\lambda)\times d\lambda} \quad (22)$$

Here, $RET_{\mathrm{OA}}(OH_{\mathrm{exp}})$ and $RET_{\mathrm{tot}}(OH_{\mathrm{exp}})$ denote the rate of energy transfer per volume (in $W\ m^{-3}$) to the air mass in question due to light absorption by OA and the total carbonaceous aerosol, respectively. We note that while $RET_{\mathrm{OA}}(OH_{\mathrm{exp}})$ and $RET_{\mathrm{tot}}(OH_{\mathrm{exp}})$ are extensive properties, $W_{\mathrm{OA}}(OH_{\mathrm{exp}})$ does not depend on the loading or scattering/lensing, provided that scattering/lensing similarly affects BC and OA present in the same air mass (e.g. BC and OA have a similar size distribution).

We also note that $W_{\mathrm{OA}}(OH_{\mathrm{exp}})$ depends on the photon flux, $S(\lambda)$, but we consider this dependence to be trivial compared to the variability in the aerosol emissions and their light absorbing properties (error bars considering these variabilities are shown in Fig. 8D). Errors in W_{OA} were propagated by Monte Carlo simulations using the uncertainties from the estimated MAC values of BC and OA fractions and the variability in f_{OA}. Our ~~error~~ sensitivity analysis suggests that the major part of the variance in predicting W_{OA} for primary emissions stems from the variability in the POA mass fraction. In contrast, the SOA mass absorption cross-sections at lower wavelengths are the most critical factor for assessing the relative importance of BrC absorptivity in aged emissions.

Fig. 8D shows that the fractional energy transfer to the air mass, W_{OA}, due to the absorption by the primary organic aerosol was around 10% of that of the total carbonaceous aerosol for our samples. This percentage is comparable to that observed by Fu et al. (2012), in spite of f_{OA} in their samples being much higher, because of the high OA MACs in our samples (Table 1). Moreover, with aging, the fraction of OA is enhanced, resulting in a sizeable increase W_{OA}, from ~0.1 to ~0.3 (Fig. 8D), highlighting that SOA formation in biomass burning plumes is an atmospherically relevant source of BrC. We note that our data are more representative of flaming conditions. More data are needed

on the chemical nature of primary particulate emissions and of the contributing SOA precursors as well as the absorptivity of these primary and secondary products, for better constraining the influence of biomass-burning related BrC on the Earth's climate.

6. CONCLUSIONS

We determined wavelength-dependent MAC values of BC, POA and SOA, as well as k_{OA} for methanol and water extracts of fresh and aged OA, for wood-burning emissions through smog-chamber experiments. To our knowledge, this is the first determination of these properties for wood-burning OA. We showed that the MAC_{OA}(370nm) values calculated based on k_{OA} through Mie analysis correlated well with those estimated from online filter based measurements. This correlation between independent MAC measurements supports the quality of both methods. While MAC_{OA}(370nm) values computed based on $k_{OA,methanol}$ were a 2-fold lower than those estimated from online filter based measurements, calculations based on $k_{OA,water}$ could only explain 12% of the measured absorption, suggesting that BrC species in POA and SOA are mostly water insoluble. The MAC_{OA} was found to vary by more than one order of magnitude. Similar to previous reports, this variability could be related to the variability in the ratio of the mass concentrations of BC and OA (M_{BC}/M_{OA}) due to very different mechanisms of oxidative aging and burn-to-burn variability.

The MAC_{POA} and MAC_{SOA} determined for wavelengths between 370 and 660 nm followed a power-law dependence on λ with an absorption Ångström exponent of 4.6 and 5.6 for POA and SOA, respectively. In addition to following this power law, the MACs of POA and SOA appeared to be constant for OH exposures up to 40 x 10^6 molecules cm^{-3} h.

The mean MAC_{POA}(370nm) obtained under our conditions was 5.5 $m^2\ g^{-1}$, considerably higher than previously reported values for open biomass burning. ~~The mean MAC_{SOA}(370nm) was 2.4 $m^2\ g^{-1}$ under our experimental conditions, 2.3 times lower than the mean MAC_{POA}(370nm) but approximately an order of magnitude higher than MAC values estimated for ambient oxygenated aerosols or reported for SOA from biogenic and traditional anthropogenic precursors~~. The mean MAC_{SOA}(370nm) was 2.2 $m^2\ g^{-1}$ (one-sigma variability: 1.6 – 3.1 $m^2\ g^{-1}$ according to a GSD = 1.39) under our experimental conditions, 2.3 times lower than the mean MAC_{POA}(370nm) but approximately an order of magnitude higher than MAC values estimated for ambient oxygenated aerosols or

reported for SOA from biogenic and traditional anthropogenic precursors. We propose that the important role of oxidized phenols and aromatics in forming wood-burning SOA (Bruns et al., 2016) is the cause of this observation. This hypothesis is supported by our observed reaction rates with OH, and by the water-insolubility of the BrC in aged OA.

Overall, the absorption by organic aerosols was estimated to contribute 10-30% of the total solar absorption of wood-combustion aerosols, where 10% represents the primary OA and 30% the aged OA. SOA formation in biomass burning plumes is therefore an atmospherically relevant source of BrC.

Acknowledgements. The research leading to these results has received funding from the European Research Council grant (ERC-CoG 615922-BLACARAT) and by the Competence Centre Energy and Mobility (CCEM) project 807.

References

Alexander, D. T. L., Crozier, P. A. and Anderson, J. R.: Brown carbon spheres in East Asian outflow and their optical properties., Science, 321(5890), 833–6, doi:10.1126/science.1155296, 2008.

Andreae, M. O. and Gelencsér, A.: Black carbon or brown carbon? the nature of light-absorbing carbonaceous aerosols, Atmos. Chem. Phys., 6(3), 3419–3463, doi:10.5194/acpd-6-3419-2006, 2006.

Barmet, P., Dommen, J., DeCarlo, P. F., Tritscher, T., Praplan, A. P., Platt, S. M., Prévôt, A. S. H., Donahue, N. M. and Baltensperger, U.: OH clock determination by proton transfer reaction mass spectrometry at an environmental chamber, Atmos. Meas. Tech., 5(3), 647–656, doi:10.5194/amt-5-647-2012, 2012.

Bertrand, A., Stefenelli, G., Bruns, E. A., Pieber, S. M., Prévôt, A. S. H., Wortham, H., Temime-roussel, B., Slowik, J. G., Haddad, I. El and Marchand, N.: Primary emissions and secondary aerosol production potential from woodstoves for residential heating : influence of the stove technology and combustion efficiency, Atmos. Environ., 169, doi:10.1016/j.atmosenv.2017.09.005, 2017.

Di Blasi, C.: Modeling chemical and physical processes of wood and biomass pyrolysis, Prog. Energy Combust. Sci., 34(1), 47–90, doi:10.1016/j.pecs.2006.12.001, 2008.

Bond, T. C., Habib, G. and Bergstrom, R. W.: Limitations in the enhancement of visible light absorption due to mixing state, J. Geophys. Res. Atmos., 111(20), 1–13, doi:10.1029/2006JD007315, 2006.

Bond, T. C., Doherty, S. J., Fahey, D. W., Forster, P. M., Berntsen, T., Deangelo, B. J., Flanner, M. G., Ghan, S., Kärcher, B., Koch, D., Kinne, S., Kondo, Y., Quinn, P. K., Sarofim, M. C., Schultz, M. G., Schulz, M., Venkataraman, C., Zhang, H., Zhang, S., Bellouin, N., Guttikunda, S. K., Hopke, P. K., Jacobson, M. Z., Kaiser, J. W., Klimont, Z., Lohmann, U., Schwarz, J. P., Shindell, D., Storelvmo, T., Warren, S. G. and Zender, C. S.: Bounding the role of black carbon in the climate system: a scientific assessment, J. Geophys. Res. Atmos., 118(11), 5380–5552, doi:10.1002/jgrd.50171, 2013.

Bruns, E. A., Krapf, M., Orasche, J., Huang, Y., Zimmermann, R., Drinovec, L., Močnik, G., El-Haddad, I., Slowik, J. G., Dommen, J., Baltensperger, U. and Prévôt, A. S. H.: Characterization of primary and secondary wood combustion products generated under different burner loads, Atmos. Chem. Phys., 15(5), 2825–2841, doi:10.5194/acp-15-2825-2015, 2015.

Bruns, E. A., El Haddad, I., Slowik, J. G., Kilic, D., Klein, F., Baltensperger, U. and Prévôt, A. S. H.: Identification of significant precursor gases of secondary organic aerosols from residential wood combustion., Sci. Rep., 6, 27881, doi:10.1038/srep27881, 2016.

Bruns, E. A., Slowik, J. G., Haddad, I. El, Kilic, D., Klein, F., Dommen, J., Temime-Roussel, B., Marchand, N., Baltensperger, U. and Prévôt, A. S. H.: Characterization of gas-phase organics using proton transfer reaction time-of-flight mass spectrometry : fresh and aged residential wood combustion emissions, Atmos. Chem. Phys., 705–720, doi:10.5194/acp-17-705-2017, 2017.

Cavalli, F., Viana, M., Yttri, K. E., Genberg, J. and Putaud, J.-P.: Toward a standardised thermal-optical protocol for measuring atmospheric organic and elemental carbon: the EUSAAR protocol, Atmos. Meas. Tech., 3(1), 79–89, doi:doi:10.5194/amt-3-79-2010, 2010.

Chakrabarty, R. K., Moosmüller, H., Chen, L. W. A., Lewis, K., Arnott, W. P., Mazzoleni, C., Dubey, M. K., Wold, C. E., Hao, W. M. and Kreidenweis, S. M.: Brown carbon in tar balls from smoldering biomass combustion, Atmos. Chem. Phys., 10(13), 6363–6370, doi:10.5194/acp-10-6363-2010, 2010.

Chakrabarty, R. K., Arnold, I. J., Francisco, D. M., Hatchett, B., Hosseinpour, F., Loria, M., Pokharel, A. and Woody, B. M.: Black and brown carbon fractal aggregates from combustion of two fuels widely used in asian rituals, J. Quant. Spectrosc. Radiat. Transf., 122, 25–30, doi:10.1016/j.jqsrt.2012.12.011, 2013.

Chen, Y. and Bond, T. C.: Light absorption by organic carbon from wood combustion, Atmos. Chem. Phys., 10, 1773-1787, doi:10.5194/acp-10-1773-2010, 2010.

China, S., Mazzoleni, C., Gorkowski, K., Aiken, A. C., and Dubey, M. K.: Morphology and mixing state of individual freshly emitted wildfire carbonaceous particles, Nat. Commun., 4, 1–7, doi:10.1038/ncomms-3122-2013, 2013.

Ciarelli, G., Haddad, I. El, Bruns, E. and Aksoyoglu, S., Möhler, O., Baltensperger, U. and Prévôt, A. S. H.: Constraining a hybrid volatility basis set model for aging of wood burning emissions using smog chamber experiments, Geosci. Model. Dev., 2303-2320, doi:10.5194/gmd-2303-2017, 2017.

Clarke, A., McNaughton, C., Kapustin, V., Shinozuka, Y., Howell, S., Dibb, J., Zhou, J., Anderson, B. E., Brekhovskikh, V., Turner, H. and Pinkerton, M.: Biomass burning and pollution aerosol over North America: organic components and their influence on spectral optical properties and humidification response, J. Geophys. Res. Atmos., 112(12), 1–13, doi:10.1029/2006JD007777, 2007.

Collaud Coen, M., Weingartner, E., Apituley, A., Ceburnis, D., Fierz-Schmidhauser, R., Flentje, H., Henzing, J. S., Jennings, S. G., Moerman, M., Petzold, A., Schmid, O., and Baltensperger, U.: Minimizing light absorption measurement artifacts of the Aethalometer: evaluation of five correction algorithms, Atmos.Meas. Tech., 3, 457–474, doi:10.5194/amt-3-457-2010, 2010.

Corbin, J. C., Lohmann, U., Sierau, B., Keller, A., Burtscher, H. and Mensah, A. A.: Black carbon surface oxidation and organic composition of beech-wood soot aerosols, Atmos. Chem. Phys., 15(20), 11885–11907, doi:10.5194/acp-15-11885-2015, 2015a.

Corbin, J. C., Keller, A., Lohmann, U., Burtscher, H., Sierau, B. and Mensah, A. A.: Organic emissions from a wood stove and a pellet stove before and after simulated atmospheric aging, Aerosol Sci. Technol., 49(11), 1037–1050, doi:10.1080/02786826.2015.1079586, 2015b.

Corbin, J. C.; Pieber, S. M.; Czech, H.; Zanatta, M.; Jakobi, G.; Massabò, D.; Orasche, J.; El Haddad, I.; Mensah, A. A.; Stengel, B.; Drinovec, L.; Mocnik, G.; Zimmermann, R.; Prévôt, A. S. H. and Gysel, M.: Brown and black carbon emitted by a marine engine operated on heavy fuel oil and distillate fuels: optical properties, size distributions and emission factors, J. Geophys. Res. Atmos., 123, 6175-6195, doi:10.1029/2017JD027818, 2018.

DeCarlo, P. F., Kimmel, J. R., Trimborn, A., Northway, M. J., Jayne, J. T., Aiken, A. C., Gonin, M., Fuhrer, K., Horvath, T., Docherty, K. S., Worsnop, D. R. and Jimenez, J. L.: Field deployable, high resolution, time-of-flight aerosol mass spectrometer, Anal. Chem., 78(24), 8281–8289, doi:8410.1029/2001JD001213, 2006.

Denier Van Der Gon, H. A. C., Bergström, R., Fountoukis, C., Johansson, C., Pandis, S. N., Simpson, D. and Visschedijk, A. J. H.: Particulate emissions from residential wood combustion in Europe - revised estimates and an evaluation, Atmos. Chem. Phys., 15(11), 6503–6519, doi:10.5194/acp-15-6503-2015, 2015.

Drinovec, L., Močnik, G., Zotter, P., Prévôt, A. S. H., Ruckstuhl, C., Coz, E., Rupakheti, M., Sciare, J., Müller, T., Wiedensohler, A. and Hansen, A. D. A.: The "dual-spot" aethalometer: an improved measurement of aerosol black carbon with real-time loading compensation, Atmos. Meas. Tech., 8(5), 1965–1979, doi:10.5194/amt-8-1965-2015, 2015.

Feng, Y., Ramanathan, V. and Kotamarthi, V. R.: Brown carbon: a significant atmospheric absorber of solar radiation, Atmos. Chem. Phys., 13(17), 8607–8621, doi:10.5194/acp-13-8607-2013, 2013.

Forrister, H., Liu, J., Scheuer, E., Dibb, J., Ziemba, L., Thornhill, L. K., Anderson, B., Diskin, G., Perring, A. E., Schwarz, J. P., Campuzan-Jost, P., Day, D. A., Palm, B. B., Jimenez, J. L., Nenes, A., Weber, R. J.: Evolution of brown carbon in wildfire plumes, Gephys. Res. Lett.,42, 4623-4630, doi: 10.1002/2015GL063897, 2015.

Fu, J. S., Hsu, N. C., Gao, Y., Huang, K., Li, C., Lin, N. H. and Tsay, S. C.: Evaluating the influences of biomass burning during 2006 BASE-ASIA: a regional chemical transport modeling, Atmos. Chem. Phys., 12(9), 3837–3855, doi:10.5194/acp-12-3837-2012, 2012.

847 Grieshop, A. P., Logue, J. M., Donahue, N. M. and Robinson, A. L.: Laboratory investigation of photochemical
848 oxidation of organic aerosol from wood fires – part 1: measurement and simulation of organic aerosol evolution,
849 Atmos. Chem. Phys., 9, 2227–2240, doi:10.5194/acp-9-2227-2009, 2009.

850 Gueymard, C.; Myers, D.; Emery, K.: Proposed Reference Irradiance Spectra for Solar Energy Systems Testing,
851 Solar Energy, 73, 6, 443–467, 2002.
852

853 Gundel, L. A., Dod, R. L., Rosen, H. and Novakov.: The relationship between optical attenuation and black carbon
854 concentration for ambient and source particles, Sci. Total Environ., 36, 197-202, 1984.

855 Haslett, S. L.; Thomas, J. C.; Morgan, W. T.; Hadden, R.; Liu, D.; Allan, J. D.; Williams, P. I.; Keita, S.; Liousse, C.
856 and Coe, H.: Highly controlled, reproducible measurements of aerosol emissions from combustion of a common
857 African biofuel source, Atmos. Chem. Phys, 385-403, doi:10.5194/acp-18-385-2018, 2018.
858

859 Hecobian, A., Zhang, X., Zheng, M., Frank, N., Edgerton, E. S. and Weber, R. J.: Water-soluble organic aerosol
860 material and the light-absorption characteristics of aqueous extracts measured over the southeastern United States,
861 Atmos. Chem. Phys., 10(13), 5965–5977, doi:10.5194/acp-10-5965-2010, 2010.

862 Heringa, M. F., DeCarlo, P. F., Chirico, R., Tritscher, T., Dommen, J., Weingartner, E., Richter, R., Wehrle, G.,
863 Prévôt, A. S. H. and Baltensperger, U.: Investigations of primary and secondary particulate matter of different wood
864 combustion appliances with a high-resolution time-of-flight aerosol mass spectrometer, Atmos. Chem. Phys.,
865 11(12), 5945–5957, doi:10.5194/acp-11-5945-2011, 2011.

866 Hoffer, A., Gelencsér, A., Guyon, P., Kiss, G., Schmid, O., Frank, G. P., Artaxo, P. and Andreae, M. O.: Optical
867 properties of humic-like substances (HULIS) in biomass-burning aerosols, Atmos. Chem. Phys., 6, 3563-3570,
868 doi:10.5194/acp-6-3563-2006, 2006.

869 Jo, D. S., Park, R. J., Lee, S., Kim, S. W. and Zhang, X.: A global simulation of brown carbon: Implications for
870 photochemistry and direct radiative effect, Atmos. Chem. Phys., 16(5), 3413–3432, doi:10.5194/acp-16-3413-2016,
871 2016.

872 Kirchstetter, T. W., Novakov, T. and Hobbs, P. V.: Evidence that the spectral dependence of light absorption by
873 aerosols is affected by organic carbon, J. Geophys. Res. D Atmos., 109(21), 1–12, doi:10.1029/2004JD004999,
874 2004.

875 Krapf, M., Haddad, I. El, Bruns, E. A., Haddad, I. El, Molteni, U., Daellenbach, K. R., Prévôt, A. S. H.,
876 Baltensperger, U., Dommen, J. : Labile peroxides in secondary organic aerosol labile peroxides in secondary organic
877 aerosol, Chem 1, 603–616, doi:10.1016/j.chempr.2016.09.007, 2016.

878 Lack, D. A. and Langridge, J. M.: On the attribution of black and brown carbon light absorption using the Ångström
879 exponent, Atmos. Chem. Phys., 13(20), 10535–10543, doi:10.5194/acp-13-10535-2013, 2013.

880 Lambe, A. T., Cappa, C. D., Massoli, P., Onasch, T. B., Forestieri, S. D., Martin, A. T., Cummings, M. J.,
881 Croasdale, D. R., Brune, W. H., Worsnop, D. R. and Davidovits, P.: Relationship between oxidation level and
882 optical properties of secondary organic aerosol, Environ. Sci. Technol., 47(12), 6349–6357, doi:10.1021/es401043j,
883 2013.

884 Laskin, A., Laskin, J. and Nizkorodov, S. A.: Chemistry of atmospheric brown carbon, Chem. Rev., 115(10), 4335–
885 4382, doi:10.1021/cr5006167, 2015.

886 Lee, H. J., Aiona, P. K., Laskin, A., Laskin, J. and Nizkorodov, S. A.: Effect of solar radiation on the optical
887 properties and molecular composition of laboratory proxies of atmospheric brown carbon, Environ. Sci. Technol.,
888 48(17), 10217–10226, doi:10.1021/es502515r, 2014.

889 Lewis, K., Arnott, W. P., Moosmüller, H. and Wold, C. E.: Strong spectral variation of biomass smoke light
890 absorption and single scattering albedo observed with a novel dual-wavelength photoacoustic instrument, J.

Geophys. Res. Atmos., 113(16), 1–14, doi:10.1029/2007JD009699, 2008.

Lin, G., Penner, J. E., Flanner, M. G., Sillman, S., Xu, L. and Zhou, C.: Radiative forcing of organic aerosol in the atmosphere and on snow: effect of SOA and brown carbon, J. Geophys. Res. - Atmos., 119(12), 7453–7476, doi:10.1002/2013JD021186.Received, 2014.

Liu, J., Scheuer, E., Dibb, J., Ziemba, L. D., Thornhill, K. L., Anderson, B. E., Wisthaler, A., Mikoviny, T., Devi, J. J., Bergin, M. and Weber, R. J.: Brown carbon in the continental troposphere, Geophys. Res. Lett., 41, 2191–2195, doi:10.1002/2013GL058976, 2014.

Liu, J., Lin, P., Laskin, A., Laskin, J., Kathmann, S. M., Wise, M., Caylor, R., Imholt, F., Selimovic, V. and Shilling, J. E.: Optical properties and aging of light absorbing secondary organic aerosol, Atmos. Chem. Phys., 16, 12815-12827, doi:10.5194/acp-2016-482, 2016.

Liu, D. T., Whitehead, J., Alfarra, M. R., Reyes-Villegas, E., Spracklen, D. V., Reddington, C. L., Kong, S. F., Williams, P. I., Ting, Y. C., Haslett, S., Taylor, J. W., Flynn, M. J., Morgan, W. T., McFiggans, G., Coe, H., and Allan, J. D.: Black-carbon absorption enhancement in the atmosphere determined by particle mixing state, Nat. Geosci., 10, 184–188, doi:10.1038/ngeo2901, 2017.

Liu, P. F., Abdelmalki, N., Hung, H. M., Wang, Y., Brune, W. H. and Martin, S. T.: Ultraviolet and visible complex refractive indices of secondary organic material produced by photooxidation of the aromatic compounds toluene and m-xylene, Atmos. Chem. Phys., 15(3), 1435–1446, doi:10.5194/acp-15-1435-2015, 2015a.

Liu, P. S. K., Deng, R., Smith, K. A., Jayne, J. T., Williams, L.R., Canagaratna, M. R., Moore, K., Onasch, T. B., Worsnop, D.R., and Deshler, T.: Transmission efficiency of an aerodynamic focusing lens system: comparison of model calculations and laboratory measurements for the aerodyne aerosol mass spectrometer,Aerosol Sci. Tech., 41, 721–733, 2007.

Liu, S., Aiken, A. C., Gorkowski, K., Dubey, M. K., Cappa, C. D., Williams, L. R., Herndon, S. C., Massoli, P., Fortner, E. C., Chhabra, P. S., Brooks, W. A., Onasch, T. B., Jayne, J. T., Worsnop, D. R., China, S., Sharma, N., Mazzoleni, C., Xu, L., Ng, N. L., Liu, D., Allan, J. D., Lee, J. D., Fleming, Z. L., Mohr, C., Zotter, P., Szidat, S. and Prévôt, A. S. H.: Enhanced light absorption by mixed source black and brown carbon particles in UK winter, Nat. Commun., 8435, doi:10.1038/ncomms9435, 2015b.

Lu, Z., Streets, D. G., Winijkul, E., Yan, F., Chen, Y., Bond, T. C., Feng, Y., Dubey, M. K., Liu, S., Pinto, J. P. and Carmichael, G. R.: Light absorption properties and radiative effects of primary organic aerosol emissions, Environ. Sci. Technol., 49, 4868–4877, doi:10.1021/acs.est.5b00211, 2015.

Massabò, D., Caponi, L., Bernardoni, V., Bove, M. C., Brotto, P., Calzolai, G., Cassola, F., Chiari, M., Fedi, M. E., Fermo, P., Giannoni, M., Lucarelli, F., Nava, S., Piazzalunga, A., Valli, G., Vecchi, R. and Prati, P.: Multi-wavelength optical determination of black and brown carbon in atmospheric aerosols, Atmos. Environ., 108, 1–12, doi:10.1016/j.atmosenv.2015.02.058, 2015.

Massabò, D., Bernardoni, V., Bove, M. C., Brunengo, A., Cuccia, E., Piazzalunga, A., Prati, P., Valli, G. and Vecchi, R.: A multi-wavelength optical set-up for the characterization of carbonaceous particulate matter, J. Aerosol Sci., 60, 34–46, doi:10.1016/j.jaerosci.2013.02.006, 2013.

Moosmüller, H., Chakrabarty, R. K. and Arnott, W. P.: Aerosol light absorption and its measurement: A review, J. Quant. Spectrosc. Radiat. Transf., 110(11), 844–878, doi:10.1016/j.jqsrt.2009.02.035, 2009.

Moosmüller, H., Chakrabarty, R. K., Ehlers, K. M. and Arnott, W. P.: Absorption Ångström coefficient, brown carbon, and aerosols: Basic concepts, bulk matter, and spherical particles, Atmos. Chem. Phys., 11(3), 1217–1225, doi:10.5194/acp-11-1217-2011, 2011.

Petzold, A. and Schönlinner, M.: Multi-angle absorption photometry - A new method for the measurement of aerosol light absorption and atmospheric black carbon, J. Aerosol Sci., 35(4), 421–441,

doi:10.1016/j.jaerosci.2003.09.005, 2004.

Platt, S. M., El Haddad, I., Zardini, A. A., Clairotte, M., Astorga, C., Wolf, R., Slowik, J. G., Temime-Roussel, B., Marchand, N., Ježek, I., Drinovec, L., Močnik, G., Möhler, O., Richter, R., Barmet, P., Bianchi, F., Baltensperger, U. and Prévôt, A. S. H.: Secondary organic aerosol formation from gasoline vehicle emissions in a new mobile environmental reaction chamber, Atmos. Chem. Phys., 13(18), 9141–9158, doi:10.5194/acp-13-9141-2013, 2013.

Romonosky, D. E., Laskin, A., Laskin, J. and Nizkorodov, S. A.: High-resolution mass spectrometry and molecular characterization of aqueous photochemistry products of common types of secondary organic aerosols, J. Phys. Chem. A, 119(11), 2594–2606, doi:10.1021/jp509476r, 2015.

Saleh, R., Hennigan, C. J., McMeeking, G. R., Chuang, W. K., Robinson, E. S., Coe, H., Donahue, N. M. and Robinson, A. L.: Absorptivity of brown carbon in fresh and photo-chemically aged biomass-burning emissions, Atmos. Chem. Phys., 13(15), 7683–7693, doi:10.5194/acp-13-7683-2013, 2013.

Saleh, R., Robinson, E. S., Tkacik, D. S., Ahern, A. T., Liu,S., Aiken, A. C., Sullivan, R. C., Presto, A. A., Dubey, M. K., Yokelson, R. J., Donahue, N. M., and Robinson, A.L.: Brownness of organics in aerosols from biomass burning linked to their black carbon content, Nat. Geosci., 7, 2–5, doi:10.1038/ngeo2220, 2014.

Schauer, J. J., Mader, B. T., Deminter, J. T., Heidemann, G., Bae, M. S., Seinfeld, J. H., Flagan, R. C., Cary, R. A., Smith, D., Huebert, B. J., Bertram, T., Howell, S., Kline, J. T., Quinn, P., Bates, T., Turpin, B., Lim, H. J., Yu, J. Z., Yang, H., and Keywood, M. D.: ACE-Asia intercomparison of a thermaloptical method for the determination of particle-phase organic and elemental carbon, Environ. Sci. Technol., 37, 993–1001, 2003.

Shafizadeh, F.: The chemistry of pyrolysis and combustion. The chemistry of solid Wood, ACS Symp. Ser., 207, 489–529, doi:10.1021/ba-1984-0207.ch013\r10.1021/ba-1984-0207.ch013, 1984.

Slowik, J. G., E. S. Cross, J.-H. Han, P. Davidovits, T. B. Onasch, J. T. Jayne, L. R. Williams, M. R. Canagaratna, D. R. Worsnop, R. K. Chakrabarty, H. Moosmüller, W. P. Arnott, J. P. Schwarz, R. S. Gao, D. W. Fahey, G. L. Kok and A. Petzold.: An inter-comparison of instruments measuring black carbon content of soot particles, *Aerosol Sci. Technol. 41*, 3, 295-314, 2007.

Sumlin, B. J., Pandey, A., Walker, M. J., Pattison, R. S., Williams, B. J., and Chakrabarty, R. K.: Atmospheric photooxidation diminishes light absorption by primary brown carbon aerosol from biomass burning, Environ. Sci. Technol. Lett., 4(12), 540-545, doi:10.1021/acs.estlett.7b00393, 2017.

Sun, H., Biedermann, L. and Bond, T. C.: Color of brown carbon: A model for ultraviolet and visible light absorption by organic carbon aerosol, Geophys. Res. Lett., 34(17), 1–5, doi:10.1029/2007GL029797, 2007.

Ulevicius, V., Bozzetti, C., Vlachou, A., Plauškait, K., Mordas, G., Dudoitis, V., Abbaszade, G., Remeikis, V., Garbaras, A., Masalaite, A., Blees, J., Fröhlich, R., Dällenbach, K. R., Canonaco, F., Slowik, J. G., Dommen, J., Zimmermann, R., Schnelle-kreis, J., Salazar, G. A. and Agrios, K., Szidat, S., Haddad, I. El., and Prévôt, A. S. H. : Fossil and non-fossil source contributions to atmospheric carbonaceous aerosols during extreme spring grassland fires in Eastern Europe, Atmos. Chem. Phys., 16, 5513–5529, doi:10.5194/acp-16-5513-2016, 2016.

Wang, X., Heald, C. L., Ridley, D. A., Schwarz, J. P., Spackman, J. R., Perring, A. E., Coe, H., Liu, D. and Clarke, A. D.: Exploiting simultaneous observational constraints on mass and absorption to estimate the global direct radiative forcing of black carbon and brown carbon, Atmos. Chem. Phys., 14(20), 10989–11010, doi:10.5194/acp-14-10989-2014, 2014.

Weingartner, E., Saathoff, H., Schnaiter, M., Streit, N., Bitnar, B. and Baltensperger, U.: Absorption of light by soot particles: determination of the absorption coefficient by means of aethalometers, J. Aerosol Sci., 34(10), 1445–1463, doi:10.1016/S0021-8502(03)00359-8, 2003.

Yang, H. and Yu, J. Z.: Uncertainties in charring correction in the analysis of elemental and organic carbon in atmospheric particles by thermal/optical methods, Environ. Sci. Technol., 36 (23), 5199–5204, 2002.

Zhang, X., Lin, Y. –H., Surratt, J. D., Zotter, P. and Prévôt, A. S. H.: Light-absorbing soluble organic aerosol in Los-Angeles and Atlanta: A contrast in secondary organic aerosol, Geophys. Res. Lett, 38, 2011.

Zhao, R., Lee, A. K. Y., Huang, L., Li, X., Yang, F. and Abbatt, J. P. D.: Photochemical processing of aqueous atmospheric brown carbon, Atmos. Chem. Phys., 15(11), 6087–6100, doi:10.5194/acp-15-6087-2015, 2015.

Zotter, P., Herich, H., Gysel, M., El-Haddad, I., Zhang, Y., Močnik, G., Hüglin, C., Baltensperger, U., Szidat, S. and Prévôt, A. S. H.: Evaluation of the absorption Ångström exponents for traffic and wood burning in the Aethalometer based source apportionment using radiocarbon measurements of ambient aerosol, Atmos. Chem. Phys., 17, 4229-4249, doi:10.5194/acp-17-4229-2017, 2017.

Zotter, P., Herich, H., Gysel, M., El-haddad, I., Zhang, Y. and Močnik, G.: Evaluation of the absorption Ångström exponents for traffic and wood burning in the Aethalometer-based source apportionment using radiocarbon measurements of ambient aerosol, , 4229–4249, doi:10.5194/acp-17-4229-2017, 2017.

Old Figure

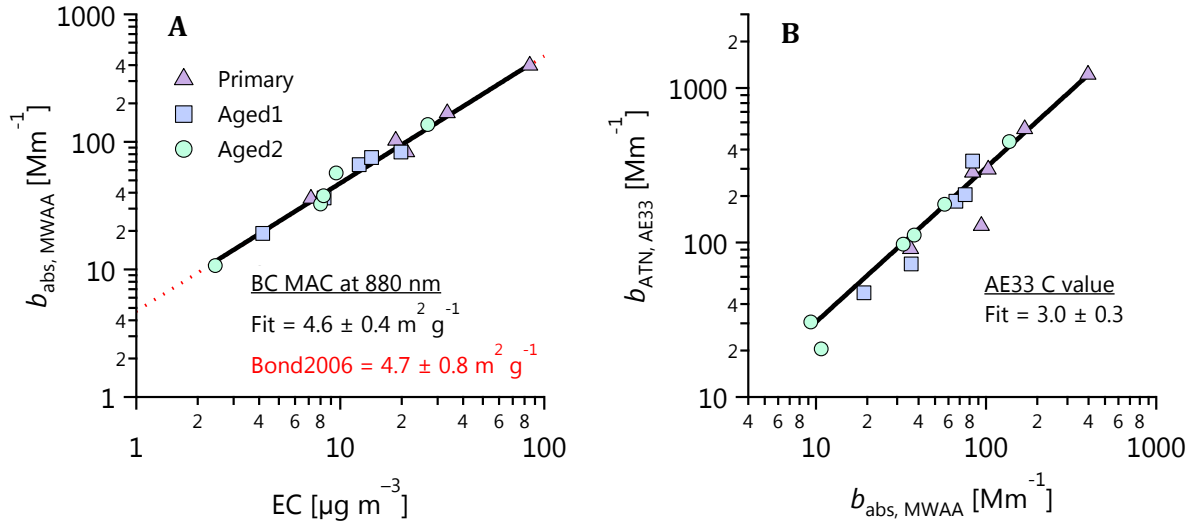

New Figure

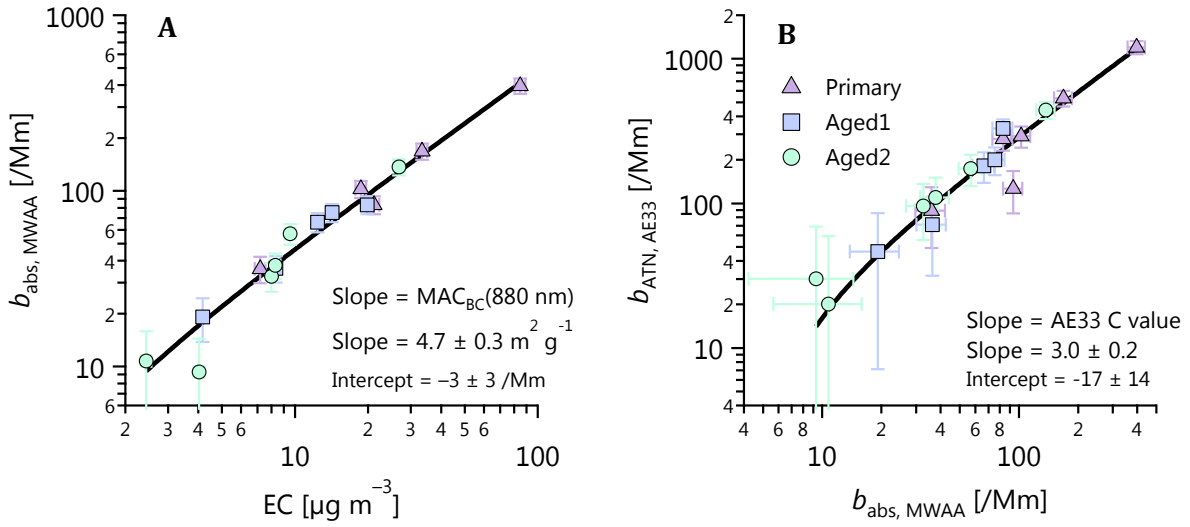

Figure 1: Determination of (A) MAC_{BC}(880nm) and (B) aethalometer *C* value using MWAA absorption measurements, thermal/optical EC (EUSAAR2 protocol) and aethalometer attenuation measurements. MWAA absorption measurements at 880 nm is determined by extrapolating the absorption coefficients at 850 nm using an *α* determined from the ratio between the absorption coefficients at 850 nm and 635nm. The aerosols were either primary (no OH exposure), Aged 1 (~$1x10^7$ molec OH cm^{-3} h), or Aged 2 (~$4x10^7$ molec OH cm^{-3} h). No difference in MAC or *C* value was discernable with aging (see also Fig. S2). ~~Also shown is the MAC of pure BC recommended by Bond et al. (2006) (dotted line in A).~~ The *C* value derived from σ_{ATN} recommended by Drinovec et al. (2015) = 2.6 compares well with the value derived in Fig. 1B.

Old Figure

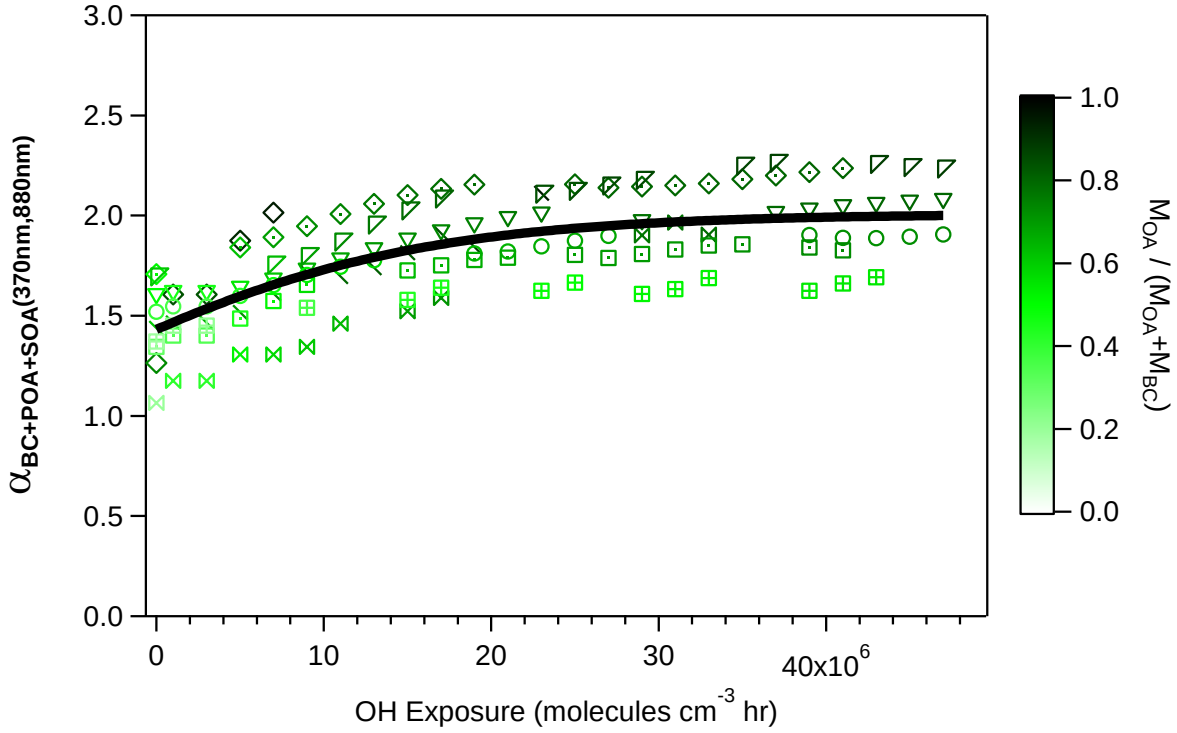

New Figure:

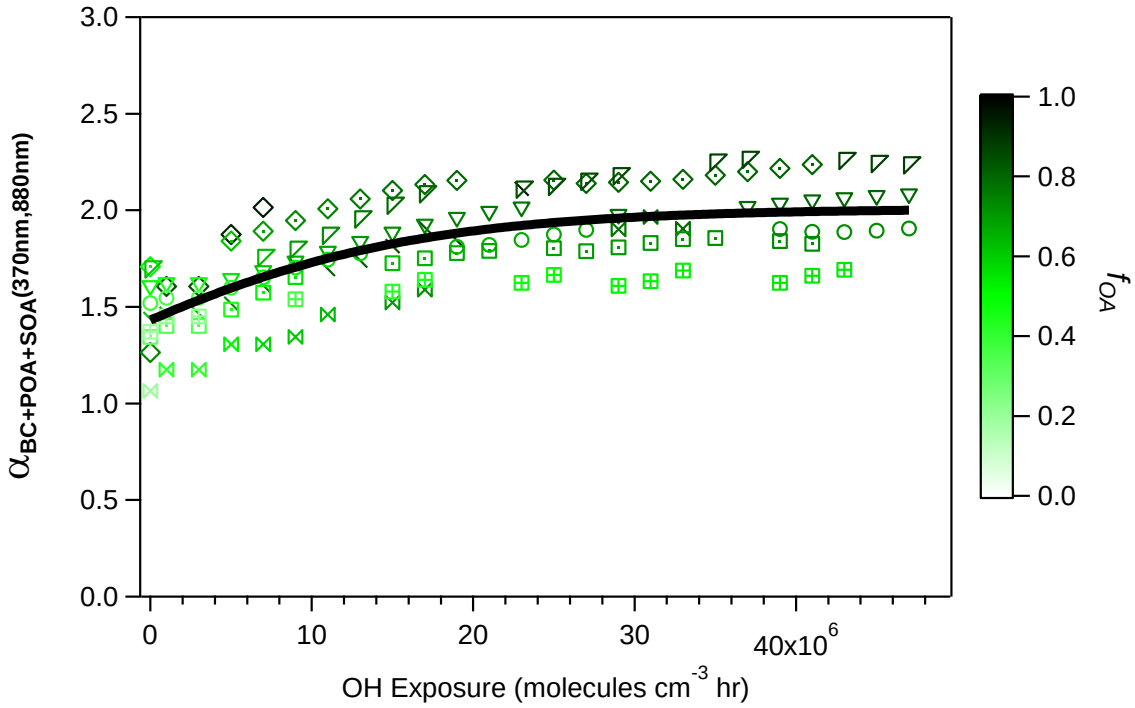

Figure 2: Evolution during photochemical aging of $\alpha_{\mathrm{BC+POA+SOA}}(370\mathrm{nm}, 880\mathrm{nm})$ (two-wavelength Ångström exponent calculated using total absorption data at 370 nm and 880 nm), where the different symbols denote individual experiments. Data are colored by the OA mass fraction $f_{\mathrm{OA}} = M_{\mathrm{OA}}/(M_{\mathrm{OA}} + M_{\mathrm{BC}})$. The black line is a fit to guide the eye.

Old Figure:

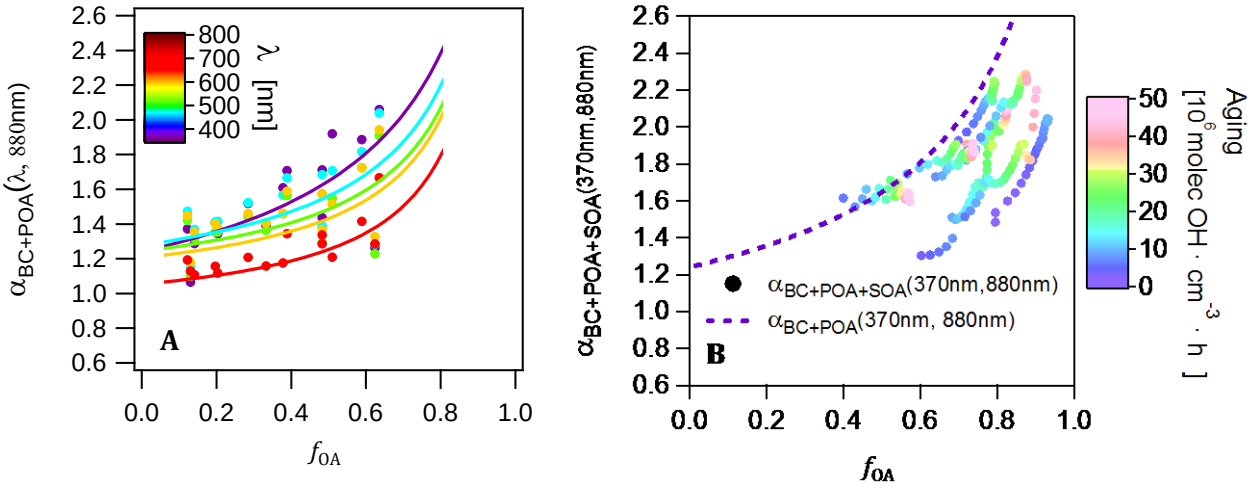

New Figure:

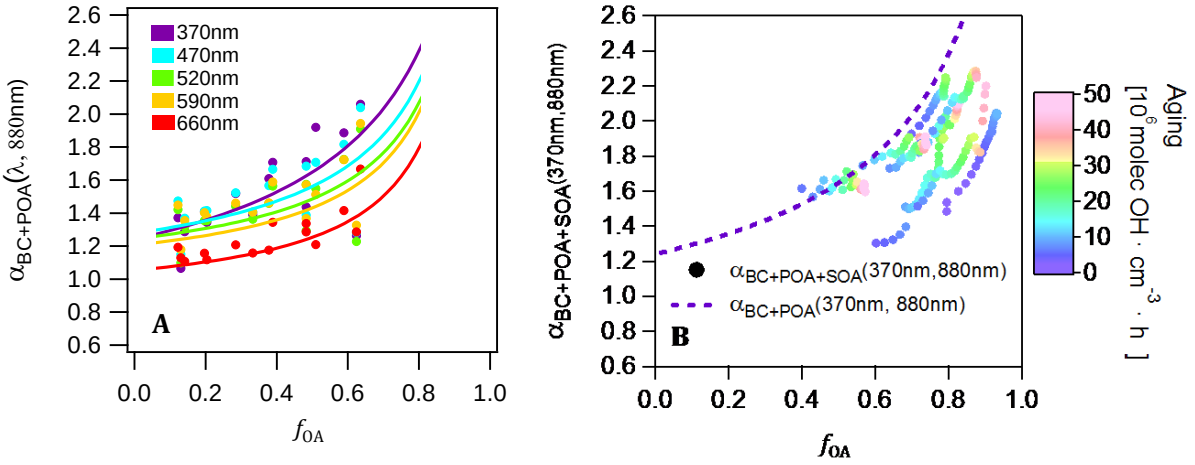

~~**Figure 3: (A) Relationship of $\alpha_{\mathrm{BC+POA}}(\lambda, 880\mathrm{nm})$ to f_{OA} for seven wavelengths. Lines are fits of Eq. (13) to the data. (B) Relationship of $\alpha_{\mathrm{BC+POA+SOA}}(370\mathrm{nm}, 880\mathrm{nm})$ to f_{OA} for several experiments. Data in (A) and (B) are colored by the wavelength and OH exposure, respectively.**~~

Figure 3: (A) Relationship of $\alpha_{\mathrm{BC+POA}}$ (λ, 880nm) to f_{OA} for seven wavelengths for primary emissions. Data are colored by the wavelength. Curves are fits of Eq. (13) to the data. Each point represents the average of one experiment and therefore the variability in f_{OA} is related to the variability in the emission composition between experiments. (B) Relationship of $\alpha_{\mathrm{BC+POA+SOA}}(370\mathrm{nm}, 880\mathrm{nm})$ to f_{OA} for several experiments for aged aerosols. Data are color coded by the OH exposure. The variability in f_{OA} is due to SOA formation with aging; data from several experiments are shown which explains the wide range of f_{OA} at low OH exposures. Note that more data are included in A than B, as primary emissions for some experiments were not aged.

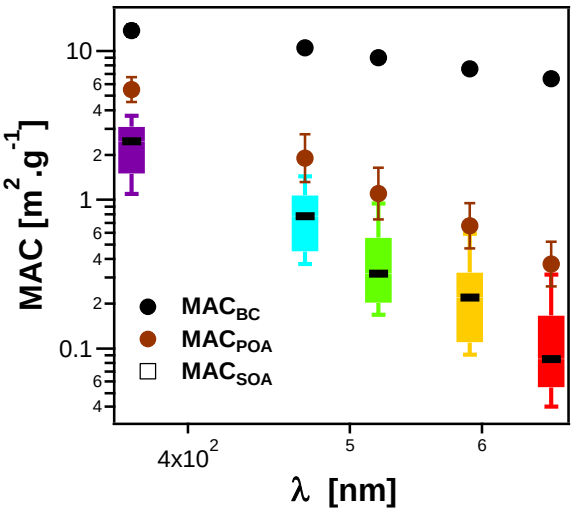

Figure 4: $MAC_{SOA}(\lambda)$ calculated from several smog chamber experiments plotted as box-whiskers as a function of wavelength (also shown by the color of the bars). The thick black lines, the boxes and the whiskers mark the medians, the quartiles and the 10th and the 90th percentiles, respectively. Also shown are the $MAC_{BC}(\lambda)$ and $MAC_{POA}(\lambda)$ reported in Table 1. Note that MAC_{SOA}(880nm) and MAC_{POA}(880nm) are zero by definition.

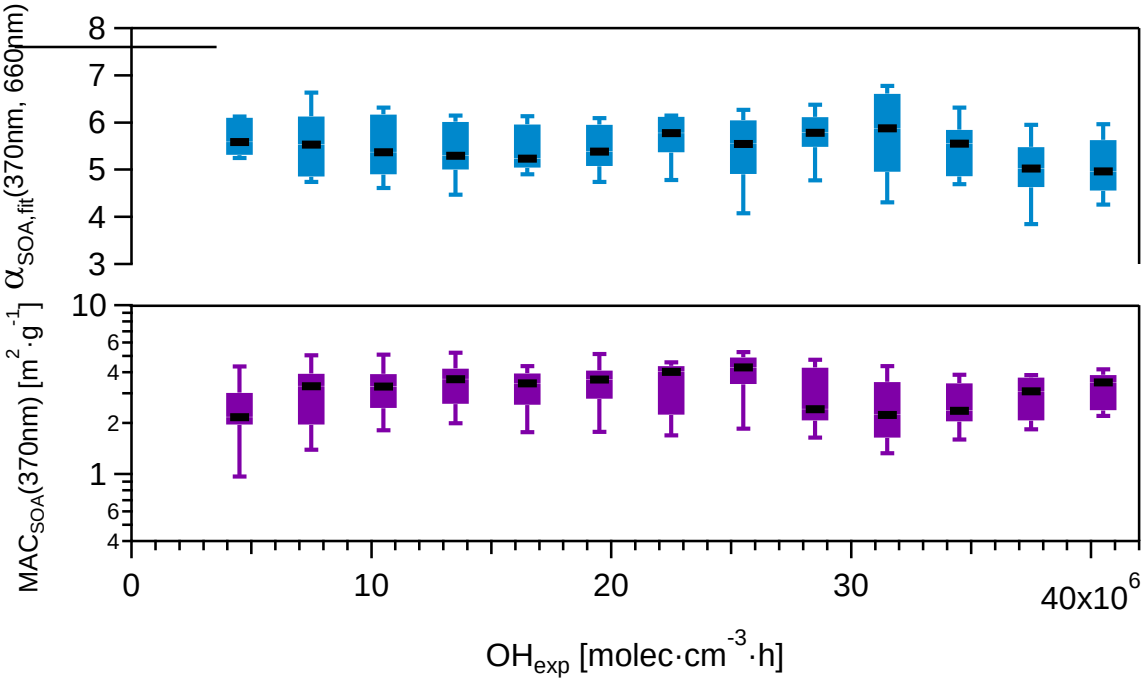

Figure 5: MAC_{SOA}(370nm) and $\alpha_{SOA,fit}$(370nm, 660nm) calculated from several smog chamber experiments plotted as a function of OH exposure. The box marks the 25th and 75th percentile, while the whiskers mark the 10th and the 90th percentile. MAC_{SOA}(370nm) was obtained using Eq. (19). $\alpha_{SOA,fit}$(370nm, 660nm) was obtained from fitting the MAC_{SOA} values in the range 370-660 nm for the different experiments against the wavelength. $\alpha_{SOA,fit}$(370nm, 660nm) is the slope of the linear fit applied after log transforming the data. $MAC_{SOA}(\lambda)$ for higher wavelengths are shown in Fig. S10.

Old Figure:

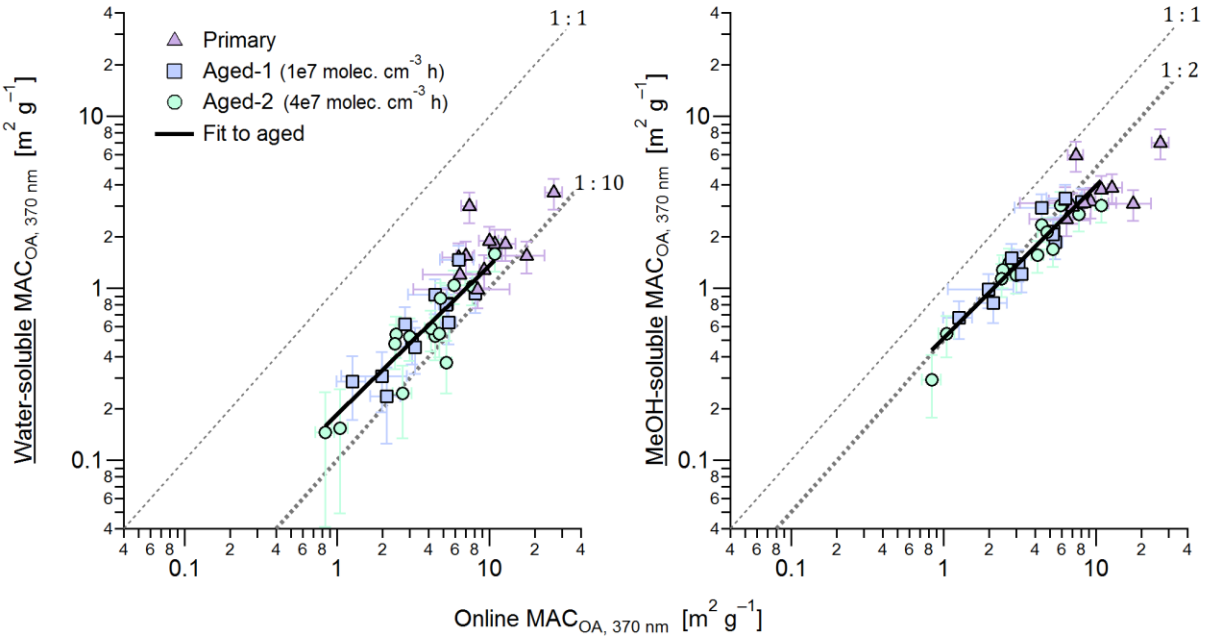

New Figure:

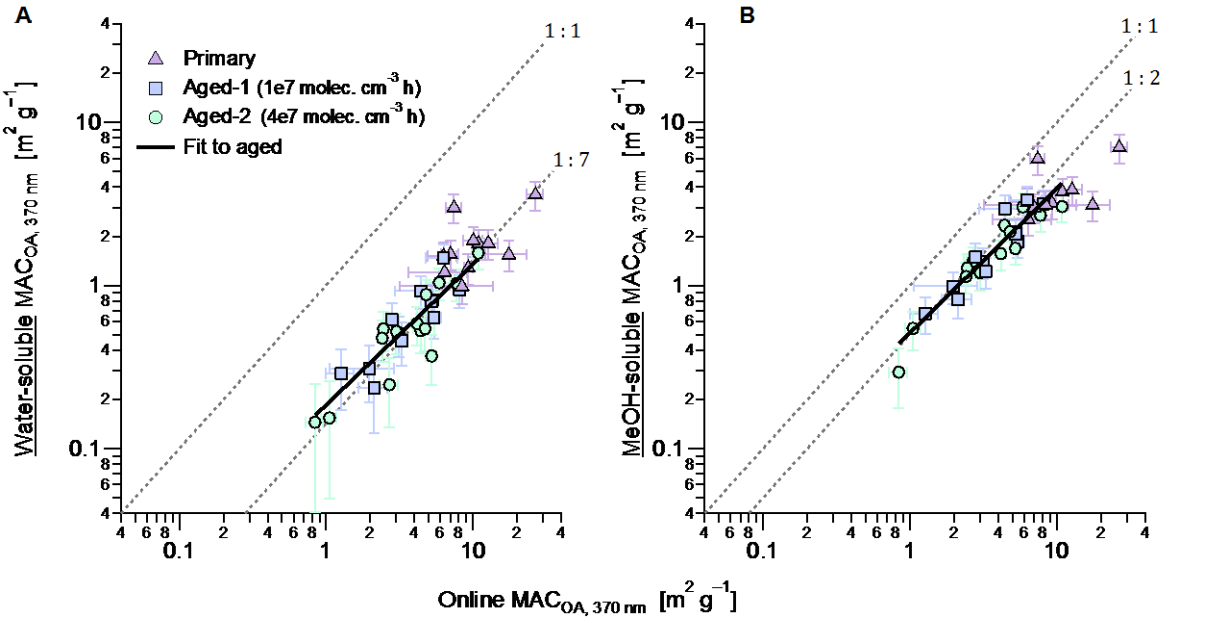

~~**Figure 6: Comparison of the MAC_{OA}(370nm) of aged aerosols determined from online and offline measurements of absorption. The offline filter extraction method directly quantified properties of total OA (ordinate), while the average of MAC_{SOA} and MAC_{POA} from the online measurements weighted with respective mass concentrations is shown on the abscissa. (A) offline measurements of water-soluble OA, (B) methanol-soluble OA.**~~

Figure 6: Comparison of the MAC_{OA}(370nm) of aged aerosols determined from online and offline absorption measurements. The offline filter-extraction method directly quantified properties of total OA (ordinate), while the average of MAC_{SOA} and MAC_{POA} weighted with respective mass concentrations is shown on the abscissa. The panels show offline measurements of (A) water-soluble OA, (B) methanol-soluble OA. Fits are to aged data only due to the

significantly smaller scatter of those data, although primary data on average follow similar trends. The fitted slopes and intercepts are, respectively, (A) 0.13 ± 0.02 and 0.05 ± 0.06 m^2g^{-1} and (B) 0.12 ± 0.1 and 0.38 ± 0.03 m^2g^{-1}.

Old Figure

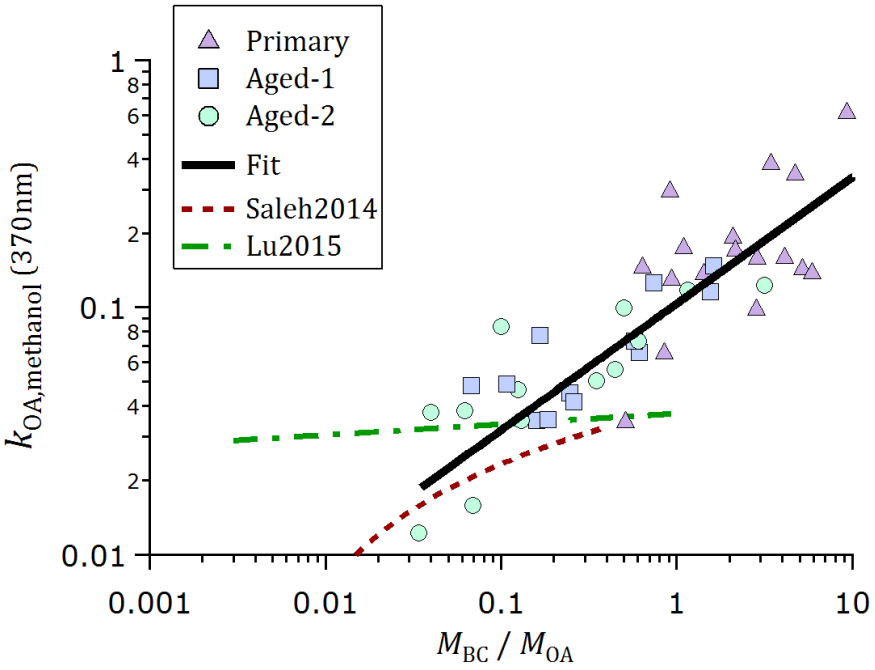

New Figure

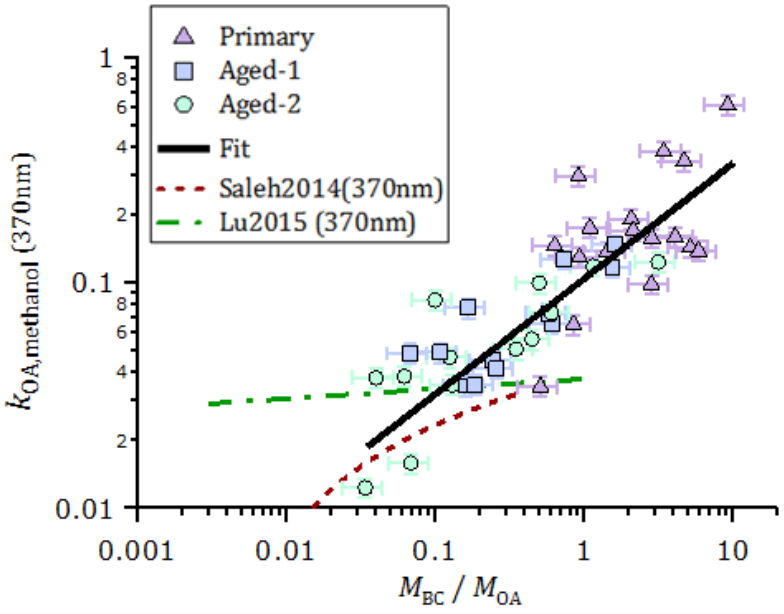

~~**Figure 7: Imaginary part of the OA refractive index at 370 nm, obtained from offline UV/vis spectroscopy of methanol OA extracts, plotted as a function of f_{OA}. The ordinary least-squares fit is $\log(k_{OA,370}) = \log(M_{BC}/M_{OA})(0.51 \pm 0.07) + (-0.98 \pm 0.05)$.**~~

Figure 7: Imaginary part of the OA refractive index at 370 nm, obtained from offline UV/vis spectroscopy of methanol OA extracts, plotted as a function of f_{OA}. The data could be empirically represented by a linear function in the log-log space, in the measurement range. The ordinary least-squares fit is $(k_{OA,nm}) = \log(M_{BC}/M_{OA})(0.51 \pm 0.07) + (-0.98 \pm 0.05)$. Also shown are parameterizations of k_{OA}(370 nm) for open burning against M_{BC}/M_{OA} estimated based on the online k_{OA} (550 nm) measurements in Saleh et al. (2014) and Lu et al. (2015), using the k_{OA} wavelength dependence reported by the respective authors.

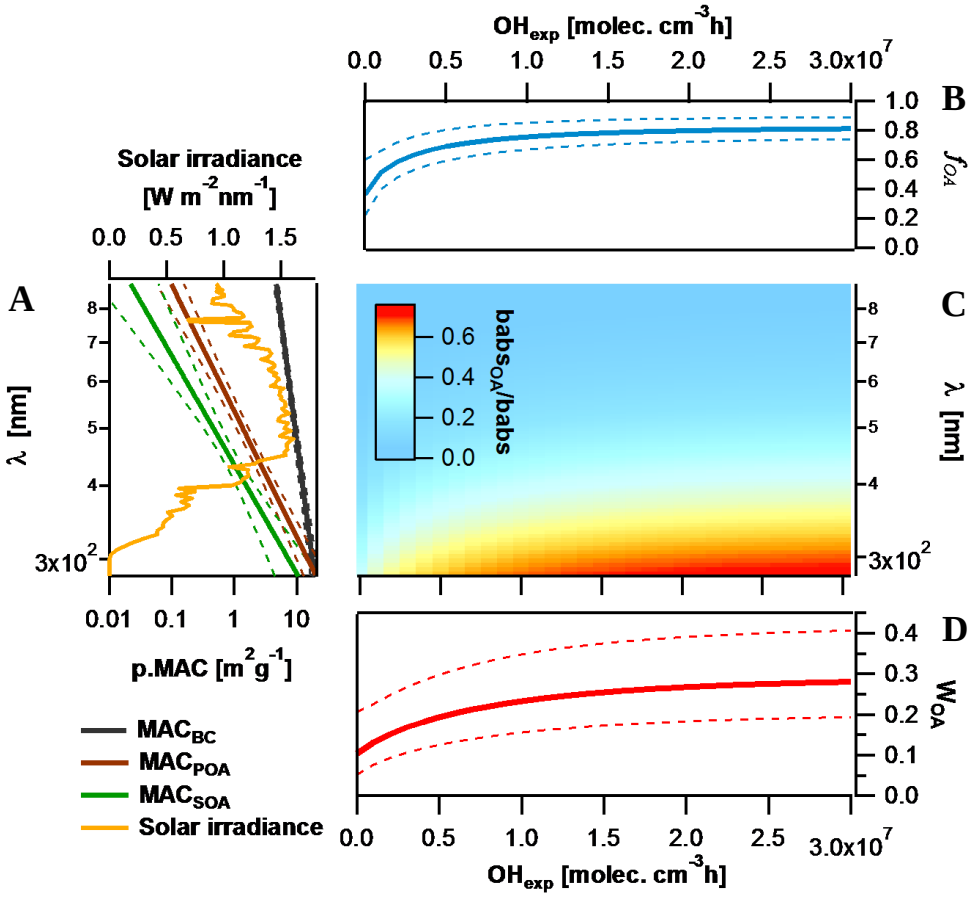

Figure 8: Impact of BrC absorption on total primary and secondary wood-burning-aerosol absorption. (A) MACs of different particle components (BC, POA and SOA) along with their corresponding standard deviations plotted as a function of wavelength based on smog chamber data and compared to the solar irradiance spectrum. (B) Species average relative abundance in the smog chamber (f_{OA}) plotted as a function of the OH exposure. (C) Image plot showing the OA absorption coefficient relative to the total aerosol absorption as a function of wavelength and OH exposure. (D) Rate of energy transfer due to BrC light absorption relative to the total carbonaceous aerosol absorption (W_{OA}) estimated as a function of aging using the solar flux, the fractions of the different components and their MACs.

Table 1: Geometric mean and standard deviations of the determined MACs of BC, POA and SOA at different wavelengths. Uncertainties were obtained from fits of Eq. (13) for $MAC_{BC,}$ MAC_{POA} , while for MAC_{SOA} uncertainties GSD values are geometric standard deviation values on the MAC_{SOA} average values from all experiments. These uncertainties do not include uncertainties related to the determination of MAC_{BC}(880nm). By definition, BrC absorbance at 880 nm is zero.

	BC		POA		SOA	
λ (nm)	GM (m^2 g^{-1})	GSD	GM (m^2 g^{-1})	GSD	GM (m^2 g^{-1})	GSD
370	13.7	1.1	5.5	1.21	2.2	1.39
470	10.5	1.06	1.9	1.45	0.72	1.61
520	9	1.04	1.1	1.49	0.34	1.75
590	7.6	1.03	0.67	1.42	0.2	1.97
660	6.5	1.01	0.37	1.41	0.09	2.42
880	4.6	0.7	0*		0*	

*By definition

Supporting information for:

Production of particulate brown carbon during atmospheric aging of residential wood-burning emissions

Nivedita K. Kumar[1], Joel C. Corbin[1*], Emily A. Bruns[1], Dario Massabó[2], Jay G. Slowik[1], Luka Drinovec[3,4], Griša Močnik[3,4], Paolo Prati[2], Athanasia Vlachou[1], Urs Baltensperger[1], Martin Gysel[1], Imad El-Haddad[1] and André S. H. Prévôt[1]

[1]Laboratory of Atmospheric Chemistry, Paul Scherrer Institute, 5232 Villigen, Switzerland

[2]Department of Physics & INFN, University of Genoa, via Dodecaneso 33, 16146, Genova, Italy

[3]Aerosol d.o.o, Kamniška 41, 1000 Ljubljana, Slovenia

[4]Condensed Matter Physics, Jožef Stefan Institute, 1000 Ljubljana, Slovenia

*Now at National Research Council Canada, Ottawa, Canada

Correspondence to: I. El-Haddad (imad.el-haddad@psi.ch), A. S. H. Prévôt (andre.prevot@psi.ch)

Wall loss correction

Solving the equations in Section 3.1 requires the determination of the time-dependent concentrations of the different absorbing species, which may be governed by their photochemical production or decay as well as by diffusion, electrostatic and gravitational losses to the walls. Assuming all particles are equally lost to the walls, an inert, non-volatile species, *X*, follows a first order decay:

$$X(t) = X(t_0) \cdot \exp(\tau^{-1}(t - t_0) \quad \text{(S1)}$$

Here, t and t_0 denote the time of interest and reference time, respectively. The time constant τ is the lifetime of X with respect to particle wall losses. We determined τ by fitting $b_{abs}(t, 880nm)$ to Equation S1. Only the last period of each experiment was chosen for fitting, when secondary organic aerosol production rates are smaller. On average, τ equals 3.9±0.8 hours for our chamber. The wall loss corrected absorption coefficient, $b_{abs}^{WLC}(t, 880\,nm)$, varied less than 8% throughout the experiment, with higher values in the first period of

measurements. Therefore we conclude that the first order decay is an appropriate approach for the wall loss correction of inert particulate properties. We ascribe the residual variations of $b_{\mathrm{abs}}^{\mathrm{WLC}}(t, 880\,nm)$ to a combination of uncertainties, including the aethalometer compensation parameter and possible small changes of MAC_{BC}(880nm) with aging.

For the extrapolation of our data to ambient environments we computed the average SOA mass formed as a function of OH exposure during the different experiments. This step requires the correction of OA mass for particle wall losses, which has been achieved by assuming two cases: (1) condensable oxidized gases do not interact with wall-deposited particles and (2) condensable oxidized gases condense at similar rates onto the suspended and wall-deposited particles (Pierce et al., 2008). We did not consider the deposition of oxidized vapors onto the clean Teflon walls, which would require knowledge of the saturation vapor pressures of the compounds, the condensed phase bulk properties and the vapor-wall equilibration rates. It is likely that the large particle condensational sinks utilized here (with a particle surface area concentration of several hundreds of μm^2 cm^{-3}), outcompeted vapor deposition onto the walls. Therefore, we consider the vapor deposition to the clean Teflon wall to be of a minor importance compared to burn-to-burn variability and other experimental uncertainties.

Solving the mass balance equations of the suspended organic aerosol, $[OA_{sus}(t)]$, and the organic aerosol on the walls yields the expressions in Equations (S2) and (S3), when considering scenario (1) and (2), respectively:

$$\left[M_{OA,wlc,1}(t)\right]=\left[M_{OA,sus}(t)\right]+\int_0^t \tau^{-1}\left[M_{OA,sus}(t)\right]dt \quad \text{(S2)}$$

$$\left[M_{OA,wlc,2}(t)\right]=\left[M_{OA,sus}(t)\right]*\exp(\tau^{-1}t) \quad \text{(S3)}$$

Here, $[M_{OA,wlc}(t)_j]$ is the wall-loss-corrected OA concentration. The results presented in Fig. 8 in the manuscript are the average time-series of all experiments considering both scenarios, and associated ranges entail both the experiment-to-experiment variability and the uncertainties related to wall loss corrections.

Supplementary figures

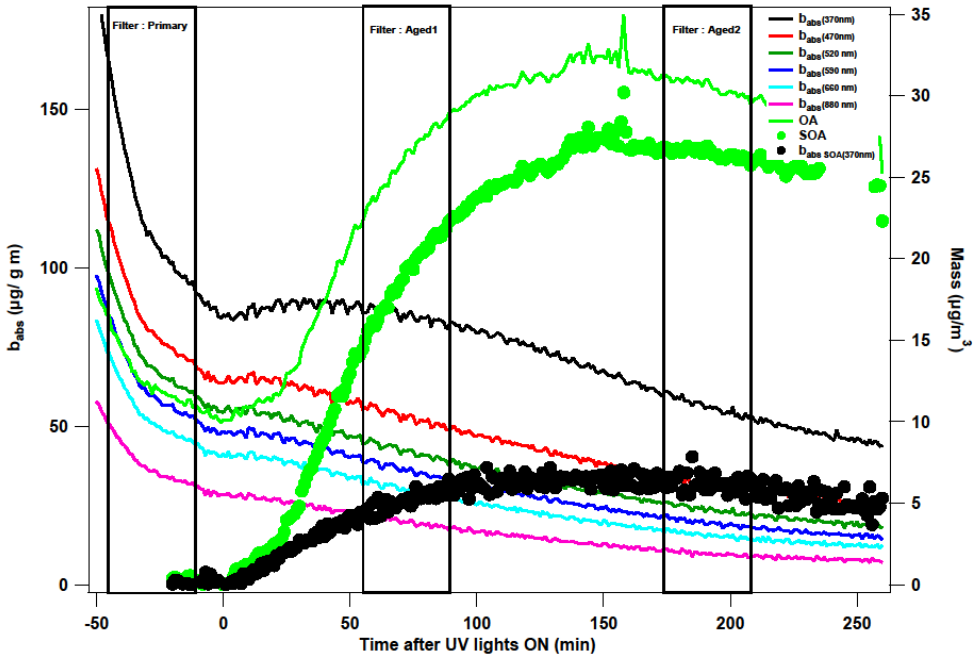

Figure S1: Absorption coefficients of fresh and aged emissions measured at 6 different wavelengths (i.e. 370 – 880 nm) using the aethalometer. The OA is measured using an AMS. Dotted lines are primary-subtracted OA (SOA) and absorption coefficient (b_{absSOA}(370nm)) . The black boxes mark the times where the primary, slightly aged (Aged1, OH exposure ~1x10^{7}molecules cm^{-3} h) and heavily aged filters (Aged2, OH exposure ~ 4x10^7 molecules cm^{-3} h) were collected.

Old Figure:

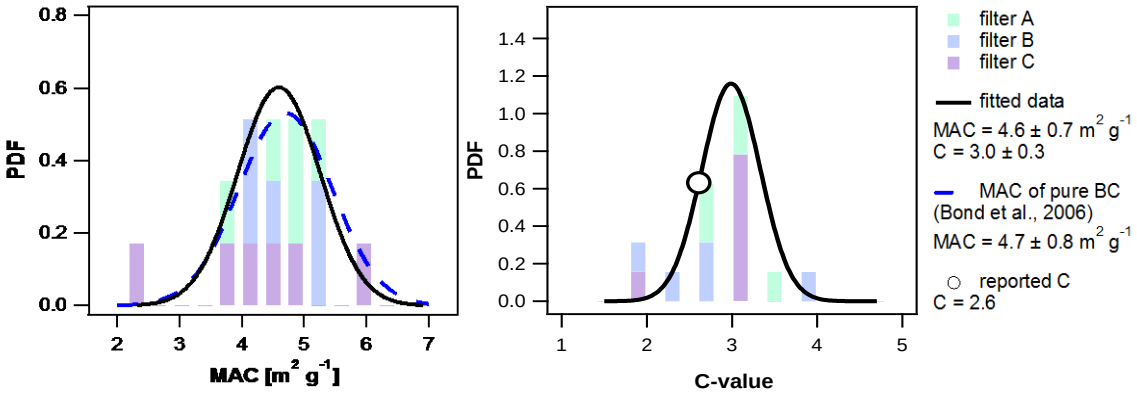

New Figure:

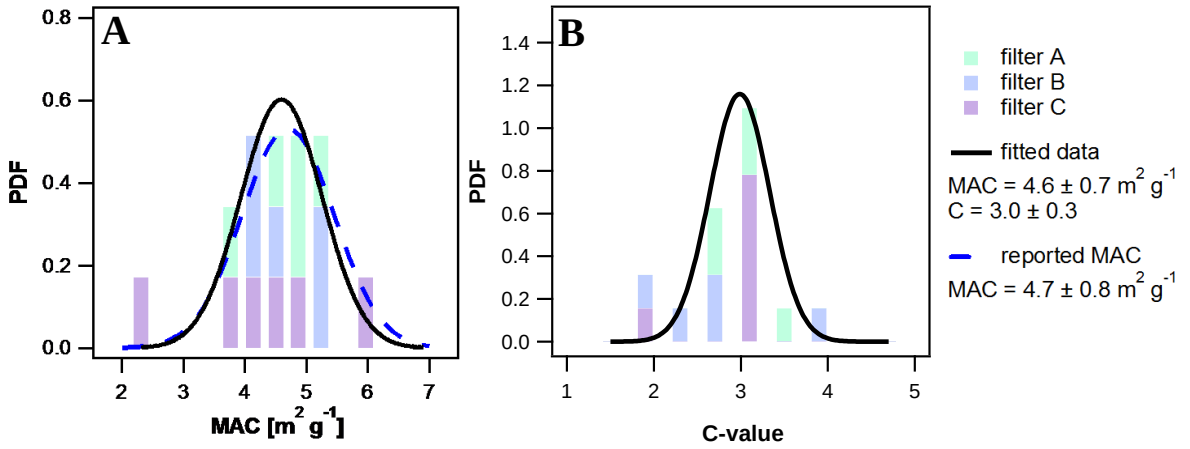

Figure S2: (a) Probability density function (PDF) comparing the MAC values determined by normalizing MWAA absorption measurements of offline primary (filter A), slightly aged (filter B: Aged1) and aged filter (filter C: Aged2) samples to EC (EUSAAR2) measurements of the same samples (bold line). A literature value for pure BC is also shown (Bond et al., 2006) (dashed blue line). (b) PDF comparing aethalometer attenutation measurements at 880 nm and MWAA absorption measurements at 850 nm to retrieve the aethalometer *C* value.

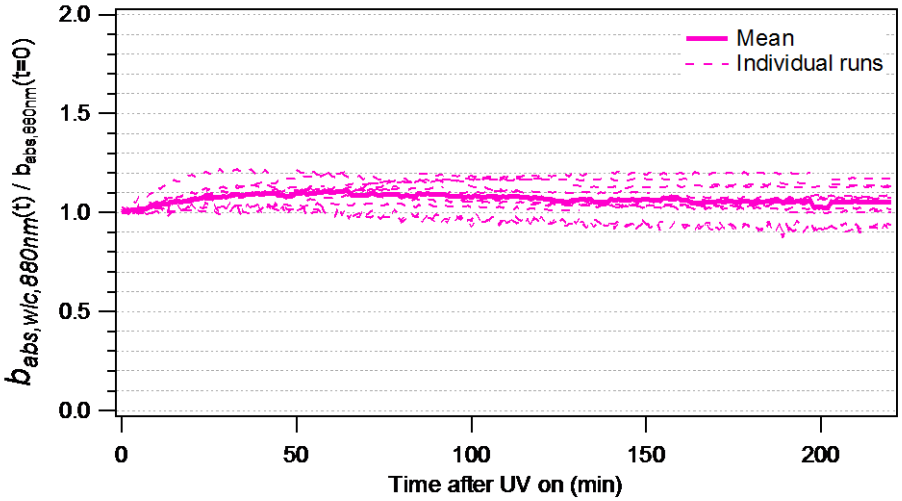

Figure S3: Wall-loss-corrected aethalometer absorption coefficient at 880 nm normalized to start-of-experiment absorption. The lack of any trend in this plot illustrates that the wall loss correction is appropriate and that only a negligible absorption increase occurs due to additional lensing by SOA.

Old Figure:

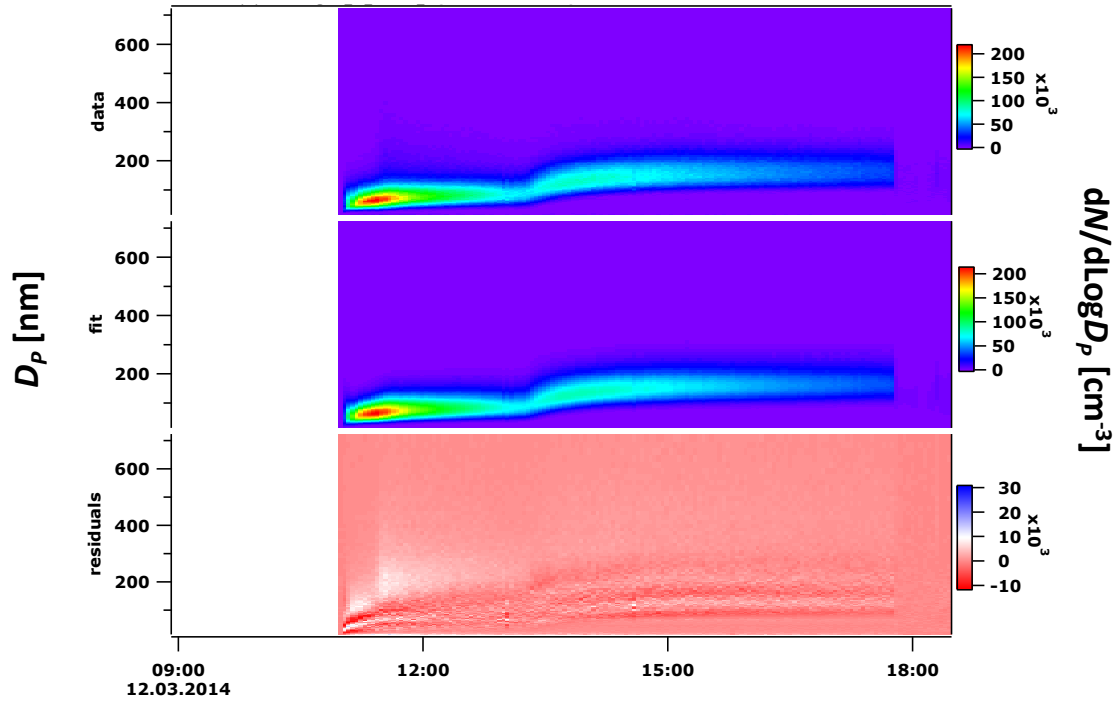

New Figure:

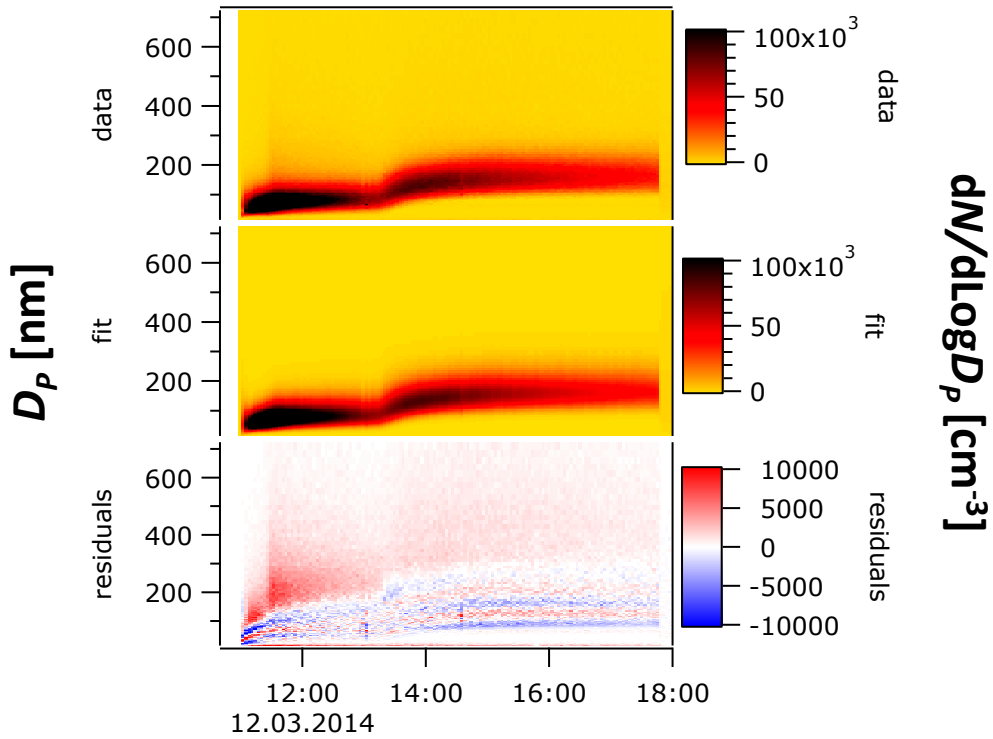

Figure S4: SMPS measurements (top), lognormal fits (middle; f_{POA}=0.51), and fit residuals (bottom) of the size distribution of biomass burning organic aerosol during a typical aging experiment.

Old Figure:

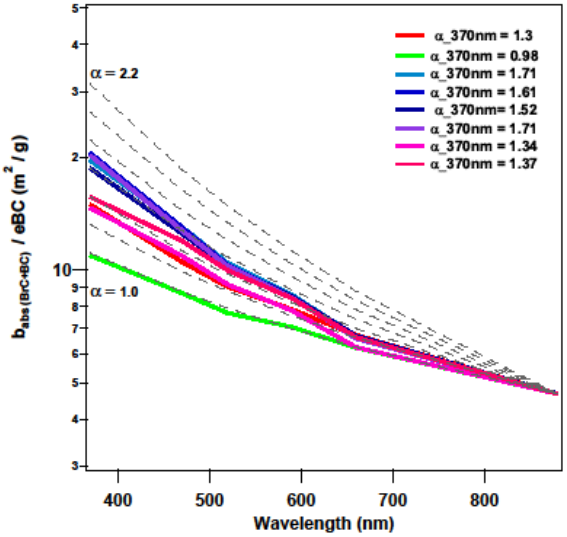

New Figure:

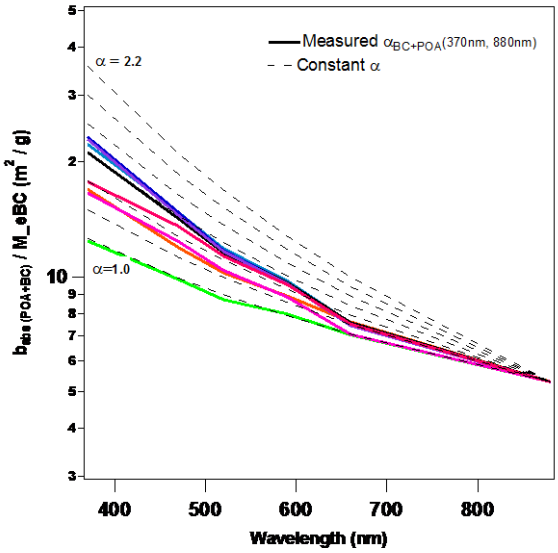

~~**Figure S5: Absorption coefficients of fresh wood burning emissions measured using an aethalometer normalized to the eBC mass as a function of wavelength. In the legend each color denotes the α_{BC+POA}(370nm,880nm) for an individual experiment. The dashed lines mark the literature range of α values obtained for primary biomass burning emissions.**~~

Figure S5: Absorption coefficients of fresh wood burning emissions measured using an aethalometer normalized to the eBC mass as a function of wavelength. In the legend each color denotes the α_{BC+POA}(370nm,880nm) for an individual experiment. The dashed lines mark the absorption profiles calculated assuming a constant α_{BC+POA} in the range 370-880nm. The range of α values, is set between 1-2.2 (with an increment of 0.2), based on literature reports for primary biomass burning emissions from residential heating. The observed absorption spectra have steeper gradients with decreasing wavelength compared to the lines of constant alpha. This systematic decrease in $\alpha(\lambda, 880nm)$ with increasing λ reflects the more-efficient light absorption by BrC at shorter wavelengths (Moosmüller et al., 2011), and shows that the power law wavelength dependence is an inaccurate oversimplification for this mixed aerosol.

Old Figure:

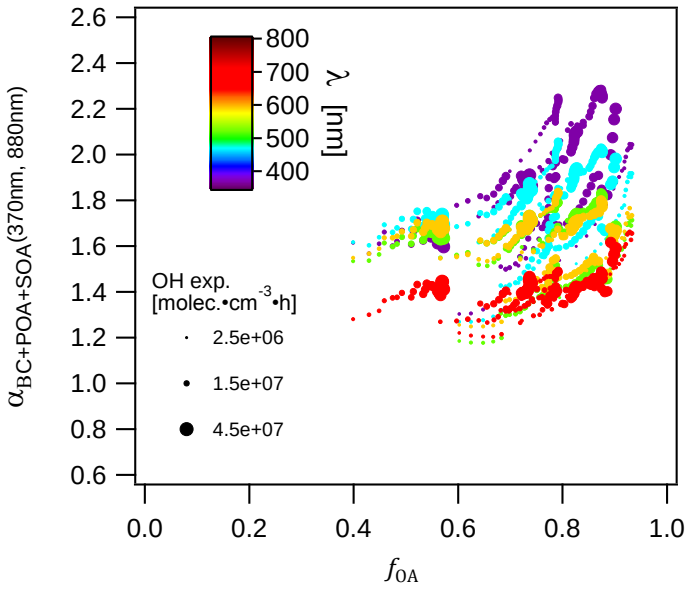

New Figure:

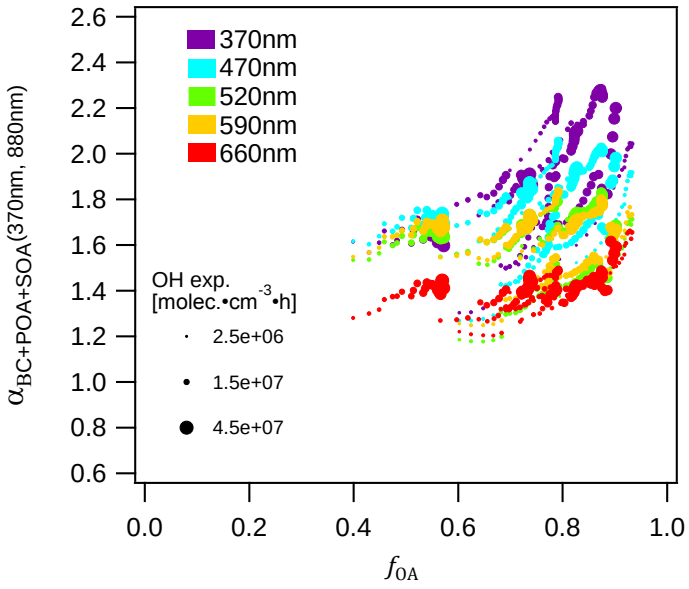

Figure S6: Relationship of $\alpha_{BC+POA+SOA}(\lambda, 880nm)$ to f_{OA} for seven wavelengths, with symbol sizes indicating OH exposure.

Old Figure:

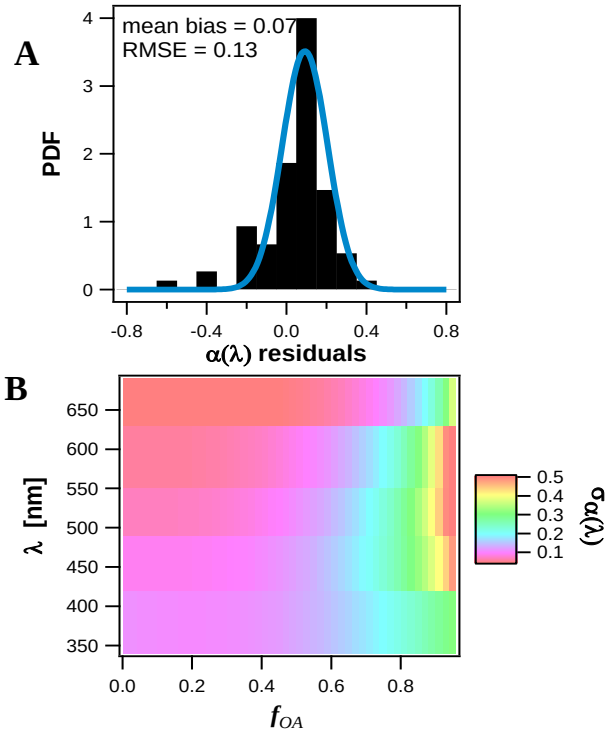

New Figure:

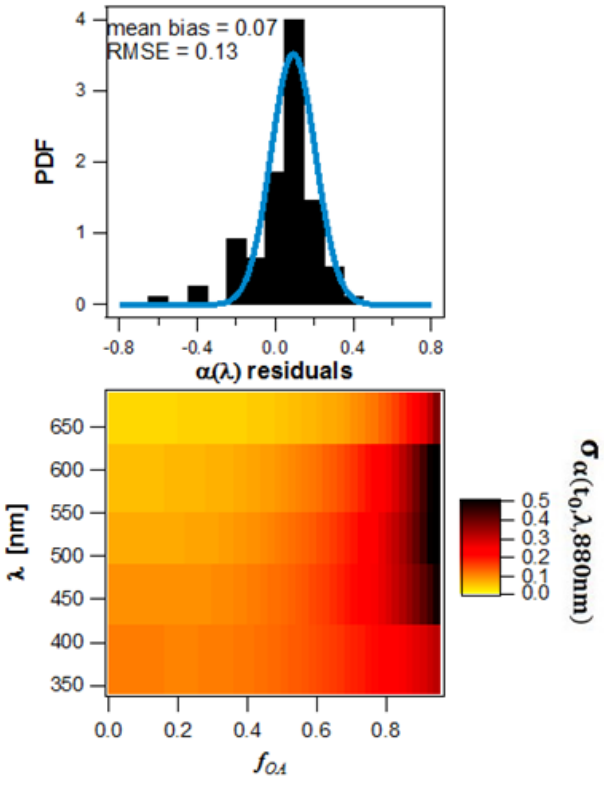

~~**Figure S7: Analysis of the fitting errors of $\alpha(\lambda, 880\text{nm})$ of primary emissions as a function of f_{OA}. Panel A shows the α residual as a probability density function. Panel B is an image plot of the $\alpha(\lambda, 880\text{nm})$ uncertainty as a function of f_{OA} estimated based on error propagation, using Equation 13 and assuming $MAC_{POA}(\lambda)$, $MAC_{BC}(\lambda)$ and f_{OA} to be independent variables (assuming negligible covariance between these quantities). The image plot in panel B shows that at short wavelengths and low fractions of OA, the estimated error on α is less than 0.1. However, with increasing OA fraction and at longer wavelength the uncertainty increases. It should be noted that this increasing uncertainty is not greater than 0.5 even at OA fractions of 0.99, corresponding to an α of ~ 2.2.**~~

Figure S7: Analysis of the fitting errors of $\alpha(\lambda, 880\text{nm})$ of primary emissions as a function of f_{OA}. Panel A shows the α residual as a probability density function. Panel B is an image plot of the $\alpha(\lambda, 880\text{nm})$ error, $\sigma_{\alpha(t_0,\lambda,880\text{nm})}$, as a function of f_{OA} at different wavelengths. $\sigma_{\alpha(t_0,\lambda,880\text{nm})}$ is obtained from the error propagation of Eq. (13) solved for different wavelengths, using the geometric mean and standard deviation of $MAC_{POA}(\lambda)$ and $MAC_{BC}(\lambda)$. This error term represents the variability in or the confidence level on the $\alpha(t_0, \lambda, 880\text{nm})$ at different wavelengths. As $\alpha(t_0, \lambda, 880\text{nm})$ depends on $M_{OA}/\ b_{abs}(t_0, 880\text{nm})$ in Equation 13, $\sigma_{\alpha(t_0,\lambda,880\text{nm})}$ also does. We expressed $M_{OA}/b_{abs}(t_0, 880\text{nm})$ as f_{OA}, using σ_{ATN} to estimate EC mass from b_{ATN}(880nm). At short wavelengths and low OA fractions, the confidence level on α is within 0.1. However, with increasing f_{OA}, and at longer wavelength the uncertainty in predicting α increases.

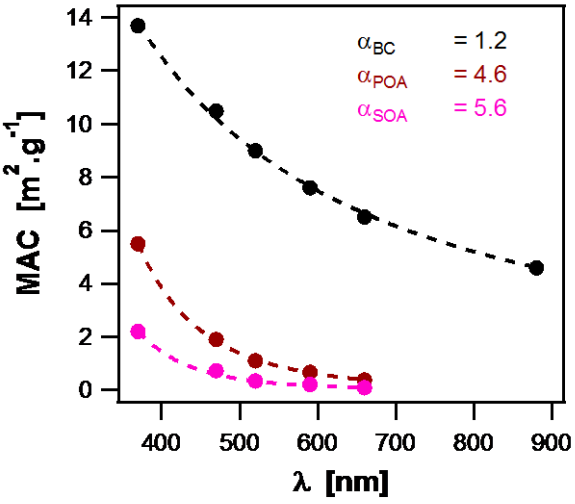

Figure S8: Power law fits through the average MAC of BC, POA and SOA calculated from Aethalometer measurements plotted as a function of wavelength. Note that MAC_{SOA}(880nm) and MAC_{POA}(880nm) are zero by definition.

Old Figure:

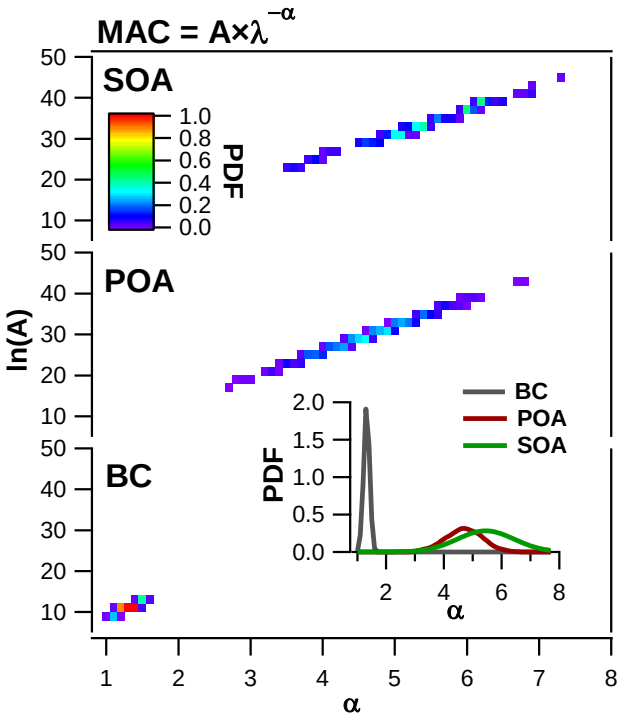

New Figure:

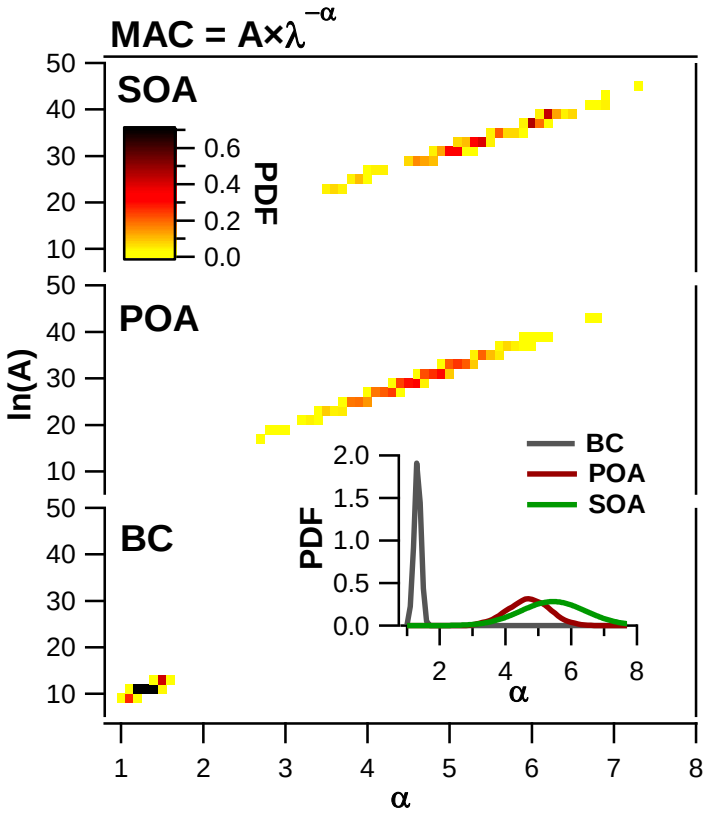

Figure S9: Probability distributions of α and ln(A) describing the optical properties of BC, POA and SOA. Parameters for representing these distributions as a bivariate normal joint density function are shown in Table S1. The equation needed to generate these probabilities is $f(\mathrm{X}) = \frac{|\Sigma|^{-\frac{1}{2}}}{2\pi} \exp\left(-\frac{1}{2}(\mathrm{X}-\mu)^{\mathrm{T}}\Sigma^{-1}(\mathrm{X}-\mu)\right)$ **, where** $\mu = \begin{pmatrix} \mu_{\alpha} \\ \mu_{\ln(A)} \end{pmatrix}$**; represents the average α and ln(A) values and** $\Sigma = \begin{pmatrix} \sigma_{\alpha}^2 & \rho\sigma_{\alpha}\sigma_{\ln(A)} \\ \rho\sigma_{\alpha}\sigma_{\ln(A)} & \sigma_{\ln(A)}^2 \end{pmatrix}$ **is the covariance matrix. As α and ln(A) are determined from fitting the MAC vs. λ, their covariance is high. Therefore the selection of these parameters to represent the MAC profiles of BC, POA and SOA, should not be done independently but by using the probability density function above and the parameters in Table S1.**

Table S1: Parameters for normal joint density function.

	BC	**POA**	**SOA**
μ	$\begin{pmatrix} 1.2 \\ 10.0 \end{pmatrix}$	$\begin{pmatrix} 4.6 \\ 29.2 \end{pmatrix}$	$\begin{pmatrix} 5.6 \\ 33.3 \end{pmatrix}$
Σ	$\begin{pmatrix} 0.09 & 0.054 \\ 0.054 & 0.61 \end{pmatrix}$	$\begin{pmatrix} 0.64 & 2.6 \\ 2.6 & 4.1 \end{pmatrix}$	$\begin{pmatrix} 1.36 & 11.4 \\ 11.4 & 8.35 \end{pmatrix}$

Old Figure:

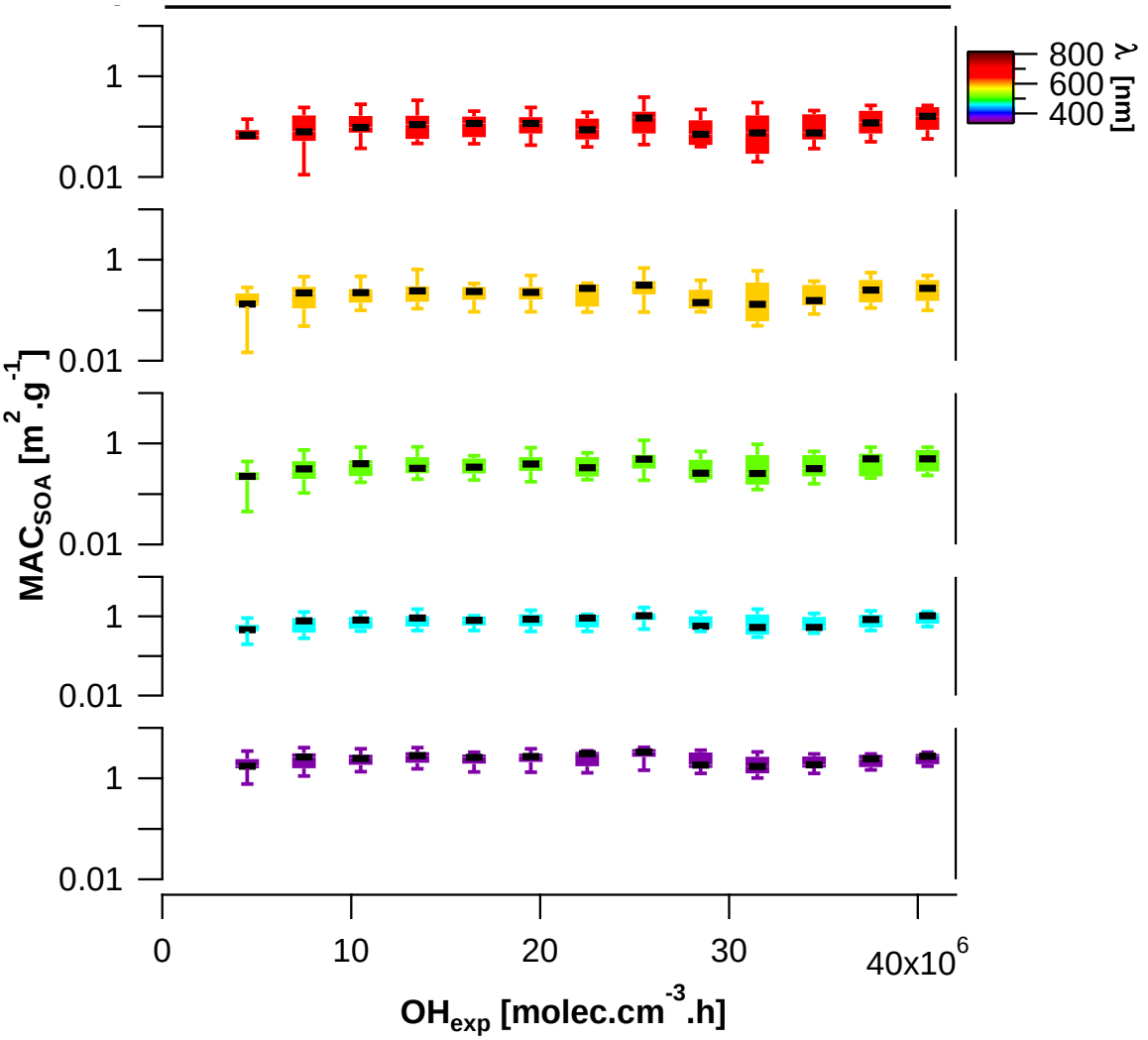
800
600
400
λ [nm]
1
0.01
MAC$_{SOA}$ [m^2.g^{-1}]
0
10
20
30
40x10^6
OH$_{exp}$ [molec.cm^{-3}.h]

New Figure:

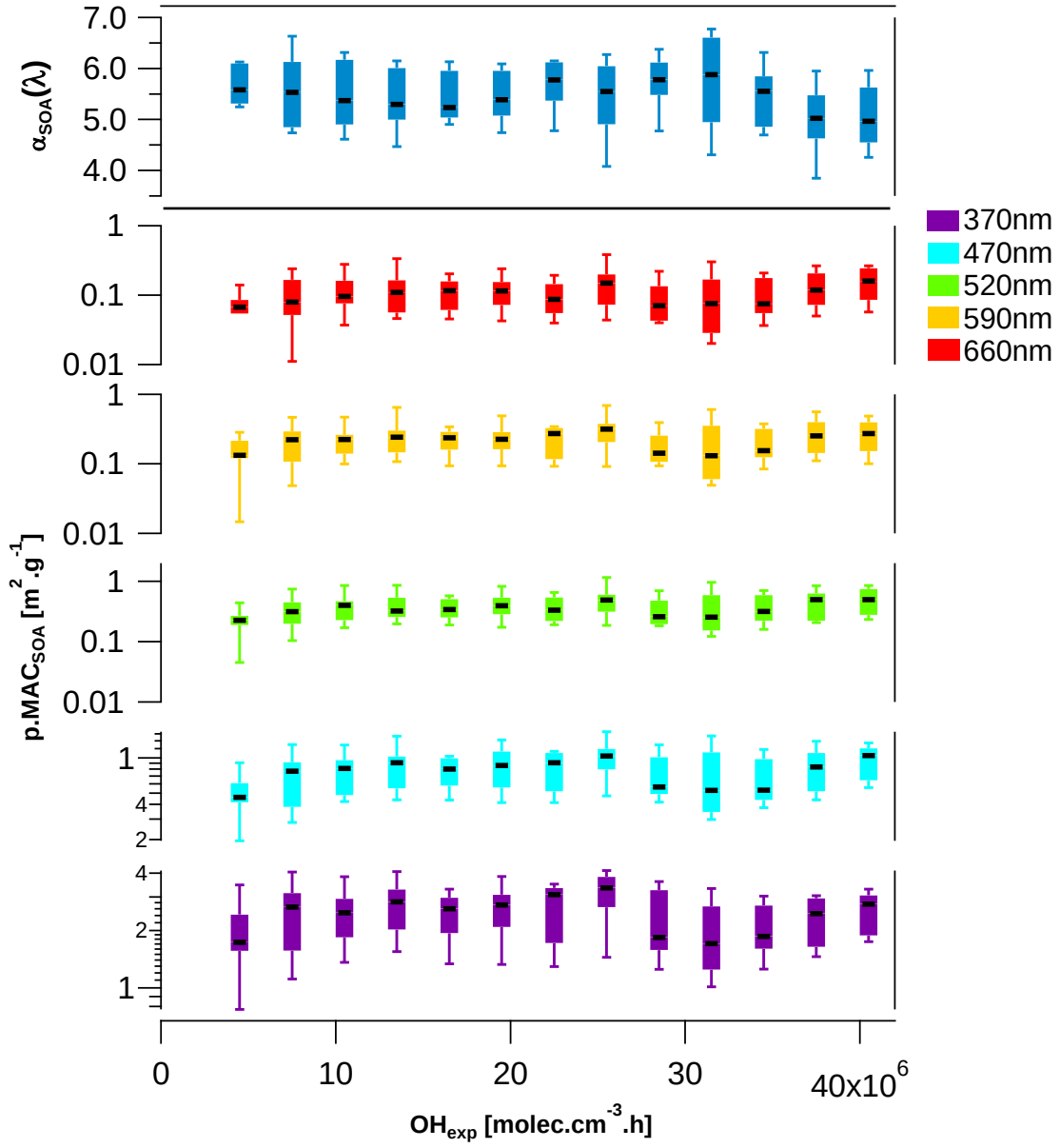

Figure S10: MAC_{SOA} as a function of OH exposure color coded according to the wavelength.

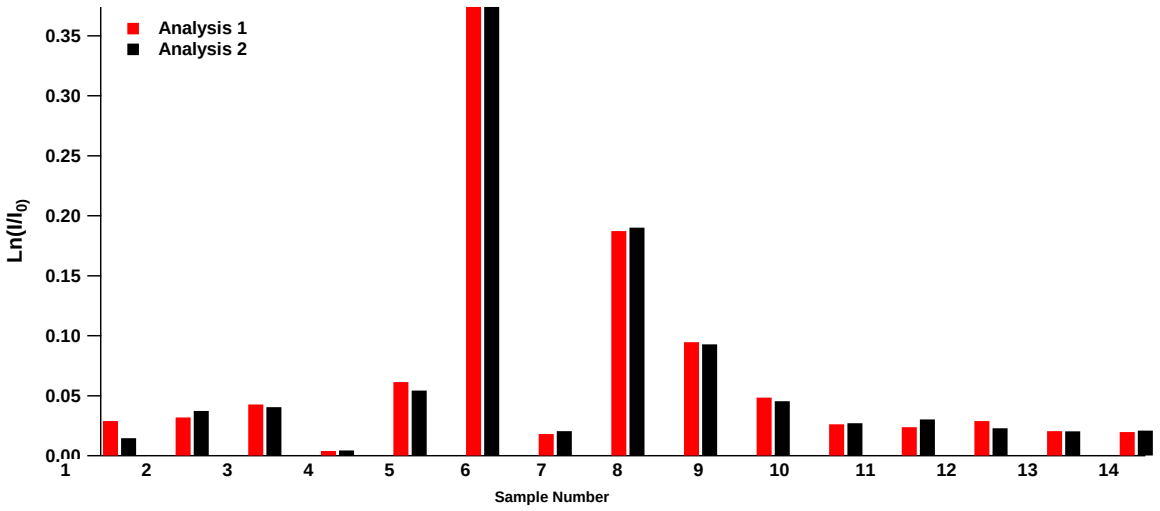

Figure S11: Absorbance measurements from UV-visible analysis of water extracted filters from several wood burning experiments showing very good repeatability (consistent within 10%).

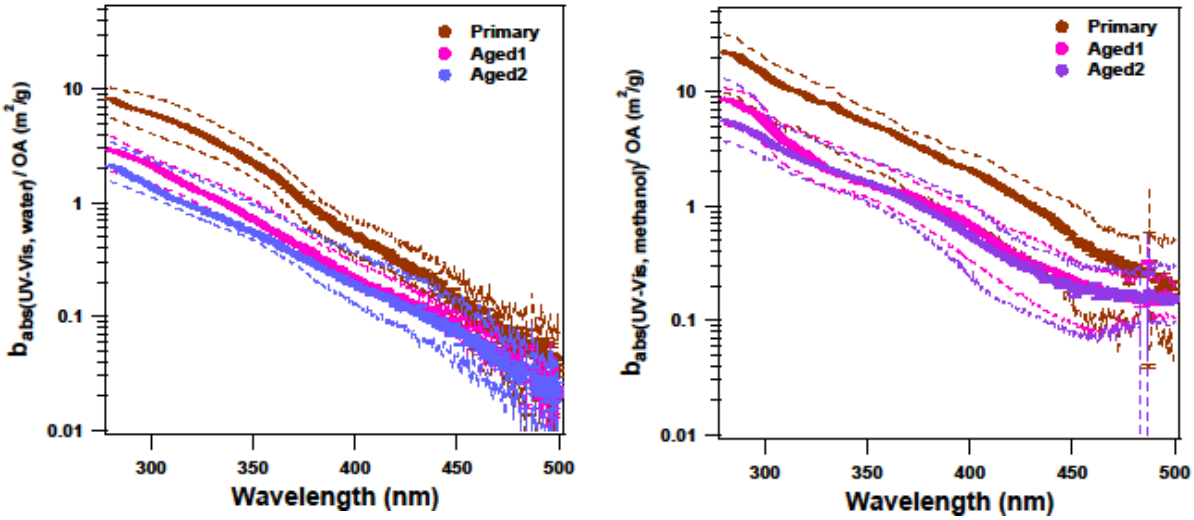

Figure S12: MAC_{bulk} (bulk absorbance of extracts normalized to AMS-measured OA) of primary, slightly aged (Aged1, OH exposure ~ $1x10^7$molecules cm^{-3} h) and aged emissions (Aged2, OH exposure ~ $4x10^7$ molecules cm^{-3} h) for (A) water and (B) methanol extracts. The bold lines indicate the medians, and the dashed lines mark the 25th and 75th percentiles. At 450–500 nm, the methanol-extract absorption shows a constant absorptivity feature which was not present before aging, suggesting that the absorbing species may be partially-oxidized (partially-solubilized) primary OA, or reflect light-absorbing SOA.

Old Figure:

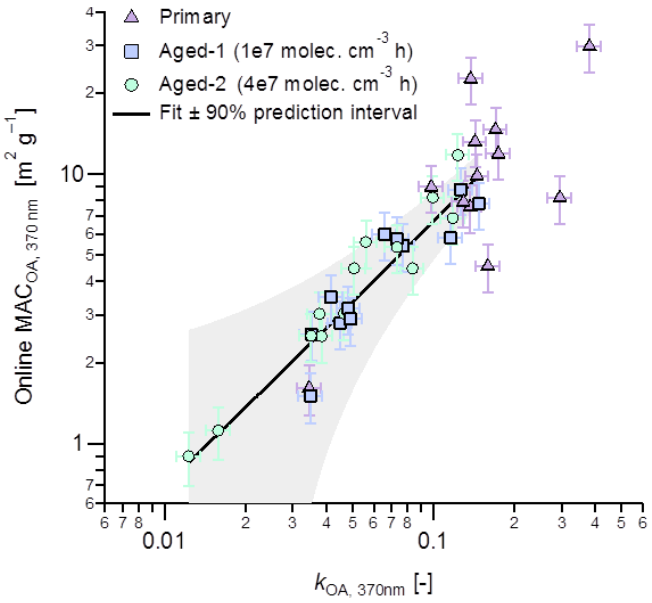

New Figure:

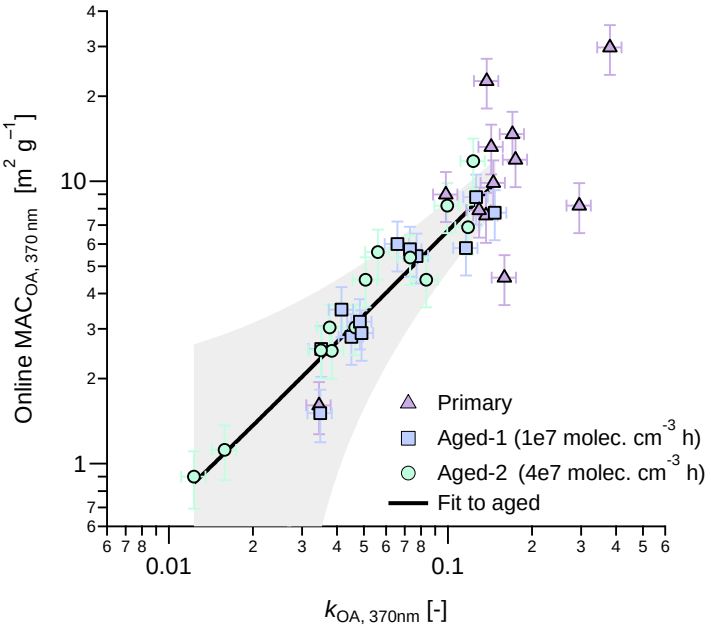

~~**Figure S13: MAC_{OA} at λ = 370 nm calculated from aethalometer measurements vs. k_{OA} at λ = 370 nm from the UV-visible measurements of the methanol extracts.**~~

Figure S13: MAC_{OA} at λ = 370 nm calculated from aethalometer measurements vs. k_{OA} at λ = 370 nm from the UV/visible measurements of the methanol extracts. The shaded region shows the 90% confidence interval of a weighted orthogonal regression (slope 66 ± 9 m^2g^{-1}, intercept 0.0 ± 0.3 m^2g^{-1}) to illustrate the relatively small range of variability in the data for aged samples.

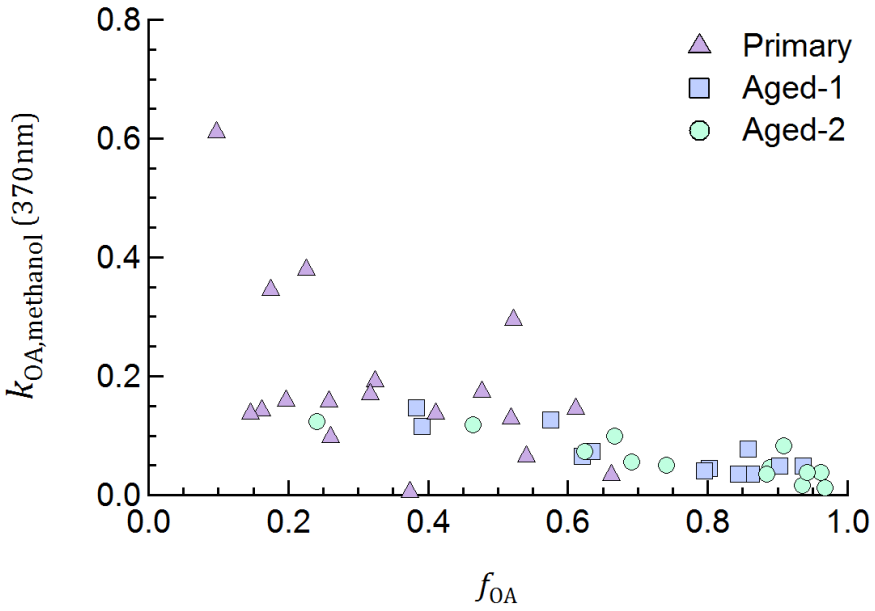

Figure S14. Similar to Fig. 7 in the main text, but plotted against f_{OA} for comparison to the other figures in this work.

References

Pierce, J. R., Engelhart, G. J., Hildebrandt, L., Weitkamp, E. A., Pathak, R. K., Donahue, N. M., Robinson, A. L., Adams, P. J. and Pandis, S. N.: Constraining particle evolution from wall losses, coagulation, and condensation-evaporation in smog-chamber experiments: optimal estimation based on size distribution measurements, Aerosol Sci. Technol., 42, 1001–1015, doi:10.1080/02786820802389251, 2008.

Bond, T. C., Habib, G. and Bergstrom, R. W.: Limitations in the enhancement of visible light absorption due to mixing state, J. Geophys. Res. Atmos., 111(20), 1–13, doi:10.1029/2006JD007315, 2006.